ISSN 0021-9673

VOL. 637 NO. 2 MAY 14, 1993

THIS ISSUE COMPLETES VOL. 637

JOURNAL OF CHROMATOGRAPHY

INCLUDING ELECTROPHORESIS AND OTHER SEPARATION METHODS

ELSEVIER

JOURNAL OF CHROMATOGRAPHY

INCLUDING ELECTROPHORESIS AND OTHER SEPARATION METHODS

Scope. The *Journal of Chromatography* publishes papers on all aspects of **chromatography, electrophoresis** and related methods. Contributions consist mainly of research papers dealing with chromatographic theory, instrumental developments and their applications. The section *Biomedical Applications*, which is under separate editorship, deals with the following aspects: developments in and applications of chromatographic and electrophoretic techniques related to clinical diagnosis or alterations during medical treatment; screening and profiling of body fluids or tissues related to the analysis of active substances and to metabolic disorders; drug level monitoring and pharmacokinetic studies; clinical toxicology; forensic medicine; veterinary medicine; occupational medicine; results from basic medical research with direct consequences in clinical practice. In *Symposium volumes*, which are under separate editorship, proceedings of symposia on chromatography, electrophoresis and related methods are published.

Submission of Papers. The preferred medium of submission is on disk with accompanying manuscript (see *Electronic manuscripts* in the Instructions to Authors, which can be obtained from the publisher, Elsevier Science Publishers B.V., P.O. Box 330, 1000 AH Amsterdam, Netherlands). Manuscripts (in English; *four* copies are required) should be submitted to: Editorial Office of *Journal of Chromatography*, P.O. Box 681, 1000 AR Amsterdam, Netherlands, Telefax (+31-20) 5862 304, or to: The Editor of *Journal of Chromatography, Biomedical Applications*, P.O. Box 681, 1000 AR Amsterdam, Netherlands. Review articles are invited or proposed in writing to the Editors who welcome suggestions for subjects. An outline of the proposed review should first be forwarded to the Editors for preliminary discussion prior to preparation. Submission of an article is understood to imply that the article is original and unpublished and is not being considered for publication elsewhere. For copyright regulations, see below.

Publication. The *Journal of Chromatography* (incl. *Biomedical Applications*) has 40 volumes in 1993. The subscription prices for 1993 are:

J. Chromatogr. (incl. *Cum. Indexes, Vols. 601–650*) + *Biomed. Appl.* (Vols. 612–651):
Dfl. 8520.00 plus Dfl. 1320.00 (p.p.h.) (total *ca.* US$ 5622.75)

J. Chromatogr. (incl. *Cum Indexes, Vols. 601–650*) only (Vols. 623–651):
Dfl. 7047.00 plus Dfl. 957.00 (p.p.h.) (total *ca.* US$ 4573.75)

Biomed. Appl. only (Vols. 612–622):
Dfl. 2783.00 plus Dfl. 363.00 (p.p.h.) (total *ca.* US$ 1797.75).

Subscription Orders. The Dutch guilder price is definitive. The US$ price is subject to exchange-rate fluctuations and is given as a guide. Subscriptions are accepted on a prepaid basis only, unless different terms have been previously agreed upon. Subscriptions orders can be entered only by calender year (Jan.–Dec.) and should be sent to Elsevier Science Publishers, Journal Department, P.O. Box 211, 1000 AE Amsterdam, Netherlands, Tel. (+31-20) 5803 642, Telefax (+31-20) 5803 598, or to your usual subscription agent. Postage and handling charges include surface delivery except to the following countries where air delivery via SAL (Surface Air Lift) mail is ensured: Argentina, Australia, Brazil, Canada, China, Hong Kong, India, Israel, Japan*, Malaysia, Mexico, New Zealand, Pakistan, Singapore, South Africa, South Korea, Taiwan, Thailand, USA. *For Japan air delivery (SAL) requires 25% additional charge of the normal postage and handling charge. For all other countries airmail rates are available upon request. Claims for missing issues must be made within six months of our publication (mailing) date, otherwise such claims cannot be honoured free of charge. Back volumes of the *Journal of Chromatography* (Vols. 1–611) are available at Dfl. 230.00 (plus postage). Customers in the USA and Canada wishing information on this and other Elsevier journals, please contact Journal Information Center, Elsevier Science Publishing Co. Inc., 655 Avenue of the Americas, New York, NY 10010, USA, Tel. (+1-212) 633 3750, Telefax (+1-212) 633 3764.

Abstracts/Contents Lists published in Analytical Abstracts, Biochemical Abstracts, Biological Abstracts, Chemical Abstracts, Chemical Titles, Chromatography Abstracts, Current Awareness in Biological Sciences (CABS), Current Contents/Life Sciences, Current Contents/Physical, Chemical & Earth Sciences, Deep-Sea Research/Part B: Oceanographic Literature Review, Excerpta Medica, Index Medicus, Mass Spectrometry Bulletin, PASCAL-CNRS, Referativnyi Zhurnal, Research Alert and Science Citation Index.

US Mailing Notice. *Journal of Chromatography* (ISSN 0021-9673) is published weekly (total 52 issues) by Elsevier Science Publishers (Sara Burgerhartstraat 25, P.O. Box 211, 1000 AE Amsterdam, Netherlands). Annual subscription price in the USA US$ 4573.75 (subject to change), including air speed delivery. Application to mail at second class postage rate is pending at Jamaica, NY 11431. **USA POSTMASTERS**: Send address changes to *Journal of Chromatography*, Publications Expediting, Inc., 200 Meacham Avenue, Elmont, NY 11003. Airfreight and mailing in the USA by Publications Expediting.

See inside back cover for Publication Schedule, Information for Authors and information on Advertisements.

0021-9673/93/$06.00

This issue is printed on acid-free paper.

Printed in the Netherlands

CONTENTS

(Abstracts/Contents Lists published in Analytical Abstracts, Biochemical Abstracts, Biological Abstracts, Chemical Abstracts, Chemical Titles, Chromatography Abstracts, Current Awareness in Biological Sciences (CABS), Current Contents/Life Sciences, Current Contents/Physical, Chemical & Earth Sciences, Deep-Sea Research/Part B: Oceanographic Literature Review, Excerpta Medica, Index Medicus, Mass Spectrometry Bulletin, PASCAL-CNRS, Referativnyi Zhurnal, Research Alert and Science Citation Index)

REGULAR PAPERS

(Continued overleaf)

SHORT COMMUNICATIONS

Column liquid chromatography

Supercritical fluid chromatography

Electrophoresis

Journal of Chromatography, 637 (1993) 119–128
Elsevier Science Publishers B.V., Amsterdam

CHROM. 24 897

Variance of a zone migrating in a linear medium

II. Time-varying non-uniform medium

Leonid M. Blumberg

Hewlett-Packard Co., 2850 Centerville Road, Wilmington, DE 19808 (USA)

(First received September 8th, 1992; revised manuscript received December 14th, 1992)

ABSTRACT

A model of dispersion of a solute migrating in a non-uniform (coordinate-dependent) time-varying medium has been proposed. Only two quantities, plate height and velocity of the solute required for the complete model. Derivatives of the variance of the zone have been found for the general case of a linear (independent of solute concentration) medium, and for many special cases. For the practically important case where the local plate height and the local gradient of the solute velocity are nearly coordinate-independent within the zone, a simple model of the evolution of the variance of the zone has been derived. A consistent definition of the local plate height has been constructed. It has been shown that the currently accepted method of calculation of the variance of the zone is valid only under the certain conditions which were not known before.

INTRODUCTION

Chromatographic conditions may change during the analysis (*time-variance*) and/or along the column (*non-uniformity*), see Table I.

Many types of *temporal* and *spatial* variations of chromatographic conditions specific for particular chromatographic techniques have been analyzed in the literature [3–25]. However, no unified general theory describing the underlying effects of these changes is known.

Certainly, a specific study is well suited for the analyses of particular circumstances of a given technique. It can take into account all the details of the technique. A general theory, on the other hand, allows to see the broad picture of many separation techniques and provide the answers applicable to all of them. It can also serve as a framework and a guide for the more detailed studies. For instance, it has been recently shown [26] that, as long as a separation is *linear* (concentration independent) and *ideal* (infinitely short injection time, *etc.*), no focusing [15–26] can improve chromatographic resolution. If, on the other hand, the conditions were not ideal (which, in practice, is always the case) the focusing can recover [26] the losses in resolution. These conclusions were based on the theory described in this paper. They can guide a study of focusing in many separation techniques.

The purpose of this paper is to develop the foundation for the *kinetic* theory of separation in an arbitrary linear medium (time-varying and/or non-uniform). The study of the evolution of the variance of the zone is viewed as a corner stone for such theory. This paper is part 2 in the series dedicated to that study.

In the first part of the series [2], the theory for an arbitrary *time-invariant* medium (Table I), has been developed. The theory was derived from the basic principles of dispersion of migrating solutes.

In this paper, this theory has been further extended. Although the theory covers the entire

0021-9673/93/$06.00

TABLE I

CLASSIFICATION OF CHROMATOGRAPHIC MEDIA BY THE TYPES OF CHANGES

Media	Changes	Ref.	Examples
Time-invariant uniform	No changes	1[a]	Isocratic LC, isothermal GC with low-pressure drops
Time-invariant non-uniform	Changes in distance only	2[a]	Supercritical fluid chromatography (SFC), isoelectric focusing, isothermal GC
Time-varying uniform	Changes in time only	3–12	Programmed-temperature GC with low-pressure drops
Time-varying non-uniform	Changes in time and distance	13–25	Programmed temperature GC, chromathermography, gradient elution LC, programmed-pressure SFC

[a]And references cited therein.

Table I, its main focus has been the most complicated case of the *time-varying* non-uniform media.

Model

The model of a mass-conservative migration and dispersion of a solute in a time-varying non-uniform medium can be represented by the partial differential equation [2]

$$\frac{\partial m}{\partial s} = \frac{\partial^2}{\partial x^2}(D_{\text{eff}} m) - \frac{\partial}{\partial x}(um) \qquad (1)$$

where x and s are, respectively, distance and time coordinates for the medium, m is *specific mass* (per unit length) of the solute, D_{eff} is local *effective diffusivity* [27] of the solute, and u is local *velocity* of the solute.

In this study, the scope of the model is limited by the following assumptions.

(C1) *Linearity* of the medium. Quantities $D_{\text{eff}} = D_{\text{eff}}(x, s)$ and $u = u(x, s)$ do not depend on m.

In addition, D_{eff} is not negative, and at any time, both D_{eff} and u are bounded within any bounded interval of x while their gradients are bounded when x approaches infinity. More specifically:

(C2) $0 \leq s < \infty$ implies: $0 \leq D_{\text{eff}} < \infty$ and $|u| < \infty$ when $|x| < \infty$; $|\partial D_{\text{eff}}/\partial x| < \infty$ and $|\partial u/\partial x| < \infty$ when $x \rightarrow \pm\infty$.

Finally, m is not negative, and the second moment of the zone is bounded at any time, *i.e.*

(C3) $m = m(x, s) \geq 0$, and $\int_{-\infty}^{\infty} x^2 m \, dx < \infty$ when $0 \leq s < \infty$.

Of these conditions, only C1 represents the practically meaningful limitation. It means, *e.g.*, that the results of this theory can not be applied to many cases of preparative chromatography [14] where frequently, due to the column overloading, the conditions are substantially *non-linear*. In the analytical chromatography, however, the overloading is typically avoided, and the results of the theory are valid. Also, only this condition is *substantially different* from its counterpart in ref. 2 reflecting the much broader scope of this treatment. Whereas in ref. 2, the quantities D_{eff} and u were only allowed to be functions of the distance, x, (*time-invariant non-uniformity*), here they can depend on the time, s, as well (medium can be *time-varying* and/or non-uniform).

Conditions in the collections C2 and C3 are either the statements of the physically existing facts (non-negative mass and effective diffusivity), or of the limitations which always exist in practice. Interpretation of all these conditions is obvious with the one possible exception of the bounded second moment of the zone. The latter means that the width of the zone expressed via the *standard deviation* of the zone is required to be bounded. A simple example of a zone with the non-bounded variance (see Appendix 1) is of certain theoretical interest.

THEORY

Many derivations in this section are similar to those in ref. 2. However, the possibility of the changes of the properties of the medium in time

(excluded in ref. 2) requires special attention. As before [2], a distinction between an arbitrary coordinate x in the medium and the coordinate, z, of the center of mass of a migrating zone is carefully maintained. Additionally, here, similar distinction between an arbitrary time variable s and the migration time of the zone, t (the time when the center of mass of the zone is at z), is recognized.

Implications of conditions C1–C3

Conditions C3 imply that the amount, M, of the solute in the zone is bounded. Additionally, due to the mass conservative nature of the eqn. 1, M is constant [2]. In other words,

$$M = \int_{-\infty}^{\infty} m \, dx = \text{constant} < \infty \tag{2}$$

The second of the conditions C3 also implies that at any instant, $s = t$, of time

$$z = z(t) = \frac{1}{M} \int_{-\infty}^{\infty} xm(x, t) \, dx < \infty \tag{3}$$

i.e. the coordinate, z, of the center of mass of the zone is bounded as well. If necessary, the function $z = z(t)$ can be inverted[a] to $t = t(z)$. Relations $z = z(t)$ and $t = t(z)$ can be used to transform any function of z into a function of t and vice versa. Finally, together, eqns. 2 and 3 imply a known relation

$$\int_{-\infty}^{\infty} (z - x)m \, dx = 0 \tag{4}$$

Modified model

Effective diffusivity, D_{eff}, in eqn. 1 represents the rate of diffusion of a solute per unit of time [27] (*temporal* rate of diffusion). Better known in chromatography is the rate of *dispersion* of the zone per unit of its displacement in the column (*spatial rate* of dispersion). In a uniform time-invariant chromatography that rate known as a column *plate height*, relates to the effective diffusivity as [27]

$$H = \frac{2D_{\text{eff}}}{u} \tag{5}$$

In an arbitrary medium, the quantity H in eqn. 5 represents the *local* rate of dispersion of the solute per unit of its displacement in the medium, and, therefore, can be identified with the *local plate height* in the medium [2] (see Discussion for the direct definition of the local plate height). Substitution of eqn. 5 in eqn. 1 yields

$$\frac{\partial m}{\partial s} = \frac{1}{2} \cdot \frac{\partial^2}{\partial x^2} (Hum) - \frac{\partial}{\partial x} (um) \tag{6}$$

This model describes the mass-conservative migration of a zone directly through the two best known basic concepts in chromatography: a column plate height and velocity of a solute.

Velocity of the zone

In a non-uniform medium, different parts of the zone can migrate with different velocities. Nevertheless, the concept of the single (*aggregate*) *velocity*, $\tilde{u}$, *of the zone* as a whole can be defined. If the location of the zone is identified with the coordinate, z, eqn. 3, of its center of mass, and t is the time required for the zone to migrate to z then the velocity of the zone becomes

$$\tilde{u} = \frac{dz}{dt} \tag{7}$$

It can be shown (see Appendix 2) that

$$\tilde{u} = \frac{1}{M} \left(\int_{-\infty}^{\infty} um \, dx \right)_{s=t} = \frac{1}{M} \int_{-\infty}^{\infty} u(x, t)m(x, t) \, dx \tag{8}$$

Evolution of the spatial variance of the zone

The changes in the *spatial variance*

$$\sigma^2 = \frac{1}{M} \int_{-\infty}^{\infty} (x - z)^2 m \, dx \tag{9}$$

of the zone can be described by the derivative $d\sigma^2/dz$ [2]. It can be shown (see Appendix 3) that

[a] If the velocity of the zone reverses direction, the relation $t(z)$ can become multi-valued.

$$\frac{d\sigma^2}{dz} = \frac{1}{\tilde{u}M}\left(\int_{-\infty}^{\infty} Hum\,dx + 2\int_{-\infty}^{\infty}(x-z)um\,dx\right)_{s=t(z)} = \tilde{H} + \frac{2}{\tilde{u}M}\left(\int_{-\infty}^{\infty}(x-z)um\,dx\right)_{s=t(z)} \quad (10)$$

where

$$\tilde{H} = \frac{1}{\tilde{u}M}\left(\int_{-\infty}^{\infty} Hum\,dx\right)_{s=t} \quad (11)$$

is the *zonal* plate height, *i.e.* the (*aggregate*) plate height for the entire zone [2].

Special cases

So far, no limits to the degree of the variation of H and u in distance or time were imposed. For example, the gradient of velocity of the solute was allowed to change its sign *within* the zone. That can significantly distort the shape of the zone and even split a zone of a pure solute in several pockets. In analytical chromatography, however, efforts are made to avoid such extremes and keep the variation of the gradients

$$g_H = g_H(x,s) = \frac{\partial H}{\partial x} \quad \text{and} \quad g_u = g_u(x,s) = \frac{\partial u}{\partial x} \quad (12)$$

within the zone at the low level. Under such conditions, eqn. 10 can be simplified.

(C4) *Moderate media.* Within the zone located at z, the plate height and the solute velocity are linear functions of x:

$$H(x,t(z)) = H(z,t(z)) + g_H(z,t(z))(x-z),$$

for all x where $m(x,t(z)) \neq 0$; (13)

$$u(x,t(z)) = u(z,t(z)) + g_u(z,t(z))(x-z),$$

for all x where $m(x,t(z)) \neq 0$ (14)

For a moderate medium, eqn. 10 can be rewritten (see Appendix 4) as

$$\frac{d\sigma^2}{dz} = H + \frac{2\sigma^2}{u}\cdot\frac{\partial u}{\partial x}\left(1+\frac{1}{2}\cdot\frac{\partial H}{\partial x}\right) \quad \text{or}$$

$$\frac{d\sigma^2}{dz} = H + \frac{2\sigma^2 g_u}{u}\left(1+\frac{g_H}{2}\right) \quad (15)$$

(C5) *Partially moderate media.* Within the zone located at z, the solute velocity is linear functions of x, eqn. 14 (while the plate height can change arbitrarily).
In this case[a] (see Appendix 4),

$$\frac{d\sigma^2}{dz} = \tilde{H} + \frac{2\sigma^2}{u}\cdot\frac{\partial u}{\partial x} \quad \text{or} \quad \frac{d\sigma^2}{dz} = \tilde{H} + \frac{2\sigma^2 g_u}{u} \quad (16)$$

(C6) *Smooth media* (a stronger case of the moderate media). Within the zone located at z, the solute velocity is a linear function of x, eqn. 14, while the plate height does not depend on x:

$$H(x,t(z)) = H(z,t(z))$$

for all x where $m(x,t(z) \neq 0$ (17)

This is the simplest of the time-varying non-uniform media (see Discussion). Due to $g_H = 0$, eqn. 15 becomes

$$\frac{d\sigma^2}{dz} = H + \frac{2\sigma^2}{u}\cdot\frac{\partial u}{\partial x} \quad \text{or} \quad \frac{d\sigma^2}{dz} = H + \frac{2\sigma^2 g_u}{u} \quad (18)$$

(C7) *Uniform media.* Within the zone located at z, the plate height and the solute velocity do not depend on x, *i.e.* along with eqn. 17, one has:

$$u(x,t(z)) = u(z,t(z))$$

for all x where $m(x,t(z)) \neq 0$. (19)

Eqns. 15 and 18 become

$$\frac{d\sigma^2}{dz} = H \quad (20)$$

Notice, that this familiar relation [28,29] remains valid even if the medium changes in time (time-variance).

(C8) *Moderate time-invariant media.* During the passage of the center of mass of the zone through the coordinate z, the medium remains moderate, C4, and time-invariant. The latter means that

[a] Eqn. 16 was instrumental for the derivations in ref. 26.

$$\left.\frac{\partial H}{\partial s}\right|_{s=t(z)} = 0 \quad \text{and} \quad \left.\frac{\partial u}{\partial s}\right|_{s=t(z)} = 0$$

for all x where $m(x, t(z)) \neq 0$. (21)

As partial derivatives of H and u over s vanish due to this condition, the partial derivatives of these quantities over x become the same as the full derivatives over x. Furthermore, since only $x = z$ is considered in eqn. 15 (see notations in Appendix 4), the derivatives over x are the same as the derivatives over z. Eqn. 15 becomes

$$\frac{d\sigma^2}{dz} = H + \frac{2\sigma^2}{u} \cdot \frac{du}{dz}\left(1 + \frac{1}{2} \cdot \frac{dH}{dz}\right) \quad (22)$$

The quantity

$$\tau^2 = \frac{\sigma^2}{u^2} \quad (23)$$

can be referred to as a *temporal variance of the zone*[a]. After the substitution of eqn. 23 into eqn. 22, the latter becomes (see Appendix 5)

$$\frac{d\tau^2}{dz} = \frac{H}{u^2} + \frac{\tau^2}{u} \cdot \frac{du}{dz} \cdot \frac{dH}{dz} \quad (24)$$

Significance of eqns. 22 and 24 is discussed in the next section.

(C9) *Smooth time-invariant media* [2]. During the passage of the center of mass of the zone through the coordinate z, the medium remains smooth, C6, and time-invariant, eqn. 21.

This case has been studied in ref. 2. The same arguments which led from eqn. 15 to eqns. 22 and 24, lead [2] to

$$\frac{d\sigma^2}{dz} = H + \frac{2\sigma^2}{u} \cdot \frac{du}{dz}, \quad (25)$$

$$\frac{d\tau^2}{dz} = \frac{H}{u^2} \quad (26)$$

The latter allows to calculate the net temporal variance of the zone at any z as

$$\tau^2 = \int d\tau^2 = \int \frac{H\, dz}{u^2} \quad (27)$$

Other forms of eqns. 26 and 27 (see Discussion) were known before [35–38].

(C10) *Gaussian zone.*

$$m(x, t(z)) = \frac{M}{\sigma\sqrt{2\pi}} \cdot \exp\left(-\frac{(x-z)^2}{2\sigma^2}\right)$$

is a Gaussian function of x when the zone is at z. For the Gaussian zone, eqn. 10 can be rewritten (see Appendix 6) as[b]

$$\frac{d\sigma^2}{dz} = \tilde{H} + \frac{2\sigma^2}{\tilde{u}}\tilde{g}_u \quad (28)$$

where

$$\tilde{g}_u = \frac{1}{M}\left(\int_{-\infty}^{\infty} g_u m\, dx\right)_{s=t}$$

is the average gradient of velocity of the solute in the zone.

This concludes the analysis of the special cases. Notice the structural similarity of eqns. 15 and 22, and eqns. 16, 18, 25 and 28. It is also worth mentioning that the special cases C4–C9 prescribe their conditions only in the vicinity of the certain coordinate z, and only at the time when the zone is there. In that sense, the conditions can be viewed as the zonal and the instantaneous ones. Obviously, the results are valid when the conditions are broader. For example, a certain region in the medium can be always smooth; or, at a given time, the entire medium can be smooth; and, finally, the entire medium can be always smooth.

DISCUSSION

The theory developed in the previous section is founded on the two basic principles of chromatographic separation in any medium: migration and dispersion of the zones. The small number of elements in the foundation of the theory assures broad application of its results

[a] When $t^2(z) \gg \tau^2$ (large values of z), the temporal variance of the *zone*, eqn. 23, is a good approximation to the temporal variances of the *solute mass-flow* or the *concentration-time curve* at z [30–34].

[b] Eqn. 28 was the basis for the formulation of the generalized conclusion in ref. 26.

[2,26]. Some implications of the theory are discussed below.

Implications of the time-variance

The time-variance enters into the relations for $d\sigma^2/dz$ (see Theory) in a subtle way. For instance, integration in eqn. 10 is done only over the distance variable x with the fixed s, and the equation itself is very similar to its time-invariant counterpart [2]. In the equations describing the special cases, variable t is even less visible (all quantities σ^2, H, $\tilde{H}$, u, g_H, g_u, $\tilde{g}_u$ in these equations are functions of the single variable z). Nevertheless, the influence of the time-variance is significant.

First of all, full derivatives over dz in the time-invariant equations are replaced with partial derivatives over ∂x in their time-varying counterparts. What is more, the time-varying equations are more complex because parameters H, u, *etc.* in these equations are not as directly related to their counterparts in the model eqn. 6, as they are in a time-invariant medium.

Consider, *e.g.*, the plate height in the time-invariant eqns. 22, 24–27. Notice, that the plate height in eqn. 6 is a function $H = H(x)$ of a single variable x [2]. Substitution of $x = z$ results in the function $H = H(z)$ for all eqns. 22, 24–27. In other words, quantity H eqns. 22, 24–27 is **the same function** as the one in eqn. 6. In the time-varying eqns. 15, 16, 18 and 20, the plate height is also a function of the single variable z, but now it is defined as $H = H(z, t(z))$ (see Appendix 4). To derive $H(z, t(z))$, the function $t = t(z)$ (see comments to eqn. 3) must be known. To find $t = t(z)$, notice that $\tilde{u} = u(z, t)$ for all eqns. 15, 16, 18 and 20 (see Appendix 4). Therefore, eqn. 7 becomes

$$\frac{dz}{dt} = u(z, t) \tag{29}$$

where the function $u(x, s)$ is known from eqn. 6. The function $t = t(z)$ can be found by solving eqn. 29 for $z = z(t)$ and inverting the latter relation to get $t = t(z)$, or by solving equation

$$\frac{dt}{dz} = \frac{1}{u(z, t)} \tag{30}$$

directly for $t = t(z)$. These manipulations are not as trivial (see Appendix 7) as the substitution $x = z$ which is valid only for the time-invariant media.

Comparison of new and previously known results

It is important that the previously known special cases follow from the broader theory. If that does not occur, the sources of the inconsistency must be identified.

Notice that eqn. 10 developed here for an arbitrary medium has its narrower precedent in the theory developed before [2] for the time-invariant medium. It has also been shown above that the new and broader relations such as eqns. 16, 18 and 28 converge to the previously known [2] eqn. 25 while eqn. 24 converges to the previously known [2] eqn. 26 when the appropriate conditions [2] are reproduced.

Eqn. 26 was also previously known [35–38] in its approximate form

$$\tau_i^2 = \frac{H_i z_i}{u_i^2} \tag{31}$$

where H_i and u_i were, respectively, the plate height and solute velocity in a short column segment z_i, and τ_i^2 was the contribution of that segment to the total τ^2. The latter was calculated as

$$\tau^2 = \sum \tau_i^2 = \sum \frac{H_i z_i}{u_i^2} \tag{32}$$

Previously [35–38], eqn. 32 was viewed as the **self-evident** rule of addition of the small contributions, τ_i^2, to the total τ^2 in **any** time-invariant medium. The theory developed in the previous section provides an example of a time-invariant medium where the rule is **not valid**. Indeed, eqns. 31 and 32 are approximations of eqns. 26 and 27. As eqn. 24 indicates, eqns. 26 and 27 are not valid when $dH/dz \neq 0$. Invalid as well become their respective approximations eqns. 31 and 32. Discovery of the unknown limitations of the currently accepted techniques is one of the important results of the theory.

As the discussion in ref. 2 indicates, previous theories can justify eqns. 31 and 32 for the time-invariant medium which has *nearly constant*

solute velocity and plate height within the zone. The discussion in the previous paragraph, on the other hand, justifies eqns. 31 and 32 for the much broader class of the time-invariant medium, the one where the solute velocity *does not have to be nearly constant* within the zone. In other words, the theory developed in the previous section, not only reveals the limitations of the previously accepted techniques but also provides the less restrictive justifications for such techniques than the previous theories do.

For the time-invariant smooth media, all eqns. 25–27, 31 and 32 are valid. However, eqns. 31 and 32 still remain approximations of the exact and mathematically more manageable eqns. 26 and 27 which were deduced from eqn. 25. Therefore, eqn. 25 seems to be a better alternative as a starting point in the analysis of chromatography in a smooth, time-invariant medium. Eqn. 25 itself is a special case of eqn. 18 which describes the variance of the zone in *any* (not necessarily time-invariant) *smooth medium* and provides the most consistent starting point for the analysis of such medium[a]. The use of the smooth model, C6, and eqn. 18 for the analysis of many practical cases of a non-uniform chromatography can be justified by the following.

In many cases of a non-uniform chromatography [13–25, 37–40] the local plate height, H, is a much weaker function of a distance than the local solute velocity, u, is. Also, typically, in chromatography with a reasonably high efficiency (more than a hundred of plates), the largest portion of the migration of the zones from the inlet to the outlet takes place under the conditions where the widths of the zones are much narrower than the column length. As a result, typically, H and the gradient of u do not change significantly within the zone[b]. Finally, eqn. 18 is the simplest among the equations describing the time-varying non-uniform medium. (Eqn. 15 is more complicated, eqns. 16 and 28 require zonal parameters $\tilde{H}$ and $\tilde{u}$ instead of local H and u, other special cases deal only with the time-invariant medium.)

Local plate height

The concept of the plate height is one of the key concepts in chromatography. Previously known definitions of the local plate height [11,27,29,35] in a non-uniform chromatography have internal inconsistencies [11]. A new definition, free from the known inconsistencies is constructed below.

Notice, that in eqn. 5, the local plate height, H, was introduced via the local effective diffusivity, D_{eff}, and the local solute velocity. Eqn. 5 for the time-invariant uniform [27] and non-uniform [2] medium was known before.

Typically, in chromatography, H is a better known quantity than D_{eff}. A direct definition of H which does not require a knowledge of D_{eff} can be (see Appendix 8 and ref. 2):

$$H = \lim_{\sigma^2 \to 0} \frac{d\sigma^2}{dz} \tag{33}$$

CONCLUSIONS

The plate height and the solute velocity based model of a chromatographic medium has been proposed. Eqn. 10 describing evolution of the variance of the zone in any linear medium (possibly time-varying and/or non-uniform), and many special cases of that equation have been derived. When the medium is smooth (local plate height and gradient of the solute velocity are nearly coordinate-independent within the zone), the evolution of the variance of the zone is governed by the newly derived ordinary linear differential equation, eqn. 18, which can be used as the simplified model for the majority of the known non-uniform time-varying separation techniques.

Among other important results, it has been

[a] Previously [26], eqn. 18 was introduced without the derivation.

[b] This may not be true in the vicinity of joints of columns with inlets, detectors, retention gaps, *etc.* where significant upsets of velocity of solutes and/or plate height can occur *within* the zone. The non-uniformity can also be severe in case of the thick-film GC with the vacuum outlet [41]. Analysis of the extremes of the non-uniformity is also within the scope of this theory, eqn. 10. However, it is beyond the scope of this paper.

shown that the previously accepted rule of calculation of the temporal variance of the zone in an arbitrary non-uniform time-invariant medium, eqn. 32, is valid only if the medium is smooth. Also a definition, eqn. 33, of the local plate height free from the previously known inconsistencies has been constructed.

ACKNOWLEDGEMENT

The author is grateful to J. Calvin Giddings for the fruitful and encouraging discussion of the non-uniform time-varying chromatography.

APPENDIX

1. An example of the zone with unbounded variance

A zone which at a certain time, t, has specific mass

$$m = m(x,t) = \begin{cases} m_0, & |x| \leq 1 \\ m_0|x|^{-3}, & |x| > 1 \end{cases}$$

where m_0 is a constant, has bounded zeroth moment (the *total amount* of solute), M, and bounded first moment (the *center of mass* of the zone), z. Its half-height width, w, is also bounded, but its second central moment (the *variance* of the zone), σ^2, is infinite. Indeed,

$$M = \int_{-\infty}^{\infty} m\,dx = 3m_0\,, \quad z = \frac{1}{M}\int_{-\infty}^{\infty} xm\,dx = 0\,,$$

$$w = 2(1+\sqrt[3]{2}) \approx 4.52\,,$$

$$\sigma^2 = \frac{1}{M}\int_{-\infty}^{\infty}(x-z)^2 m\,dx = \frac{2}{3}\left(1+\int_1^{\infty} x^{-1}\,dx\right) = \infty$$

2. Derivation of the velocity of the zone

Due to eqn. 3 and the constancy of M one has

$$\tilde{u} = \frac{dz}{dt} = \left(\frac{1}{M}\cdot\frac{d}{ds}\int_{-\infty}^{\infty} xm\,dx\right)_{s=t}$$

$$= \left(\frac{1}{M}\int_{-\infty}^{\infty} x\frac{\partial m}{\partial s}\,dx\right)_{s=t}$$

The integral in the right-hand side of this expression can be replaced [2] with $\int_{-\infty}^{\infty} um\,dx$ yielding eqn. 8.

3. Derivation of $d\sigma^2/dz$

Due to the definition eqn. 9, one has:

$$\frac{d\sigma^2}{dt} = \frac{1}{M}\cdot\frac{d}{dt}\int_{-\infty}^{\infty}(x-z)^2 m\,dx$$

$$= \left(\frac{1}{M}\int_{-\infty}^{\infty}(x-z)^2\frac{\partial m}{\partial s}\,dx\right)_{s=t}$$

$$-\frac{1}{M}\int_{-\infty}^{\infty} 2(x-z)\frac{dz}{dt}\,m\,dx$$

In the second integral in the right-hand side of the last expression, the velocity, $\tilde{u} = dz/dt$, of the zone is not a function of x, and can be moved outside of the integral. The integral then vanishes due to the eqn. 4. The entire expression becomes

$$\frac{d\sigma^2}{dt} = \left(\frac{1}{M}\int_{-\infty}^{\infty}(x-z)^2\frac{\partial m}{\partial s}\,ds\right)_{s=t}$$

The integral in the right-hand side of this expression can be replaced [2] with

$$\int_{-\infty}^{\infty} Hum\,dx + 2\int_{-\infty}^{\infty}(x-z)u\,dx$$

which yields

$$\frac{d\sigma^2}{dt} = \frac{1}{M}\left(\int_{-\infty}^{\infty} Hum\,dx + 2\int_{-\infty}^{\infty}(x-z)um\,dx\right)_{s=t}$$

Due to eqn. 7, one has $d\sigma^2/dz = \tilde{u}^{-1}\cdot(d\sigma^2/dt)$ which, due to the previous expression, can be re-written as eqn. 10.

4. Derivation of $d\sigma^2/dz$ *for the moderate medium*

Under the condition C4, eqn. 8 becomes

$$\tilde{u} = \frac{u(z,t(z))}{M}\int_{-\infty}^{\infty} m\,dx$$

$$+\frac{g_u(z,t(z))}{M}\int_{-\infty}^{\infty}(x-z)m\,dx = u(z,t(z))$$

The second integral in that expression vanished due to the eqn. 4. The result indicates that the zone velocity becomes the same as the local velocity of the center of mass of the zone. That and condition C4 imply that eqn. 10 can be rewritten as

$$\frac{d\sigma^2}{dz} = \frac{1}{uM}\left(\int_{-\infty}^{\infty}(H+(x-z)\cdot g_H)\right.$$

$$\left.\cdot(u+(x-z)g_u)m\,dx\right.$$

$$+2\int_{-\infty}^{\infty}(x-z)(u+(x-z)g_u)m\,dx\Big)_{s=t(z)}$$

where

$$H=H(z,t(z)),\quad u=u(z,t(z)),$$

$$g_H=g_H(z,t(z))=\left.\frac{\partial H(x,t(z))}{\partial x}\right|_{x=z},$$

$$g_u=g_u(z,t(z))=\left.\frac{\partial u(x,t(z)}{\partial x}\right|_{x=z}$$

All these quantities are not functions of x. Taking that into account along with the eqn. 4, one finally has:

$$\frac{d\sigma^2}{dz}=H+\frac{1}{uM}\left(g_Hg_u\int_{-\infty}^{\infty}(x-z)^2m\,dx+2g_u\int_{-\infty}^{\infty}(x-z)^2m\,dx\right)_{s=t(z)}=H+\frac{\sigma^2}{u}g_u(2+g_H)$$

If this entire derivation was applied only to the integral term in the right-hand side of eqn. 10, the result would be eqn. 16.

5. Derivation of $d\tau^2/dz$ *for the time-invariant moderate medium*

From eqn. 23, one has

$$\frac{d\tau^2}{dz}=\frac{d}{dz}\left(\frac{\sigma^2}{u^2}\right)=\frac{1}{u^2}\left(\frac{d\sigma^2}{dz}-\frac{2\sigma^2}{u}\cdot\frac{du}{dz}\right)$$

After the replacement of $d\sigma^2/dz$ in the right-hand side of this expression with eqn. 22 one has:

$$\frac{d\tau^2}{dz}=\frac{1}{u^2}\left[H+\frac{2\sigma^2}{u}\cdot\frac{du}{dz}\left(1+\frac{1}{2}\cdot\frac{dH}{dz}\right)-\frac{2\sigma^2}{u}\cdot\frac{du}{dz}\right]=\frac{1}{u^2}\left(H+\frac{\sigma^2}{u}\cdot\frac{du}{dz}\cdot\frac{dH}{dz}\right)=\frac{H}{u^2}+\frac{\tau^2}{u}\cdot\frac{du}{dz}\cdot\frac{dH}{dz}$$

6. Derivation of $d\sigma^2/dz$ *for a Gaussian zone*

For a Gaussian zone, condition C10, $\partial m/\partial x=-[(x-z)/\sigma^2]m$. That allows to rewrite the second integral in the right-hand side of eqn. 10 as

$$\int_{-\infty}^{\infty}(x-z)um\,dx=-\sigma^2\int_{-\infty}^{\infty}u\,dm=\sigma^2\left(-(um)\Big|_{-\infty}^{\infty}+\int_{-\infty}^{\infty}\frac{\partial u}{\partial x}m\,dx\right)$$

Due to the combination of conditions C2 and C3 which force $u(\infty,\ s)\cdot m(\infty,\ s)\cdot m(-\infty,\ s)=0$ for any s, the term $-(um)\Big|_{-\infty}^{\infty}$ vanishes yielding

$$\int_{-\infty}^{\infty}(x-z)um\,dx=\sigma^2\int_{-\infty}^{\infty}\frac{\partial u}{\partial x}m\,dx$$

That along with the notations eqn. 12 allows to rewrite eqn. 10 as eqn. 28.

7. Example derivation of $z(t)$

A focusing by the constant negative gradient of a magnitude g_o which travels along the column with the constant speed [16,26] can be provided by the velocity function $u=u(x,\ s)=u_o+as-g_ox$ where initial velocity, u_o, and local acceleration, a, are constants. Eqn. 29 becomes $dz/dt=u_o+at-g_oz$. Its solution for $z(0)$ is

$$z=\frac{u_og_o}{g_o^2}(1-e^{-g_ot})+\frac{at}{g_o}$$

Inversion of this expression is not simple. However, in the special case, the expression can be significantly simplified. Notice that regardless of the initial velocity, u_o, the zone asymptotically approaches velocity $u_c=a/g_o$. If $u_o=u_c$, the previous expression for z becomes $z=u_ct$, *i.e.* the zone migrates with the constant velocity u_c. Assumption $u_o=u_c$ also simplifies eqn. 18. After the substitution $u=u_c=a/g_o$ and $g_u=-g_o$, eqn. 18 becomes $d\sigma^2/dz=H-2\sigma^2g_o^2/a$ where both g_o and a are constants.

8. Definition of the local plate height

A non-uniform medium can be nearly uniform within a small segment of its length. Indeed, other than at the points of discontinuity of the properties of the medium, there always exist such a short segment, Δx, in the path of the zone that the medium is nearly uniform within Δx. If the largest fraction of the zone is located within Δx then the migration of the zone in the vicinity of Δx is almost unaffected by the non-uniformity of the medium. The latter conditions are met when $\sigma^2\to 0$. Further, as m is not negative, it

follows from the eqn. 9 that for a non-zero amount of the solute in the zone, $\sigma^2 \rightarrow 0$ implies $m(x, t(z)) \rightarrow M\delta(x - z)$ where $\delta(x - z)$ is a Dirac's delta-function. Substitution of the last implication in eqns. 8 and 10 yields $\tilde{u} = u$ and $d\sigma^2/dz = H$ indicating that H can be measured as prescribed by eqn. 33.

SYMBOLS

D_{eff} local effective diffusivity in the medium (length^2/time)
g_H local gradient of plate height
g_u local gradient of velocity of the solute (time^{-1})
$\tilde{g}_u$ average gradient of velocity in the zone (time^{-1})
H local plate height in the medium (length)
$\tilde{H}$ plate height for the entire zone (length)
M total mass of the solute in the zone (mass)
m specific mass of a solute (mass/length)
s time coordinate (time)
t migration time of the zone (time)
u local velocity of a solute (length/time)
$\tilde{u}$ velocity of the zone (length/time)
x distance coordinate (length)
z coordinate of the center of mass of the zone (length)
σ^2 spatial variance of the zone (length^2)
τ^2 temporal variance of the zone (time^2)

REFERENCES

1 J.C. Giddings, *Unified Separation Science*, Wiley, New York, 1991.
2 L.M. Blumberg and T.A. Berger, *J. Chromatogr.*, 596 (1992) 1–13.
3 J.C. Giddings, *J. Chromatogr.*, 4 (1960) 11–20.
4 H.W. Habgood and W.E. Harris, *Anal. Chem.*, 32 (1960) 450–453.
5 H.W. Habgood and W.E. Harris, *Anal. Chem.*, 32 (1960) 1206.
6 G.H. Stewart, *Anal. Chem.*, 32 (1960) 1205.
7 J.C. Giddings, in N. Brenner, J.E. Callen and M.D. Weiss (Editors), *Gas Chromatography*, Academic Press, New York, London, 1962, pp. 57–77.
8 M.J.E. Golay, L.S. Ettre and S.D. Norem, in M. van Swaay (Editor), *Gas Chromatography*, Butterworth, London, 1962, pp. 139–151.
9 W.E. Harris and H.W. Habgood, *Programmed Temperature Gas Chromatography*, Wiley, New York, 1966.
10 E.E. Akporhonov, S. Le Vent and D.R. Taylor, *J. Chromatogr.*, 405 (1987) 67–76.
11 J. Yi. Zhang, G.M. Wang and R. Qian, *J. Chromatogr.*, 521 (1990) 71–87.
12 L.H. Wright and J.F. Walling, *J. Chromatogr.*, 540 (1991) 311–322.
13 M. Novotny, W. Bertsch and A. Zlatkis, *J. Chromatogr.*, 61 (1971) 17–28.
14 M.Z. El Fallah and G. Guiochon, *Anal. Chem.*, 63 (1991) 859–867.
15 A.A. Zhukhovitskii, O.V. Zolotareva, V.A. Sokolov and N.M. Turkel'taub, *Dokl. Akad. Nauk SSSR*, 77 (1952) 435.
16 R.W. Ohline and D.D. DeFord, *Anal. Chem.*, 35 (1963) 227–234.
17 W.A. Rubey, *J. High Resolut. Chromatogr.*, 14 (1991) 542–548.
18 W.A. Rubey, in P. Sandra (Editor), *14th International Symposium on Capillary Chromatography, Baltimore, MD, May 25–29, 1992*, Foundation for the ISCC, 1992, pp. 40–45.
19 E. Fuggerth, *Anal. Chem.*, 61 (1989) 1478–1585.
20 L.R. Snyder and D.L. Saunders, *J. Chromatogr. Sci.*, 7 (1969) 195–208.
21 L. R. Snyder, J. W. Dolan and J. R. Gant, *J. Chromatogr.*, 165 (1979) 3–30.
22 H. Poppe, J. Paanakker and M. Bronckhorst, *J. Chromatogr.*, 204 (1981) 77–84.
23 A. Wilsch and G. Schneider, *J. Chromatogr.* 357 (1986) 239–252.
24 G. Schomburg and W. Roeder, *J. High Resolut. Chromatogr.*, 12 (1989) 218–225.
25 F. Van Puyvelde and E.H. Chimovitz, *J. Supercrit. Fluids*, 3 (1990) 127–135.
26 L.M. Blumberg, *Anal. Chem.*, 64, (1992) 2459–2460.
27 J.C. Giddings, *Dynamics of Chromatography, Part I, Principles and Theory*, Marcel Dekker, New York, 1965.
28 M.J.E. Golay, in D.H. Desty (Editor) *Gas Chromatography*, Butterworth, London, 1958, pp. 36–55.
29 J.C. Giddings, *J. Gas Chromatogr.*, 2 (1964) 167–169.
30 E. Kucera, *J. Chromatogr.*, 19 (1965) 237–246.
31 O. Grubner, *Adv. Chromatogr.*, 6 (1968) 173–209.
32 E. Grushka, *J. Phys. Chem.*, 76 (1972) 2586–2593.
33 J.Å. Jönsson, in J.Å. Jönsson (Editor), *Chromatographic Theory and Basic Principles*, Marcel Dekker, New York and Basel, 1957, pp. 27–102.
34 P.J. Karol, *J. Chromatogr.*, 445 (1988) 207–210.
35 J.C. Giddings, *Anal. Chem.*, 35 (1963) 353–356.
36 D.P. Poe, D.E. Martire, *J. Chromatogr.*, 517 (1990) 3–29.
37 H.-G. Janssen, H.M.J. Snijders, J.A. Rijks, C.A. Cramers and P.J. Schoenmakers, *J. High Resolut. Chromatogr.*, 14 (1991) 438–445.
38 J.G.M. Janssen, *Dissertation*, Technical University of Eindhoven, Eindhoven, 1991.
39 J.H. Stewart, S.L. Seager and J.C. Giddings, *Anal. Chem.*, 31 (1959) 1738.
40 J.C. Giddings, S.L. Seager, L.R. Stucki and G.H. Stewart, *Anal. Chem.*, 32 (1960) 867–870.
41 C.A. Cramers and P.A. Leclercq, *CRC Critical Reviews in Analytical Chemistry*, 20–2 (1988) 117–147.

Journal of Chromatography, 637 (1993) 129–135
Elsevier Science Publishers B.V., Amsterdam

CHROM. 24 891

Design of a differential pressure detector for use in the size-exclusion chromatography of polymers

Sadao Mori

Department of Industrial Chemistry, Faculty of Engineering, Mie University, Tsu, Mie 514 (Japan)

(First received November 10th, 1992; revised manuscript received January 19th, 1993)

ABSTRACT

A differential pressure (DP) detector (a differential capillary viscometer) with four capillaries and two differential pressure transducers was constructed and its performance was evaluated. The effluent containing polymer fractions passed through one capillary while the mobile phase flowed through the other capillary, and the differential pressure between the two inlets of the capillaries was measured with a differential pressure transducer. The other two capillaries were used for the compensation of the flow fluctuation during the elution of a polymer fraction. The small increase in the pressure drop across a capillary (*i.e.*, less than 1%) for a polymer fraction was measured precisely and accurately. The delay of the response of the DP detector was observed and the size of the response delay was estimated by comparing the measured DP chromatogram with the calculated DP chromatogram. For the point-by-point calculation, the correction of the response delay for the DP chromatogram was applied and the calculated average molecular masses (M_r) were comparable to the reference data. The shear degradation of polystyrenes having $M_r > 10^6$ during passing through the size-exclusion chromatographic columns was observed.

INTRODUCTION

Several types of capillary viscometers which measure the pressure drop across a capillary or the differential pressure across two capillaries are now commercially available [1–4], in addition to laboratory-made instruments [5–7]. These viscometers are used exclusively as a molecular-mass-sensitive detector together with a concentration detector such as a refractive index (RI) detector for size-exclusion chromatography (SEC). When a polymer solution flows through a capillary, the pressure drop across the capillary is proportional to the viscosity of the polymer solution, and the intrinsic viscosity of the polymer can be calculated by knowing the pressure drop across the capillary and the sample concentration of the polymer solution. Therefore, the use of the capillary viscometer in combination with an RI detector as SEC detectors can make possible the determination of the molecular mass (M_r) of an unknown polymer by knowing the hydrodynamic volume of polymer standards by multipling the intrinsic viscosity by the molecular mass of the polymer standards.

The laboratory-made capillary viscometers reported in the literature contained one capillary and the pressure drop across a capillary was detected with two pressure transducers [6] or one differential pressure transducer [7]. However, the increase in viscosity of the sample solution eluted from SEC columns was less than 1% of the viscosity of the mobile phase, and therefore, in these laboratory-made viscometers with one capillary, the increase in the output signal of the pressure transducer for the sample solution had to be amplified, resulting in a noisy signal. Smoothing procedures were required to obtain a smoothed differential pressure signal in these viscometers [8,9].

Commercially available viscosity detectors utilize one to four capillaries, namely, single-capillary design [3], two-capillary design [4] and four-capillary bridge design [1,2]. The two-capillary

0021-9673/93/$06.00

design developed by Yau [4] utilizes two sets of capillary tubing and pressure transducer assemblies connected in series. The analytical capillary–transducer system is connected ahead of the reference capillary–transducer system and a 5–10-ml delay volume is added between them. The increase in the viscosity of the sample solution is measured by the pressure drop across the analytical capillary and the viscosity of the mobile phase by the pressure drop across the reference capillary. The two signals of the pressure drop are fed into a differential logarithmic amplifier to give a direct readout of the natural logarithmic value of the relative viscosity of the sample solution. Haney's four-capillary bridge design [1,2] measures the differential pressure across two capillaries, one for the sample solution and the other for the mobile phase, and can monitor the differential pressure directly on a strip-chart recorder.

The laboratory-made assembly is attractive owing to its relative simplicity in design, ease of data reduction and low cost compared with the commercial viscometers. In this paper, a new design with four capillaries is described. It measures the differential pressure across two capillaries, one for a sample solution and the other for the mobile phase, directly without any computational treatments. The system is simple and easy to construct in any laboratory.

EXPERIMENTAL

Differential pressure detection system

A schematic flow sheet and the assemblies of the differential pressure (DP) detection system for SEC are shown in Fig. 1. The system was composed of four capillaries, two differential pressure transducers, a delay reservoir and two SEC columns. Two of the capillaries (Nos. 1 and 3) were used for the adjustment of flow resistance on the sample and reference sides of the system, respectively. The capillaries were 1 m × 0.13 mm I.D. stainless-steel tubes. The pressure ranges of the two differential pressure transducers (Model M-7D; Tsukasa-Sokken, Tokyo, Japan) were between 0 and 507 kPa for DP0 and between 0 and 10.1 kPa for DP1. The transducers were activated by amplifiers and generated a

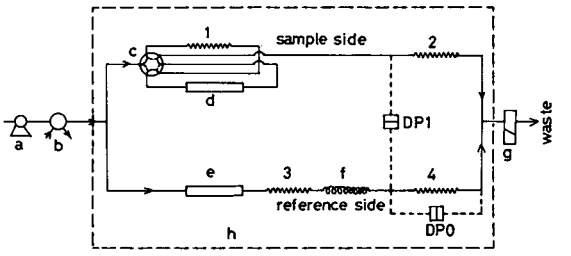

Fig. 1. Schematic flow diagram of a differential pressure detection system for SEC. a = Pump; b = sample loop injector; c = six-port valve; d = SEC column on the sample side; e = SEC column on the reference side; f = delay reservoir; g = RI detector; h = air oven; 1–4 = capillaries; DP0, DP1 = differential pressure transducers.

0–10-V output signal. These assemblies were housed in an air oven to keep them at a constant temperature.

As the mobile phase was delivered with one pump to both the sample and the reference sides at identical flow-rates, the flow resistance between the outlet of the sample loop injector and the inlet of the RI detector in Fig. 1 on both sides was adjusted to the same value by changing the length of capillary No. 1. A sample solution was injected with the sample loop injector b and was divided into two equal portions on both sides. When the sample solution was injected, the six-port valve c was on the broken-line position and the sample solution flowed into the SEC column d without passing through capillary No. 1. When the whole sample solution was introduced into the SEC column, the valve was changed to the full-line position.

The delay reservoir f was a 13 m × 1 mm I.D. stainless-steel tube with a capacity of 10 ml. This volume was approximately the same as the volume of the mobile phase in the SEC column used in this experiment. A polymer sample was fractionated in SEC columns d and e and the fractions from column d on the sample side entered capillary No. 2 and capillary No. 3 from the column e on the reference side. While the polymer fractions on the sample side passed through capillary No. 2, the polymer fractions on the reference side remained in capillary No. 3 and the delay reservoir, and only the mobile phase was flowing through capillary No. 4. The pressure difference, $\Delta\Delta P$, between the pressures

at the inlets of both capillaries Nos. 2 and 4 was measured with the differential pressure transducer DP1. The pressure drop of the mobile phase, ΔP_0, across capillary No. 4 was measured with DP0. The effluents from capillaries Nos. 2 and 4 were combined and entered the RI detector.

Size-exclusion chromatography

A Model LCP-150 syringe-type pump for liquid chromatography (Japan Spectroscopic, Tokyo, Japan) was used to deliver the mobile phase. A Model SE-11 differential refractive index detector (Showa Denko, Tokyo, Japan) was used as a concentration detector. Two Shodex SEC A-80M columns (50 cm × 8 mm I.D.) packed with polystyrene (PS) gels for polymer fractionation were used, one for the sample side and the other for the reference side. These two columns were selected so as to have similar column parameters (*i.e.*, the interstitial volume and the inner volume of the gels). The columns, capillaries Nos. 1–4, the delay reservoir and the pressure transducers were housed in a Model TU-100 air-oven (Japan Spectroscopic) at 35°C.

PS samples were PS standards with narrow M_r distributions (Pressure Chemical, Pittsburgh, PA, USA) and NBS SRM 706 PS. These polymers were dissolved in tetrahydrofuran (THF) at concentrations of 0.02–0.2%, depending on their M_r and M_r distributions. The mobile phase was THF and the flow-rate was 0.5 ml/min on each side. The injection volume of the sample solutions was 0.25 ml, so that half of the volume entered each column. Poly(vinyl chloride) (PVC), poly(vinyl acetate) (PVAc), poly(methyl methacrylate) (PMMA), poly(ethyl methacrylate) (PEMA), poly(butyl methacrylate) (PBMA) and poly(isobutyl methacrylate) (PIBMA) were purchased from several sources.

Data reduction

When the pressure drop of the mobile phase across the capillary is ΔP_0, the difference between the pressure drop, ΔP, of the polymer solution and ΔP_0 is expressed as [5]

$$\Delta\Delta P = \Delta P - \Delta P_0 = \frac{8lQ}{\pi r^4}(\eta - \eta_0) \quad (1)$$

where r is the capillary radius, l the capillary length, Q the fluid flow-rate and η and η_0 the fluid viscosity of the sample solution and the mobile phase, respectively. The value of $\Delta\Delta P$ corresponds to the differential pressure between the pressures at the inlet of the sample capillary No. 2 (ΔP) and the inlet of the reference capillary No. 4 (ΔP_0) in Fig. 1 and the differential pressure is measured with the differential pressure transducer DP1. Similarly, the value of ΔP_0 is obtained with the differential pressure transducer DP0.

For very dilute polymer concentrations, such as those existing in SEC, the intrinsic viscosity $[\eta]$ of the polymer sample is defined as [8]

$$[\eta] = \lim_{C\to 0}\frac{1}{C}\cdot\frac{\eta-\eta_0}{\eta_0} = \frac{1}{C}\cdot\frac{\eta-\eta_0}{\eta_0} = \frac{1}{C}\cdot\frac{\Delta P-\Delta P_0}{\Delta P_0} = \frac{1}{C}\cdot\frac{\Delta\Delta P}{\Delta P_0} \quad (2)$$

where C is the sample concentration and is obtained from the response of the refractive index detector.

The intrinsic viscosity of a polymer fraction eluted at a retention volume i is obtained as [7]

$$[\eta]_i = \frac{1}{C_i}\cdot\frac{\Delta\Delta P_i}{\Delta P_0} \quad (3)$$

When the RI chromatogram of a sample is divided into intervals y, then C_i is calculated as

$$C_i = \frac{Wh_i}{y\sum h_i} \quad (4)$$

where W is the mass of the sample injected into the sample column and h_i is the height of the RI chromatogram at retention volume i. The influence of temperature on the fluctuation of the height of the RI chromatogram [10] can be prevented by the use of this equation. The units of y and W in this experiment were dl and g, respectively.

Similarly, the intrinsic viscosity of the whole polymer can be calculated by using the equation

$$[\eta] = \frac{y}{W \Delta P_0} \sum \Delta\Delta P_i \quad (5)$$

RESULTS AND DISCUSSION

Performance of the system

Examples of the RI and DP chromatograms of a PS standard are shown in Fig. 2. The polymer had average M_r of 411 000. This sample had a bimodal distribution; one was the main peak and the other appeared in the high-molecular-mass region as a small peak. This distribution was observed on both chromatograms.

The single-capillary design is simple and measures the pressure drop across a stainless-steel capillary: the pressure drop ΔP_0 for pure solvent and ΔP for a sample solution. The key components of the system are DP0 and capillary No. 4 in Fig. 1. When the sample elutes from an SEC column, the increase in the viscosity of the effluent is very small because of the low sample concentration. Under typical chromatographic conditions, the increase in the viscosity due to the elution of polymer fractions is less than 1% of the background viscosity (*i.e.*, the viscosity due to the mobile phase itself). When a single-capillary system is applied to measure the pressure drop across the capillary–transducer system, this small change in the overall pressure drop must be amplified about 100-fold to display the viscometer signal properly, resulting in a low signal-to-noise ratio. An example is shown in Fig. 3. Computer smoothing procedures such as a non-linear regression [7] or fast Fourier transform smoothing [11] are required in order to obtain a smoothed viscometer signal.

When two capillaries, one for the sample solution and the other for the mobile phase, are used with two differential pressure transducers, similar assemblies to that in Fig. 1 can be considered except for the sample injection valve, capillaries Nos. 1 and 3 and the delay reservior. The six-port valve in Fig. 1 is used for sample injection in this instance. A sample solution is introduced into the SEC column on the sample side only. However, when a sample polymer passed through capillary No. 2, a difference in the pressure drops across the two capillaries was generated and, as a result, the flow-rate on the reference side was apt to increase, which, in turn, decreased the response on the pressure transducer DP1. The peak response on DP1 obtained in this system was about 15% smaller than that obtained in the system shown in Fig. 1.

A polymer sample enters the RI cell after passing through capillary No. 2 in Fig. 1. The sum of the dead volume of the connecting tubing and half the volumes of capillary No. 2 and of the RI cell was about 0.06 ml. However, the measured difference in the peak tops for a polymer sample between the two detectors was 0.15 ml (see Fig. 2). Lecacheux and Lesec [11]

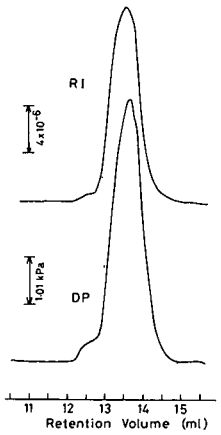

Fig. 2. RI and DP chromatograms for PS standard with M_r 411 000. Sample concentration injected, 0.11%; attenuation, RI × 4 ($\times 10^{-5}$ refractive index units full scale), DP 10 V (full scale).

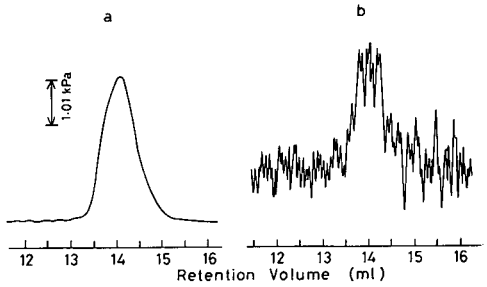

Fig. 3. DP chromatograms of PS of M_r 180 000 obtained (a) with the present system and (b) with a single-capillary design. Sample concentration injected, 0.1%; injection volume, (a) 0.25 ml and (b) 0.125 ml.

pointed out that the geometric estimate of the dead volume was not suitable and that the experimentally obtained value was greater than the geometric value. When a universal calibration graph is constructed with PS standards having narrow M_r distributions, the peak position calibration is not adequate because of not only the inaccurate estimation of the geometric dead volume but also the inconsistency of the peak tops between DP and RI chromatograms. It is easily conceivable that the polymer fraction at the peak top of a DP chromatogram does not correspond to the maximum concentration (the peak top) of the RI chromatogram, but rather has a higher M_r than that of the polymer fraction at the peak top of the RI chromatogram.

The differences between our system and the commercially available four-capillary system are as follows. The commercial system is based on a fluid analogue of a Wheatstone bridge. The polymer effluent from the SEC column enters the bridge and is divided equally into two lines: one enters the capillaries R_1 and R_3 and the other the capillaries R_2 and R_4 (after a hold-up/dilution reservoir). The effluent passed through R_1 enters R_3 and that passed through R_2 enters the hold-up/dilution reservoir. During the passage of the effluent through R_3, the mobile phase enters R_4 and the pressure difference between R_3 and R_4 is monitored. Our system, on the other hand, is not based on a Wheatstone bridge, but one capillary is attached before the SEC column on the sample side. The sample solution injected into the SEC system is divided equally into two parts and enters both the sample side and the reference side. The effluent from the SEC column on the reference side enters capillary 3 and that from the sample side enters capillary 2. The pressure difference between capillaries 2 and 4 which is occupied by the mobile phase is monitored. Our system has advantages over the commercial system: the fluctuation of the flow-rate is kept to a minimum during the measurement because the pressure drop of both sides (lines) is the same; as the pressure difference across capillaries 2 and 4 is measured as soon as the polymer effluent leaves the SEC column on the sample side, the influence of polymer degradation during passage through the capillary before entering the capillary for the measurement of the pressure drop can be neglected.

Evaluation of the measurement of PS molecular mass

The universal calibration graph constructed with PS standards is shown in Fig. 4. The molecular masses of the PS standards used for this purpose were 2100, 6200, $2.04 \cdot 10^4$, $9.72 \cdot 10^4$, $1.8 \cdot 10^5$, $4.11 \cdot 10^5$, $6.7 \cdot 10^5$, $1.8 \cdot 10^6$ and $4.48 \cdot 10^6$. Retention volumes at the peaks on the RI chromatograms were used for the calibration graph. The intrinsic viscosity of these polymers was calculated with eqn. 5.

The plot of log $[\eta]$ *versus* log M_r for the PS standards was linear in the M_r range between 10^4 and 10^6, but it was curved slightly at $M_r > 10^6$ and $<10^4$. The values of the intrinsic viscosity of PS of M_r $1.8 \cdot 10^6$ and $4.48 \cdot 10^6$ were smaller and those of PS of M_r 2100 and 6200 were higher than expected. The shear degradation during the passage of polymers with $M_r > 10^6$ through the SEC columns has been reported [12] and, therefore, the DP responses for the PS standards with $M_r > 10^6$ became smaller than expected. A molecular mass around 10^4 is known as the critical

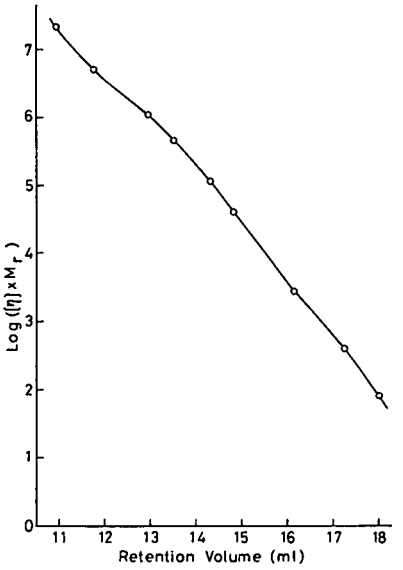

Fig. 4. Universal calibration graph of log $([\eta]M_r)$ *versus* retention volume for PS standards.

point between an oligomer and a polymer and the slope of the linear equation of log $[\eta]$ *vs.* log M_r changes at this point [13]: the slope of the equation for oligomers with $M_r < 10^4$ is smaller than that for $M_r > 10^4$. Therefore, the intrinsic viscosities of oligomers of $M_r < 10^4$ are higher than the expected values.

The RI and the DP chromatograms for NBS SRM 706 are shown in Fig. 5. The baseline of the RI chromatogram has been raised for ease of the comparison of the RI and DP chromatograms. The peak of the measured DP chromatogram [DP(a)] appeared about 0.1 ml ahead of that of the RI chromatogram.

The average molecular masses of NBS SRM 706 calculated by the conventional method using the RI chromatogram and the PS calibration graph were nearly equal to the certified values. However, average molecular masses obtained by the present method using the RI chromatogram, the DP chromatogram, the universal calibration graph in Fig. 4 and eqns. 3 and 4 are far from the NBS data certified values: $\bar{M}_n$ obtained was half the NBS value and $\bar{M}_w$ was 17% higher than the NBS value. Point-by-point calculation using the value of the dead volume of 0.06 ml was employed in this calculation.

The theoretical DP chromatogram of NBS SRM 706 can be calculated with the RI chromatogram in Fig. 5, calibration graphs of retention volume *versus* log M_r and retention volume *versus* log $([\eta]M_r)$ (Fig. 4) and eqn. 3. The result is shown in Fig. 5 [DP(b)]. The measured DP chromatogram (the experimentally obtained chromatogram) was not coincident with the calculated DP chromatogram (the theoretically obtained chromatogram). The response delay of the DP detector was observed and the difference in retention volumes at the peak positions for both DP chromatograms was about 0.175 ml. Inclusion of air in the DP chamber influenced the response delay and the peak broadening, and frequent release of the air from the DP chamber was therefore required in order to obtain reasonable results. The sampling point for the DP chromatogram was changed from $(i - 0.06)$ to $(i + 0.175)$ ml compared with the sampling point i for the RI chromatogram. This correction was effective and the average molecular masses thus calculated were comparable to the NBS certified values.

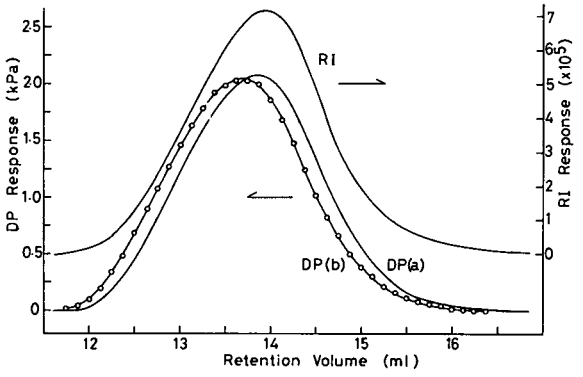

Fig. 5. RI and DP chromatograms for NBS SRM 706 PS. DP(a), measured DP chromatogram; DP(b), calculated DP chromatogram; sample concentration, 0.2%; attenuation, RI × 4, DP 10 V.

Application to polymer samples

Average molecular masses of several polymers were determined using the present system. For the point-by-point calculation, the value at a retention volume i ml for the RI chromatogram was matched against that at retention volume $(i + 0.175)$ ml for the DP chromatogram. The results are given in Table I. Good correlations between the observed values and the manufacturer's data were obtained except PMMA and PVAc.

The intrinsic viscosity of a polymer can be

TABLE I

AVERAGE MOLECULAR MASSES OF POLYMERS DETERMINED BY THE PRESENT METHOD

Polymer	Manufacturer's data		Observed	
	$M_n \times 10^{-4}$	$M_w \times 10^{-4}$	$M_n \times 10^{-4}$	$M_w \times 10^{-4}$
PVC-1	5.4	13.20	8.0	14.35
PVC-2	4.4	11.80	6.64	11.44
PVC-3	3.74	8.35	4.94	9.00
PVC-4	2.55	6.86	3.44	7.02
PVAc	8.3	33	6.7	18.9
PMMA	3.32	6.06	7.5	13.4
PEMA	14.40	39.5	18.55	36.80
PBMA	7.35	32.0	14.11	30.31
PIBMA	14.00	30.0	15.01	27.42

TABLE II

MARK–HOUWINK CONSTANTS FOR DIFFERENT POLYMERS

Polymer	Observed		Literature value		
	a	$K \times 10^4$	a	$K \times 10^4$	Ref.
PS	0.71	1.15	0.717	1.17	14
PVC	0.758	1.33	0.77	1.60	15
PVAc	0.640	2.79	0.698	1.49	16
PMMA	0.677	1.03	0.677	1.48	17
PEMA	0.712	0.783			
PBMA	0.72	0.638			
PIBMA	0.78	0.385			

calculated using an RI chromatogram, a DP chromatogram and eqn. 5. Mark–Houwink constants, a and K, can be obtained from the relationship between $[\eta]$ and M_r. The results are given in Table II.

REFERENCES

1 M.A. Haney, *J. Appl. Polym. Sci.*, 30 (1985) 3023.
2 M.A. Haney, *J. Appl. Polym. Sci.*, 30 (1985) 3037.
3 J.L. Ekmanis, in T. Havard (Editor), *International GPC Symposium, October 1989, Newton, MA, USA*, Waters Chromatography Division, Millipore Corp., Newton, MA, 1989, p. 1.
4 W.W. Yau, *Chemtracts Macromol. Chem.* 1 (1990) 1.
5 A.C. Ouano, *J. Appl. Polym. Sci., Part A-1*, 10 (1972) 2169.
6 L. Letot, J. Lesec and C. Quivoron, *J. Liq. Chromatogr.*, 3 (1980) 427.
7 F.B. Malihi, C. Kuo, M.E. Koehler, T. Provder and A.F. Kah, in T. Provder (Editor), *Size Exclusion Chromatography (ACS Symposium Series*, No. 245), American Chemical Society, Washington, DC, 1984, p. 281.
8 C.E. Lundy and R.D. Hester, *J. Liq. Chromatogr.*, 7 (1984) 1911.
9 C. Kuo, T. Provder, M.E. Koehler and A.F. Kah, in T. Provder (Editor), *Detection and Data Analysis in Size Exclusion Chomatography (ACS Symposium Series*, No. 352), American Chemical Society, Washington, DC, 1987, p. 130.
10 S. Mori, *J. Liq. Chromatogr.*, 6 (1983) 813.
11 D. Lecacheux and J. Lesec, *J. Liq. Chromatogr.*, 5 (1982) 2227.
12 P.J. Wang and B.S. Glasbrenner, *J. Liq. Chromatogr.*, 10 (1987) 3047.
13 F.L. McCrakin, *Polymer*, 28 (1987) 1847.
14 M. Kolinsky and J. Janca, *J. Polym. Sci., Polym. Chem. Ed.*, 12 (1974) 1181.
15 D. Goedhar and A. Opshoor, *J. Polym. Sci., Part A-2*, 8 (1970) 1227.
16 D. Lecacheux, J. Lesec, C. Quivoron, R. Prechner, R. Panaras and H. Benoit, *J. Appl. Polym. Sci.*, 29 (1984) 1569.
17 K.K. Chee, *J. Appl. Polym. Sci.*, 30 (1985) 1323.

Journal of Chromatography, 637 (1993) 137–143
Elsevier Science Publishers B.V., Amsterdam

CHROM. 24 985

Semi-preparative high-performance liquid chromatographic resolution of brompheniramine enantiomers using β-cyclodextrin in the mobile phase

Andrew D. Cooper[☆] and Terry M. Jefferies*

School of Pharmacy and Pharmacology, University of Bath, Claverton Down, Bath, Avon BA2 7AY (UK)

(First received December 18th, 1992; revised manuscript received February 16th, 1993)

ABSTRACT

The semi-preparative reversed-phase HPLC separation of brompheniramine enantiomers using β-cyclodextrin as a chiral mobile phase additive is described. Enantiomers were recovered free from mobile phase components on-line by a novel column switching procedure. On a 250 mm × 10 mm I.D. cyano column, a throughput of 8 mg per hour (0.65 mg per gram column packing per hour) was achieved at product optical purities of 88% and above. This was achieved using two passes through the system.

Comparison is made with other reported semi-preparative chiral separations using β-cyclodextrin, and the potential utility of the described method discussed.

INTRODUCTION

β-Cyclodextrin has found much use in recent years as a chiral resolving agent in HPLC, either as a mobile phase additive [1–3] or incorporated into stationary phases [4–6]. The cyclodextrin imparts enantioselectivity to the chromatographic system by formation of diastereomeric inclusion complexes with the analyte enantiomers [7].

The majority of reported enantiomer separations using cyclodextrins have been carried out only on an analytical scale. However, there is a need in the pharmaceutical industry for semi-preparative separation of enantiomers in order to provide milligram quantities of pure enantiomers for pharmacological investigation.

Preparative chiral separations on cyclodextrin stationary phases have been reported. Thus, β-cyclodextrin polymer gels have been used for the mg-scale resolution of racemates such as methyl mandelate [8] and indole alkaloids [9]. In these cases, low throughputs were obtained owing to the poor efficiency of these gels and the low flow-rates employed.

Vigh *et al.* [10–12] have recently shown that β-cyclodextrin-silica HPLC stationary phases may be employed to effect semi-preparative separation of isomeric compounds in displacement mode. Using two 250 × 4.6 mm I.D. Cyclobond I columns in series, up to 6 mg of various racemates were resolved in high yield and optical purity in run times of 3–6 hours [12].

Work in this laboratory has focused on the possibility of using β-cyclodextrin as a mobile phase additive for semi-preparative chiral separations in elution mode, taking advantage of the distinct selectivity obtained in this way. Hitherto, the use of mobile phase additives has largely been limited to analytical scale chiral separa-

* Corresponding author.
☆ Present address: School of Chemical Sciences, University of East Anglia, Norwich, NR4 7TJ, UK.

0021-9673/93/$06.00

tions, owing to the difficulty of separating the resolved enantiomers from the chiral additive. A novel solution to this problem has recently been presented from this laboratory, involving on-line recovery of the resolved enantiomers from the chiral eluent via column switching [13]. This was initially applied to the resolution of trimeprazine enantiomers, a racemate that is easily resolved using β-cyclodextrin (selectivity, $\alpha = 1.24$, $R_s = 2.1$ at low column loading). A throughput in excess of 1 mg per hour was obtained, using only a small column (100 mm length × 4.6 mm I.D.).

In this paper, the semi-preparative resolution of brompheniramine enantiomers by a similar procedure is presented. The separation of brompheniramine enantiomers using β-cyclodextrin-containing eluents on analytical scale has previously been described by Mularz [14], who reported selectivity, α, of only 1.13 ($R_s = 1.7$) in this case. The semi-preparative resolution of this racemate therefore provides an illustration of the application of β-cyclodextrin as an eluent additive with on-line recovery of enantiomers to racemates where only moderate selectivity is observed.

EXPERIMENTAL

Equipment and materials

The chromatograph consisted of an LDC Constametric III_G pump and LDC Spectromonitor III and Pye-Unicam LC3 UV detectors. A valve switching unit (purpose-built) was provided by ICI Research Engineering Laboratory, Alderley Park, Macclesfield, UK, and consisted of two Rheodyne 7010 valves controlled by a timer unit.

Spherisorb S5CN columns were obtained from Hichrom (Theale, Berks., UK). A Spherisorb S5C6 column was obtained from Capital HPLC (Edinburgh, UK). Lichroprep RP18 25–40 μm material was obtained from BDH (Poole, Dorset, UK). Hamilton PRP-1 12–20 μm material was donated by Hamilton (Reno, NV, USA). Recovery columns (100 × 10 mm cartridges and holders) were donated and packed by SGE (Milton Keynes, UK).

Acetonitrile (MeCN), methanol (MeOH), ethanol (EtOH) and triethylamine (TEA) (all HPLC grade), glacial acetic acid (HOAc), maleic acid (both SLR grade) and dimethylsulphoxide (Me_2SO) (AR grade) were obtained from Fisons (Loughborough, UK). β-cyclodextrin (β-CD) hydrate was donated by Wacker Chemie (Munich, Germany). Brompheniramine and pheniramine (both as racemic maleate salts) were donated by A.H. Robins (Horsham, Sussex).

Resolution of brompheniramine enantiomers

Brompheniramine enantiomers were separated on a 250 mm × 10 mm I.D. column containing 5-μm cyanopropyl-silica (Spherisorb S5CN), using a mobile phase consisting of methanol–aqueous triethylammonium acetate [0.85% TEA (v/v), acetic acid to pH 4] (5:95, v/v) containing 12 mg ml^{-1} β-cyclodextrin hydrate, at a flow-rate of 3.5 ml min^{-1}.

The instrumentation employed to effect resolution and recovery of enantiomers is shown in Fig. 1. The pump was an LDC Constametric III_G. Detector 1 was an LDC Spectromonitor III UV detector operated at 285 nm, 2.0 AUFS, and was used to monitor the separation of enantiomers. Detector 2 was a Pye-Unicam LC–UV detector operated at 290 nm, 1.28 AUFS, and

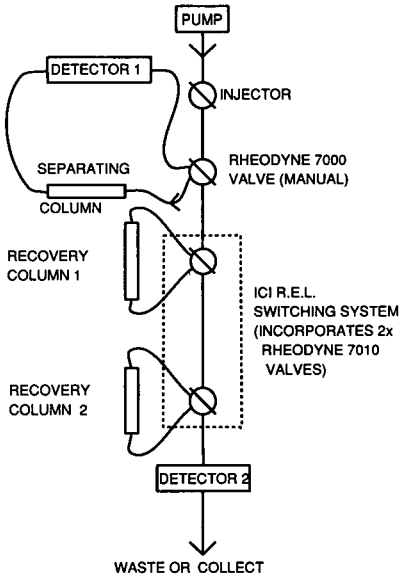

Fig. 1. Column switching system for on-line recovery of enantiomers following chiral separation.

was used to monitor the effluent from the on-line recovery system.

Injections of ±-brompheniramine maleate (5 mg) were made onto the separating column using a Rheodyne 7125 injector equipped with a 100-μl loop. Following separation, the enantiomers were switched onto two recovery columns (100 mm × 10 mm I.D.) packed with 12–20 μm polystyrene-divinylbenzene (Hamilton PRP-1) using the purpose-built valve switching system. A total of 22–24 repeat injections of racemate were made, giving a total recovery column loading of about 60 mg per enantiomer. The recovery columns were then each flushed with 180 ml of methanol–water (5:95, v/v), and the brompheniramine fractions were eluted with methanol. The separating column was by-passed during the flushing and elution stages of the procedure so as to avoid the need to re-equilibrate with mobile phase between runs.

A sample of each fraction was retained for subsequent analysis. The remainder of each fraction was evaporated to dryness, re-dissolved in mobile phase, and further purified by a second pass through the system as described above.

HPLC assay of fractions

The fractions were assayed for recovery and optical purity using a Spherisorb C6 column (150 mm × 3 mm I.D.) with a mobile phase consisting of acetonitrile–aqueous triethylammonium acetate [0.89% TEA (v/v), acetic acid to pH 4] (10:90, v/v) containing 21 mg ml^{-1} β-cyclodextrin hydrate, at a flow-rate of 1 ml min^{-1}.

Calibration standards of ±-brompheniramine maleate at 0.01, 0.05 and 0.25 mg ml^{-1} in mobile phase were prepared and injected in triplicate to produce a calibration graph for each enantiomer using peak height ratio brompheniramine : internal standard (±-pheniramine maleate).

NMR assay of fractions

The chemical purity of the fractions was assessed by comparison of their 270-MHz ^{1}H-NMR spectra in ^2H_2O with that of the unresolved standard. Recovery was also checked by NMR, by addition of one mole equivalent of maleic acid and comparison of the resulting proton signal integrals.

Optimisation of enantiomer separation

Initial optimisation was carried out on an analytical (250 mm × 4.6 mm I.D.) column packed with Spherisorb S5CN, with mobile phase flow-rate 1 ml min^{-1}.

Optimisation of recovery procedure

The recovery procedure was optimised using "off-line" experiments in which recovery columns (packed with either Lichroprep RP18 25–40 μm or Hamilton PRP-1 12–20 μm) were loaded with brompheniramine dissolved in mobile phase, and flushed with various solvents before the brompheniramine was eluted with methanol, and the recovery and optical purity assessed by NMR. In this way, the performances of the two above materials were compared, and the procedure optimised.

RESULTS

Optimisation of brompheniramine enantiomer separation

The effect of mobile phase composition on resolution of brompheniramine enantiomers at low column loading is illustrated in Table I.

It is well established that the presence of organic modifiers reduces enantioselectivity induced by β-cyclodextrin in the mobile phase [1]. Low eluent modifier levels were therefore em-

TABLE I

EFFECT OF MOBILE PHASE COMPOSITION ON RESOLUTION OF BROMPHENIRAMINE ENANTIOMERS (2 μg ON COLUMN) ON A SPHERISORB S5CN (250 × 4.6 mm I.D.) COLUMN

All eluents made up to 100% with buffer [0.8% (v/v) triethylamine, acetic acid to pH 4].

Modifier	% (v/v)	[β-CD] (mg ml^{-1})	k'_1	α	R_s
MeCN	5	16	0.9	1.14	1.0
	10	20	0.8	1.12	0.7
MeOH	3	11	1.5	1.14	0.9
	5	11	1.7	1.14	0.8
Me_2SO	5	11	1.6	1.12	1.1
		20	1.1	1.15	0.9
EtOH	5	20	0.9	1.12	0.8

ployed. It was necessary then to use a column packing of low hydrophobicity, such as cyanopropyl-silica, in order to give reasonable solute retention values. Another significant factor was cyclodextrin solubility. This was found to be reduced on addition of methanol, but enhanced by the presence of the other modifiers employed. Addition of triethylamine to the mobile phase improved peak shape but had little effect on selectivity. Selectivity was found to be maximised at pH values less than 6, with the solute molecules in cationic form.

Highest selectivity was obtained using a mobile phase containing 5% (v/v) Me_2SO and 16 mg ml^{-1} β-cyclodextrin. Highest resolution at 2 μg loading was observed with a mobile phase containing the same level of modifier but lower cyclodextrin content, due to increased retention. Differences between the resolution values obtained with the eluents investigated were generally small, as Table I shows. Highest resolution at 1 mg on column was obtained using a mobile phase containing 5% (v/v) MeOH and 11 mg ml^{-1} β-cyclodextrin. The resolution obtained using this mobile phase on a semi-preparative (10 mm I.D.) column is illustrated in Fig. 2. An amount of 5 mg was deemed to be the optimum loading on this column, on the basis of using two passes through the semi-preparative system to obtain high optical purity with minimum wastage of material.

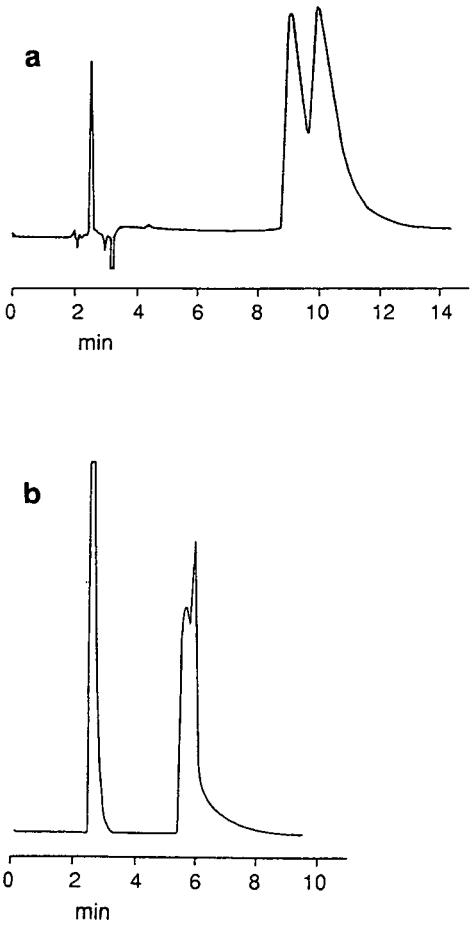

Fig. 2. Resolution of brompheniramine enantiomers on an S5CN column (250 × 10 mm I.D.). Conditions as text. (a) 10 μg ±-brompheniramine maleate on column. Detection: UV 254 nm, 0.1 AUFS; (b) 5 mg ±-brompheniramine maleate on column. Detection: UV 285 nm, 2.0 AUFS.

Optimisation of recovery procedure

The capacities of Hamilton PRP-1 and Lichroprep RP18 for brompheniramine, loaded at 1 mg ml^{-1} in the chosen eluent, were measured in off-line "breakthrough" experiments and found to be 3.8 mg per gram of packing material (PRP-1) and 2.8 mg per gram packing material (RP18). The higher capacity of the polymeric material was found to allow a much more thorough flushing step, resulting in a product free from cyclodextrin or buffer components. Hamilton PRP-1 was therefore the material used to pack the recovery columns for on-line use.

The length of the flushing step required to yield chemically pure product was found to be substantial —about 40 column volumes. However, use of a switching valve to by-pass the analytical column during flushing of the recovery columns allowed a high flow-rate to be used during flushing. This, together with the fact that a number of injections of racemate could be made before recovery column flushing, ensured that this part of the procedure made up less than 20% of the overall time involved.

Semi-preparative resolution of brompheniramine enantiomers with on-line recovery

The purity and recovery of the fractions obtained after each pass through the system are summarised in Table II. The HPLC analysis of the fractions is illustrated in Fig. 3. The more

TABLE II

OPTICAL PURITY (ENANTIOMERIC EXCESS, e.e.) AND RECOVERY OF BROMPHENIRAMINE ENANTIOMERS AFTER SEMI-PREPARATIVE RESOLUTION ON A 250 mm × 10 mm I.D. COLUMN (CONTAINING 11.8 g PACKING MATERIAL), DETERMINED BY HPLC ASSAY OF FRACTIONS

Conditions as in text.

	After 1st pass		After 2nd pass	
	Peak 1	Peak 2	Peak 1	Peak 2
Recovery (%)	68.0	72.0	49.7	35.1
e.e. (%)	82.2	75.8	95.4	88.0
Throughput (mg/h)	11.9	12.8	4.5	3.2

efficient and retentive C6 column gave near-baseline resolution of the enantiomers under analytical conditions (although was too retentive to give high throughput in semi-preparative mode).

After one pass through the system, the fractions showed enantiomeric excess values less than the 90% required for pharmacological use. The second pass resulted in a substantial improvement in optical purity.

Recoveries were 35–50% overall. No brompheniramine was detected in the eluate from the recovery columns on flushing with methanol–water. The loss of brompheniramine observed must therefore reflect the diversion of optically impure material to waste between the two collected fractions. In this respect, there is a "trade-off" between throughput, recovery and optical purity.

Fig. 4 illustrates the chemical purity of the fractions. They were found to contain up to 0.4 mol% of β-cyclodextrin, but no triethylamine or other buffer components were detected by NMR.

The optical rotations of the products as free base in dimethylformamide were determined. The first eluting peak gave a positive rotation and the second peak a negative rotation. As might be anticipated, this elution order is the reverse of that reported on a Cyclobond I column [15].

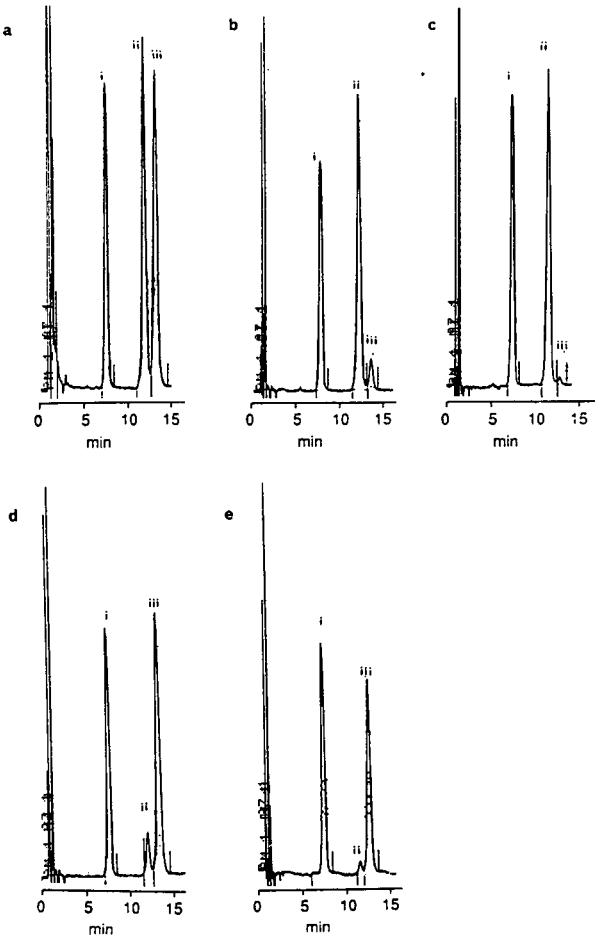

Fig. 3. Analytical resolution of brompheniramine enantiomers on S5C6 column (150 × 3 mm I.D.). Conditions as text. Peak identities: i = ±-pheniramine (I.S., 1 μg on column); ii and iii = brompheniramine enantiomers. (a) ±-Brompheniramine maleate standard, 3.5 μg on column; (b) peak 1 fraction after 1st pass; (c) peak 1 fraction after 2nd pass; (d) peak 2 fraction after 1st pass; (e) peak 2 fraction after 2nd pass.

Further confirmation of the antipodal nature of the products was provided by their NMR spectra in the presence of β-cyclodextrin. As reported by Casy and Mercer [16], the addition of β-cyclodextrin to racemic brompheniramine results in duplication of proton NMR signals. On addition of β-cyclodextrin to the resolved products, no duplication of signals was observed (resolution being too low to allow detection of the minor antipode in each fraction). On mixing

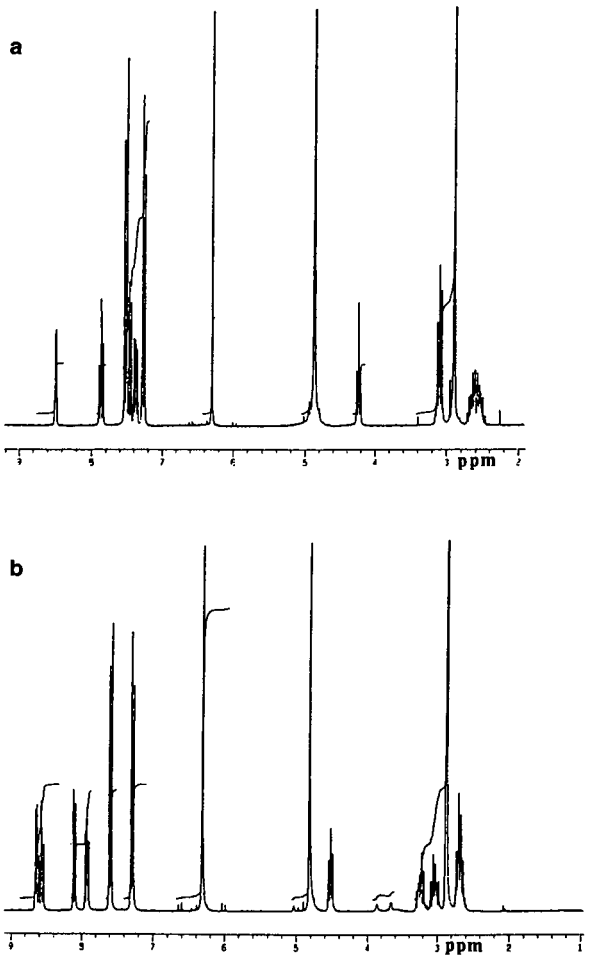

Fig. 4. 270-MHz ^{1}H-NMR spectra of brompheniramine maleate in ^2H_2O. (a) Racemate (standard). (b) HPLC peak 1 fraction after 2nd pass.

the fractions to re-form a racemate, duplication of some signals in the presence of the cyclodextrin was again observed.

DISCUSSION

Table III summarises the semi-preparative enantiomer separations carried out in this laboratory using β-cyclodextrin. It can be seen that semi-preparative product purity and throughput depend to a large extent on the selectivity obtained under analytical conditions. The work reported herein is of value in demonstrating that useful separation can be carried even when analytical selectivity is only moderate. This is particularly important, as it is rare for β-cyclodextrin to impart selectivity greater than that seen for brompheniramine. The majority of semi-preparative separations using this resolving agent are therefore likely to need the kind of approach developed here.

The throughput obtained here using β-cyclodextrin as a mobile phase additive was 0.65 mg racemate per gram column packing per hour. This is similar to the throughputs achieved by Vigh *et al.* [10–12], using a β-cyclodextrin stationary phase in displacement mode. However, the latter technique was applied to somewhat more difficult separations in elution mode than brompheniramine, and resulted in high yields of products at higher optical purities (>99%). This is not unexpected, since displace-

TABLE III

SUMMARY OF SEMI-PREPARATIVE CHIRAL SEPARATIONS CARRIED OUT USING β-CYCLODEXTRIN-CONTAINING ELUENTS

Racemate	α	e.e. (%)		Throughput [mg/(hg)]	Ref.
		Peak 1	Peak 2		
TA1	1.61	99.1	98.4	3.5	[18]
Trimeprazine	1.33	99	92	4.4	[13]
TA12	1.22	96.3	87.6	2.1	[18]
Brompheniramine	1.14	95.4	88.0	0.7	

ment mode is widely reported to be more efficient than elution mode for preparative scale separations [17].

However, the use of β-cyclodextrin as a mobile phase additive in elution mode may still be advantageous. Optimisation of semi-preparative separation in elution mode is more facile, since it is based closely on an analytical-scale separation. Use of β-cyclodextrin as an eluent additive allows more flexibility in optimisation than when a Cyclobond stationary phase is used, since column type and cyclodextrin type may be varied with ease. Furthermore, this technique will be particularly applicable to solutes where better inherent enantioselectivity is obtained using β-cyclodextrin as an eluent additive. Differences in this respect result from the modification of the cyclodextrin on bonding to the silica support to form a stationary phase.

The on-line recovery technique applied here overcomes the most obvious disadvantage of the use of chiral mobile phase additives, *i.e.* the potential difficulty in separating the resolved enantiomers from the additive. The approach used also produced products free from other buffer components. This is of particular importance in resolution of pharmaceutical racemates, which are often basic compounds requiring the addition of mobile phase components such as triethylamine to achieve efficient chromatography.

ACKNOWLEDGEMENTS

This work was supported jointly by the UK Science and Engineering Research Council and I.C.I. Pharmaceuticals through the C.A.S.E. scheme.

The provision of equipment and materials by Hamilton (Reno, NV, USA) and by Scientific Glass Engineering (Milton Keynes, UK) is gratefully acknowledged.

REFERENCES

1 D. Sybilska, *Ordered Media in Chemical Separations* (*ACS Symposium Series*, No. 326), American Chemical Society, Washington, DC, 1987 p. 218.
2 M. Gazdag, G. Szepesi and L. Huszár, *J. Chromatogr.*, 351 (1986) 128.
3 D.W. Armstrong, L.A. Spino, S.M. Han, J.I. Seeman and H.V. Secor, *J. Chromatogr.*, 411 (1987) 490.
4 K.G. Feitsma, J. Bosman, B.F.H. Drenth and R.A. de Zeeuw, *J. High Resolut. Chromatogr. Chromatogr. Commun.*, 7 (1984) 147.
5 T.J. Ward and D.W. Armstrong, *J. Liq. Chromatogr.*, 9 (1986) 407.
6 S.M. Han, Y.I. Han and D.W. Armstrong, *J. Chromatogr.*, 441 (1988) 376.
7. A. Cooper and D.D. MacNicol, *J. Chem. Soc. Perk. Trans. II*, (1978) 760.
8 A. Harada, M. Furue and S. Nozakura, *J. Polym. Sci: Polym. Chem. Ed.*, 16 (1978) 189.
9 B. Zsadon, L. Décsei, M. Szilasi, F. Tüdôs and J. Szejtli, *J. Chromatogr.*, 270 (1983) 127.
10 G. Vigh, G. Quintero and G. Farkas, *J. Chromatogr.*, 484 (1989) 237.
11 G. Vigh, G. Quintero and G. Farkas, *J. Chromatogr.*, 484 (1989) 251.
12 G. Vigh, G. Quintero and G. Farkas, *J. Chromatogr.*, 506 (1990) 481.
13 A.D. Cooper and T.M. Jefferies, *J. Pharm. Biomed. Anal.*, 8 (1990) 847.
14 E.A. Mularz, *Ph.D. Dissertation*, Seton Hall University, NJ, 1988.
15 A.D. Mercer, *Ph.D. Dissertation*, University of Bath, Bath, 1989.
16 A.F. Casy and A.D. Mercer, *Mag. Reson. Chem.*, 26 (1988) 765–774.
17 Cs. Horváth, in F. Bruner (Editor), *The Science of Chromatography* (*Journal of Chromatography Library*, Vol. 32), Elsevier, Amsterdam, 1985, pp. 179–205.
18 A.D. Cooper, *Ph.D. Dissertation*, University of Bath, Bath, 1991.

Journal of Chromatography, 673 (1993) 145–156
Elsevier Science Publishers B.V., Amsterdam

CHROM. 24 905

Rapid separation of non-ionic surfactants of polyethoxylated octylphenol and determination of ethylene oxide oligomer distribution by C1 column reversed-phase liquid chromatography

Zhendi Wang* and Merv Fingas

Emergencies Science Division, River Road Environmental Technology Centre, Environment Canada, 3439 River Road, Ottawa, K1A 0H3 (Canada)

(First received October 28th, 1992; revised manuscript received January 25th, 1993)

ABSTRACT

A rapid, simple and reproducible reversed-phase high-performance liquid chromatographic (HPLC) method was developed for the separation and characterization of individual oligomers in polyethoxylated octylphenol (PEOP) surfactants with high resolution and sensitivity, using a C1 trimethylsilyl (TMS) column. With this technique, oligomers of PEOP surfactants containing up to 40 ethylene oxide units (molecular mass distributions up to *ca.* 2000) were successfully resolved and identified. The oligomer distribution of the eight PEOP surfactants studied were calculated and depicted graphically. The effects of the mobile phase composition and of the solvents used to prepare PEOP surfactant solutions on the separation of oligomers were investigated in detail.

INTRODUCTION

Polyethoxylate alkylphenols (PEAP) are widely used as non-ionic surfactants in liquid laundry detergents, wetting agents and emulsifiers and in institutional and industrial cleaners [1,2]. They are manufactured by the addition of ethylene oxide (EO) to alkylphenols. The highly branched 4-octyl- and 4-nonylphenols are often the main raw materials used to manufacture polyethoxylated alkylphenols. The distribution of oligomers with varying lengths of the polyethoxy chain is determined mainly by the relative rates of ethoxylation of the ethylene oxide to alkylphenol in the initiation and propagation steps. As a result of their method of synthesis, these surfactants are complex mixtures in which the oligomer index (the number of EO units in each individual oligomer) varies over a considerable range.

Ethoxylated surfactants provide the blender with more versatility than their ionic counterparts. In the latter, the solubilizing power of the sulphate and sulphonate group is fixed, and it is the hydrophobic moiety which must be modified to produce differing hydrophilic–lipophilic balance (HLB) values. The hydrophilic characteristic of the ethoxylate, however, is attributed to the hydration of the ether-link oxygen atoms in the chain via hydrogen bonding, and therefore increases with increasing number of EO units. The distribution of oligomers can affect the chemical and end-use properties of these surfactants. Hence its reliable determination is important for both performance and quality control considerations. Environmental concern is another important reason to know both the

* Corresponding author.

0021-9673/93/$06.00

concentration of surfactants in water and oligomer distribution. Surfactants can have high abundance in wastewater. It has been suggested that the toxicities increase with decreasing length of the polyethoxylate chains [3].

The separation and identification of such complex samples is not trivial, and much research has been carried out in this area. Some classical and non-specific methods including metal ion complexation of the polyethoxylate chain, potentiometric titration and fission techniques [4] have been used to measure the total contents of non-ionic surfactants. These methods fail, however, to differentiate between PEAP and linear alcohol polyethoxylates, which are also widely used as non-ionic surfactants. In addition, they cannot give any information about oligomer distributions and are time consuming to perform.

Various other methods using gas chromatography (GC) or gas chromatography–mass spectrometry (GC–MS) with chemical ionization have been carried out in order to identify oligomers of PEAP. Analysis by GC is currently limited to oligomers containing relatively few ethylene oxide units. The formation of volatile derivatives prior to GC analysis is usually required [5,6] because of the lack of volatility of most non-ionic surfactants. High-temperature GC can be extended to the analysis of higher molecular mass components. For example, the high-temperature GC analysis of Triton X-100 has been reported [7]. Stephanou [8,9] reported a method using GC–MS to identify alkylphenols and linear polyethoxylated alcohols in untreated municipal wastewater. Another attempt to determine the EO distribution in complex mixtures of ethoxylated alcohols was the application of probe-distillation chemical ionization mass spectrometry [10].

One of the most suitable techniques for determining non-ionic surfactants and the oligomer distribution of PEAP is high-performance liquid chromatography (HPLC). The characterization of these surfactants has generally been performed with normal-phase columns [11–15]. The initial work on the use of normal-phase LC, with UV detection at 277 nm, to separate some commercial polyethoxylated surfactants was done by Huber *et al.* [16].

Giger and co-workers [17–20] reported on reversed-phase HPLC methods for the simultaneous determination of linear alkylbenzenesulphonates (LAS) and total polyethoxylated alkylphenols in wastewater and other environmental samples. In their methods, all oligomers of PEAP eluted as one or two peaks and the determination of individual oligomers required additional information attainable from normal-phase HPLC. Allen and Rice [21] reported the separation of alkylphenol ethoxylate adducts with up to nine or ten ethylene oxide units by reversed-phase HPLC. To our knowledge, the use of reversed-phase conditions for the separation and identification of individual oligomers of PEAP surfactants with up to 40 EO units (molecular mass distribution up to *ca.* 2000) has not previously been reported.

Escott and Chandler [22] recently reported the application of the LC–thermospray MS for the analysis of mixtures of sulphonated surfactants with in-line UV and on-line MS detection. This technique, as reported, can achieve a high degree of selectivity for the analysis of sulphonated surfactants with the addition of a sufficiently volatile ionic material to the mobile phase.

This paper presents a rapid and simple approach for the separation and identification of polyethoxylated alkylphenols with high resolution and sensitivity, and the determination of the distribution of oligomers with satisfactory reproducibility using reversed-phase HPLC with a C1 TMS (trimethylsilyl) column.

EXPERIMENTAL

Materials

The polyethoxylated octylphenol surfactant samples (Triton is the trade name for many of these surfactants) were purchased from Sigma (St. Louis, MO, USA) and Rohm and Haas (Philadelphia, PA, USA). These octylphenol-based products contained ethoxy oligomers with varying numbers of ethoxy units. PEAP, with an average of <6 EO units, will not dissolve in water (a dispersion forms), but will dissolve in methanol. PEAP, with an average of >7 EO units dissolves in both water and methanol. The sample solutions of the surfactants studied were

prepared in HPLC-grade methanol and deionized water as follows: octylphenol (0.02 μg/μl), Triton X-15 (0.02 μg/μl), Triton X-35 (0.1 μg/μl) and Triton X-45 (0.1 μg/μl) in methanol; Triton X-114 (0.2 μg/μl), Triton X-100 (0.2 μg/μl), Triton X-102 (0.5 μg/μl), Triton X-165 (0.8 μg/μl) and polyethoxylated ($n = 30$) octylphenol (1.0 μg/μl) in water. The standard solution used for testing the reversed-phase HPLC system was *tert.*-octylphenol in methanol.

Chromatography

The method development work was performed on a Shimadzu system, consisting of two LC-600 pumps, an SCL-6B system controller and a variable-wavelength SPD-6AV UV–Vis detector. The chromatograms with peak areas and retention times were recorded on a Shimadzu CR-601 Chromatopac integrator. The attenuation of the integrator was set at 4 or 5 in most measurements.

The chromatographic separation was carried out isocratically in the reversed-phase mode with a 150 mm × 4.6 mm I.D. stainless-steel C1 TMS column (CSC-C1 or Supelcosil LC-1 column, particle packing size 5 μm) purchased from Chromatography Sciences (Montreal, Canada) and Supelco (Bellefonte, PA, USA), respectively.

The mobile phase used was a mixture of deionized water (0.02 g/l of ammonium acetate was added as to improve the baseline stability) and 50–62% of HPLC-grade methanol, depending on the sample to be analysed. The column effluent was monitored at 225 nm (deuterium lamp, flow cell volume 8 μl), which is the approximate wavelength of maximum absorption of polyethoxylate octylphenols obtained from UV spectrophotometric scanning. The flow-rate was maintained at 1.0 ml/min and the column was maintained at ambient temperature (22 ± 1°C). The injection system was a Rheodyne Model 7125 sample injector equipped with a 20-μl sampling loop.

Quantification

Because all oligomers have almost identical molar absorptivities (this will be discussed later), the integrated peak area can be used directly to determine the mole fraction of each oligomer. The following equation shows how the mole fractions are related to peak area:

$$F_i = \frac{A_i}{\sum_{i=0}^{n} A_i} \quad (1)$$

where F is the mole fraction of each oligomer, A represents the peak area of the oligomer and i is the number of EO units in the ethoxylate adducts.

The average EO number may be calculated for each sample using the following equation:

$$\bar{n} = \frac{\sum_{i=0}^{n} A_i n_i}{\sum_{i=0}^{n} A_i} = \sum_{i=0}^{n} n_i F_i \quad (2)$$

where $\bar{n}$ is the average EO number of the sample and n is the number of EO units in each oligomer. After $\bar{n}$ has been obtained, the average molecular mass of each polyethoxylated alkylphenol sample can be determined with the following relationship:

$$\overline{M_r} = (M_r)_R + \bar{n}(M_r)_{EO} \quad (3)$$

where $(M_r)_R$ is the molecular mass of the octylphenol group (t-$C_8H_{17}C_6H_5$–) and $(M_r)_{EO}$ is the molecular mass of an ethylene oxide unit (CH_2CH_2O–).

If the mass fraction (M_i) of an individual oligomer containing n EO units is required, it can be determined using the following equation:

$$M_i\,(\%) = \frac{F_i[(M_r)_R + n(M_r)_{EO}]}{\overline{M_r}} \quad (4)$$

RESULTS AND DISCUSSION

Characterization of surfactant samples

In order for the method to be able to produce quantitative distributions, the following conditions should be met: (1) satisfactory separation of individual components; (2) identification of the ethoxylate peaks; (3) knowledge of the response factors of individual oligomers; and (4) sensitivity and reproducibility of detection.

Various columns and HPLC conditions were

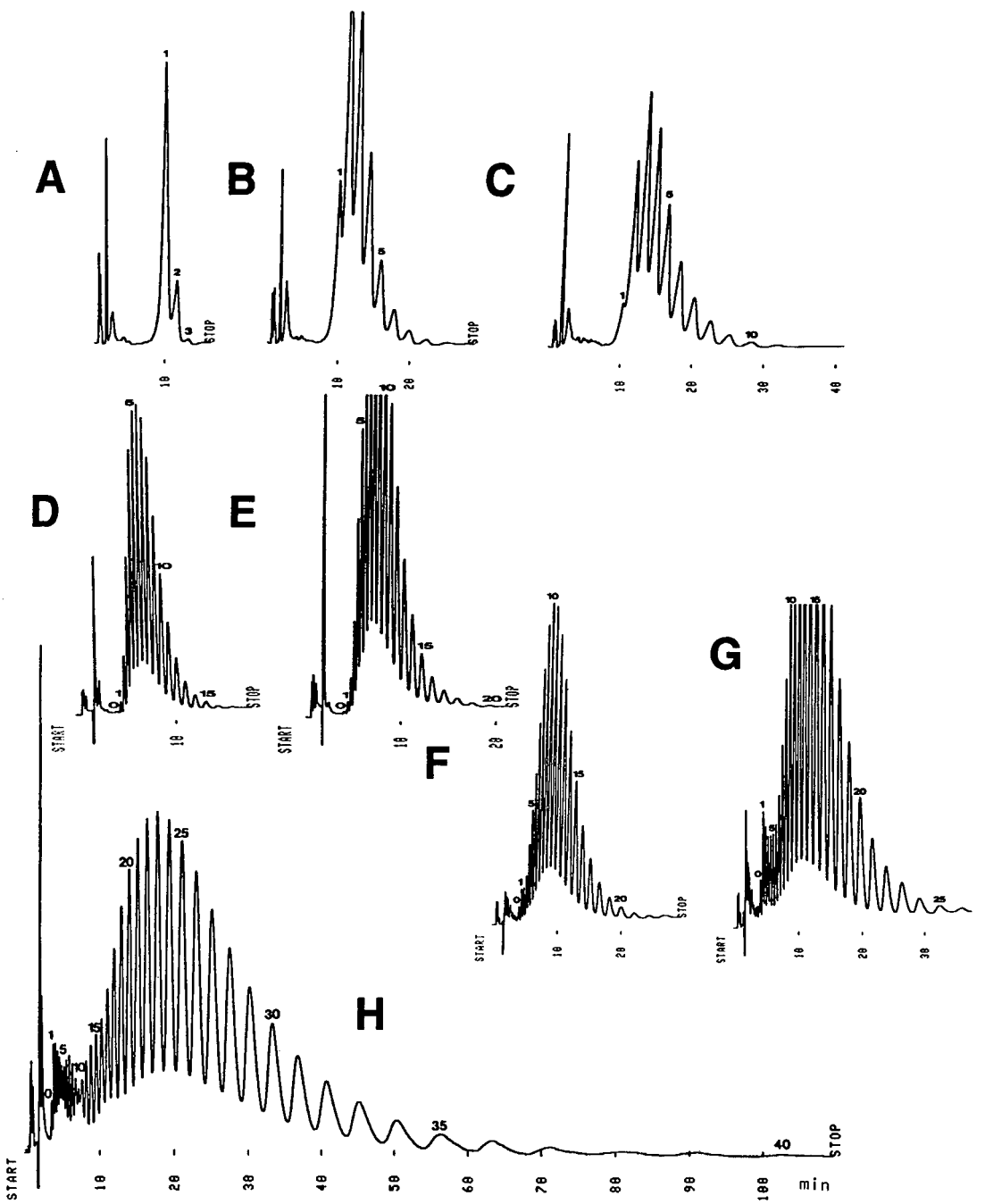

Fig. 1. HPLC of non-ionic surfactants of polyethoxylated octylphenol. (A) Triton X-15 (0.02 mg/ml); (B) Triton X-35 (0.1 mg/ml); (C) Triton X-45 (0.1 mg/ml); (D) Triton X-114 (0.2 mg/ml); (E) Triton X-100 (0.2 mg/ml); (F) Triton X-102 (0.5 mg/ml); (G) Triton X-165 (0.8 mg/ml); (H) POE (30) octylphenol (1.0 mg/ml). Conditions: CSC-C1 TMS column; temperature, 22 ± 1°C; mobile phase, methanol–water [(A)–(C) 53:47; (D)–(H) 60:40]; elution mode, isocratic; flow-rate, 1.0 ml/min; UV detection at 225 nm. The numbers assigned to the individual peaks represent the number of EO units in the oligomers; 0 represents the parent *tert.*-octylphenol. The integrator attenuation was set at 3, 4 or 5 according to the intensities of the peaks.

studied. The Wescan RP/S surfactant column separated ionic sulphate and sulphonate surfactants, but failed to separate polyethoxylated alkylphenols. Both the Supelco LC-1 C1 (TMS) column and CSC Spherisorb C1 (TMS) column separated PEAP oligomers, but better peak shapes and resolution and higher sensitivities were obtained using the latter column under comparable HPLC conditions. Consequently, all work further reported here was carried out using the CSC C1 column.

It has been demonstrated that the alkylphenol oligomers containing different numbers of EO units have nearly identical molar absorptivities at the selected UV detection wavelength because the phenyl ring is the only chromophore in the molecules [23]. Therefore, HPLC with UV detection offers the advantage that the molar response factors for the individual oligomers can be taken as identical, and serve as the basis to determine the EO distribution and average EO mole number directly from the integrated peak areas.

Fig. 1A–H show the chromatograms of eight samples of octylphenol polyethoxylate mixtures with 1–40 EO units. It can be seen that oligomers are well separated. Peak broadening is evident with increase in the number of EO units of oligomers. The small characteristic peak which was eluted prior to ethoxylate adducts and was detected in most of the samples is not part of the surfactant but is attributed to the parent *tert.*-octylphenol (EO = 0) remaining unconverted.

The numbers assigned to the individual peaks in Fig. 1A–H represent the number of EO units in each oligomer. Because of the lack of single-EO-number alkylphenol standards, the identification of these peaks was based on a comparison of the retention times with those of reference materials octylphenol (EO = 0) and Triton X-15 [its major component being EO (1) octylphenol], and on the well accepted assumption that peaks differ from each other by only 1 EO unit [16,23–25].

Reproducibility was measured by repeated analyses of the same sample. If not specifically mentioned, the measurement was carried at least four times ($n = 4$). It should be noted that the luminance of the deuterium lamp decreases as time elapses, which affects the detection sensitivity of the UV detector for the same samples.

TABLE I

RETENTION TIME AND PEAK AREA REPRODUCIBILITY IN ANALYSIS OF TRITON X-114

Peak	Retention time (min)				Peak area (counts)				Average ($\bar{x}$) (counts)	S.D. (counts)	R.S.D. (%)	F (%)[a]
	Run 1	Run 2	Run 3	Run 4	Run 1	Run 2	Run 3	Run 4				
1	4.625	4.625	4.622	4.613	12 121	11 868	11 026	11 028	11 511	568	4.93	0.311
2	4.922	4.987	4.983	4.977	63 715	63 319	63 525	61 452	63 003	1046	1.66	1.705
3	5.377	5.373	5.368	5.362	191 182	175 703	188 503	184 733	185 030	6757	3.65	5.007
4	5.770	5.765	5.758	5.750	355 404	324 687	345 217	338 206	340 879	12 898	3.78	9.224
5	6.100	6.177	6.170	6.167	443 634	411 401	433 946	423 345	428 082	13 867	3.24	11.584
6	6.638	6.633	6.625	6.620	486 022	455 984	475 745	467 963	471 429	12 677	2.69	12.757
7	7.120	7.115	7.108	7.100	499 764	483 654	496 802	491 002	492 806	7104	1.44	13.336
8	7.648	7.642	7.635	7.625	467 690	457 712	463 662	466 086	463 788	4376	0.94	12.550
9	8.225	8.222	8.217	8.205	396 676	387 800	395 056	393 334	393 217	3860	0.98	10.641
10	8.872	8.865	8.863	8.848	302 709	295 058	305 588	300 478	300 958	4455	1.48	8.144
11	9.587	9.577	9.580	9.562	212 793	206 667	221 664	212 711	213 459	6177	2.89	5.776
12	10.385	10.368	10.373	10.355	138 749	136 446	150 785	142 299	142 070	6289	4.43	3.844
13	11.270	11.243	11.258	11.240	84 957	82 894	89 696	86 018	85 891	2849	3.32	2.324
14	12.253	12.225	12.250	12.225	46 468	46 890	50 064	50 481	48 476	2089	4.31	1.312
15	13.380	13.325	13.335	13.325	28 888	28 968	30 396	31 178	29 858	1120	3.75	0.808
16	14.920	14.533	14.467	14.538	17 603	17 200	18 248	16 390	17 360	778	4.48	0.470
17	15.990	15.933	15.962	15.893	7681	7129	7569	8104	7621	401	5.26	0.206
Total area (counts)					3 756 056	3 593 380	3 747 492	3 684 808	3 695 434	65 025	1.76	
Average EO number (n)							7.43					

[a] Mole fraction of oligomers.

TABLE II

COMPARISON OF R.S.D. BY TWO CALCULATION METHODS IN ANALYSIS OF TRITON X-114

Peak	Area percentage				Average ($\bar{x}$) (%)	S.D. (%)	R.S.D. (%)	R.S.D. (%) (by area calc.)
	Run 1	Run 2	Run 3	Run 4				
1	0.323	0.330	0.294	0.299	0.311	0.018	5.79	4.93
2	1.696	1.762	1.695	1.668	1.705	0.040	2.35	1.66
3	5.090	4.890	5.030	5.013	5.007	0.084	1.68	3.65
4	9.462	9.036	9.212	9.178	9.223	0.177	1.92	3.78
5	11.811	11.449	11.580	11.489	11.583	0.162	1.40	3.24
6	12.940	12.690	12.695	12.700	12.756	0.123	0.96	2.69
7	13.306	13.460	13.257	13.325	13.337	0.087	0.65	1.44
8	12.452	12.738	12.373	12.649	12.552	0.169	1.35	0.94
9	10.561	10.792	10.542	10.675	10.642	0.116	1.09	0.98
10	8.059	8.211	8.154	8.155	8.145	0.063	0.77	1.48
11	5.665	5.751	5.915	5.773	5.776	0.104	1.80	2.89
12	3.694	3.797	4.024	3.862	3.844	0.138	3.59	4.43
13	2.262	2.307	2.393	2.334	2.324	0.055	2.37	3.32
14	1.237	1.305	1.336	1.370	1.312	0.057	4.34	4.31
15	0.769	0.806	0.811	0.846	0.808	0.032	3.96	3.75
16	0.469	0.479	0.487	0.445	0.470	0.018	3.83	4.48
17	0.204	0.198	0.202	0.220	0.206	0.010	4.85	5.26
Total (%)	100	100	100	100	100			
Average EO number (n)					7.43			

TABLE III

MOLE FRACTION (F) AND AVERAGE EO NUMBER OF TRITON X-15, X-35 AND X-45

Peak	Triton X-15			Triton X-35			Triton X-45		
	F (%)	S.D. (%)	R.S.D. (%)	F (%)	S.D. (%)	R.S.D. (%)	F (%)	S.D. (%)	R.S.D. (%)
1	80.992	0.092	0.11	11.898	0.242	2.03	3.895	0.091	2.34
2	17.389	0.075	0.43	31.531	0.278	0.88	15.251	0.399	2.62
3	1.595	0.024	1.50	26.879	0.224	0.83	21.872	0.355	1.62
4				15.701	0.189	1.20	19.820	0.240	1.21
5				7.440	0.139	1.87	14.359	0.140	0.97
6				3.678	0.166	4.51	9.674	0.129	1.33
7				1.733	0.093	5.37	6.259	0.226	3.61
8				0.790	0.044	5.57	4.006	0.209	5.22
9				0.361	0.018	4.99	2.698	0.131	4.86
10							1.555	0.065	4.18
11							0.614	0.042	6.84
Total (%)	100			100			100		
Average EO number (n)	1.21			2.99			4.32		

Hence the results vary slightly according to the time at which they were measured.

Determination of oligomer distribution

The peak areas were tabulated once each sample had been run and each peak representing different oligomers had been identified. Table I gives the retention times and the peak areas of the oligomers of Triton X-114 from four repeated analyses. The average area for each peak, standard deviation (S.D.), relative standard deviation (R.S.D.) and mole fraction (F) for each ethylene oxide adduct calculated from the average area are also given. The average EO number for Triton X-114 was determined to be 7.43.

There is another method for determining the distribution of oligomers. The data from each run are expressed as an area percentage (that is, mole fraction), and the average mole fraction for each component is then statistically calculated. These values are identical with those obtained using the first method, but R.S.D.s were general-

TABLE IV

MOLE FRACTION (F) AND AVERAGE EO NUMBER OF PEAP STUDIED

Peak	Triton X-100			Triton X-102			Triton X-165			POE(30) octylphenol		
	F (%)	S.D. (%)	R.S.D. (%)	F (%)	S.D. (%)	R.S.D. (%)	F (%)	S.D. (%)	R.S.D. (%)	F (%)	S.D. (%)	R.S.D. (%)
1	0.138	0.009	6.52	0.445	0.003	0.67	0.683	0.005	0.73	0.312	0.011	3.53
2	0.516	0.028	5.43	0.562	0.002	0.36	0.671	0.004	0.60	0.326	0.017	5.21
3	1.481	0.029	1.96	0.844	0.008	0.95	0.662	0.013	1.96	0.345	0.008	2.32
4	3.473	0.048	1.38	1.535	0.025	1.63	0.705	0.016	2.27	0.364	0.008	2.20
5	5.618	0.048	0.85	2.294	0.030	1.31	0.748	0.017	2.27	0.351	0.006	1.71
6	7.742	0.064	0.83	3.250	0.020	0.62	0.912	0.020	2.19	0.379	0.014	3.69
7	9.978	0.074	0.74	4.753	0.010	0.21	1.309	0.010	0.76	0.405	0.008	1.98
8	11.672	0.087	0.75	6.535	0.039	0.60	2.017	0.012	0.59	0.432	0.014	3.24
9	12.237	0.071	0.58	8.306	0.066	0.79	3.054	0.018	0.59	0.469	0.011	2.35
10	11.690	0.094	0.80	9.785	0.068	0.69	4.412	0.013	0.29	0.486	0.012	2.47
11	10.141	0.045	0.44	10.592	0.074	0.70	5.946	0.024	0.40	0.371	0.019	5.12
12	8.188	0.048	0.59	10.597	0.042	0.40	7.444	0.022	0.30	0.535	0.014	2.62
13	6.076	0.044	0.72	9.833	0.039	0.40	8.742	0.035	0.40	0.610	0.037	6.07
14	4.259	0.049	1.15	8.520	0.060	0.70	9.549	0.076	0.80	0.796	0.008	1.01
15	2.813	0.049	1.74	6.871	0.048	0.70	9.759	0.088	0.90	1.025	0.030	2.93
16	1.819	0.072	3.96	5.189	0.021	0.40	9.356	0.047	0.50	1.274	0.028	2.20
17	1.138	0.069	6.06	3.718	0.026	0.70	8.405	0.059	0.70	1.744	0.035	2.01
18	0.624	0.040	6.41	2.493	0.050	2.01	7.117	0.100	1.41	2.117	0.158	7.46
19	0.292	0.019	6.51	1.635	0.060	3.67	5.696	0.074	1.30	3.096	0.065	2.10
20	0.109	0.008	7.34	1.066	0.029	2.72	4.228	0.093	2.20	3.865	0.083	2.15
21				0.513	0.027	5.26	3.026	0.151	4.99	4.738	0.077	1.63
22				0.261	0.017	6.51	2.062	0.136	6.60	5.541	0.045	0.81
23				0.405	0.012	2.96	1.558	0.072	4.62	6.324	0.100	1.58
24							0.840	0.029	3.45	6.854	0.079	1.15
25							0.491	0.020	4.07	7.219	0.051	0.71
26							0.385	0.021	5.45	7.296	0.015	0.21
27							0.224	0.011	4.91	7.169	0.080	1.12
28										6.765	0.092	1.36
29										6.099	0.056	0.92
30										5.360	0.127	2.37
31										4.425	0.136	3.07
32										3.591	0.081	2.26
33										2.744	0.094	3.43
34										2.176	0.128	5.88
35										1.548	0.085	5.49
36										0.984	0.063	6.40
37										0.792	0.029	3.66
38										0.505	0.013	2.57
39										0.319	0.013	4.08
40										0.240	0.010	4.17
Total (%)	100			100			100			100		
Average EO number (n)		9.42			11.61			14.70			24.91	

ly better. Table II gives the area percentage from each run, the average mole fraction, the S.D. and the R.S.D. obtained by the second method. As a comparison, the corresponding R.S.D. obtained from direct area calculation is also shown in Table II.

Table III lists values of the mole fraction, the S.D., R.S.D. and the average EO number for Triton X-15, X-35 and X-45. Their EO units range from 1 to 11. Similarly, Table IV gives the data for another four longer chain polyethoxylated octylphenol samples [Triton X-100, X-102 and X-165 and EO (30) octylphenol] with EO units ranging from 1 to 40 and average molecular mass ranging from 206 to *ca.* 2000. All statistical data given in Tables III and IV were obtained from four analyses for each sample. The average EO number for these seven surfactants were determined to be 1.21, 2.99, 4.32, 9.42, 11.61, 14.70 and 24.91, respectively.

Figs. 2–4 depict graphically the oligomer distribution determined for samples corresponding to Tables II–IV. The Poisson distribution for the samples with lower molecular mass and the Gaussian distribution for the samples with higher molecular mass are obvious from the shapes of the curves.

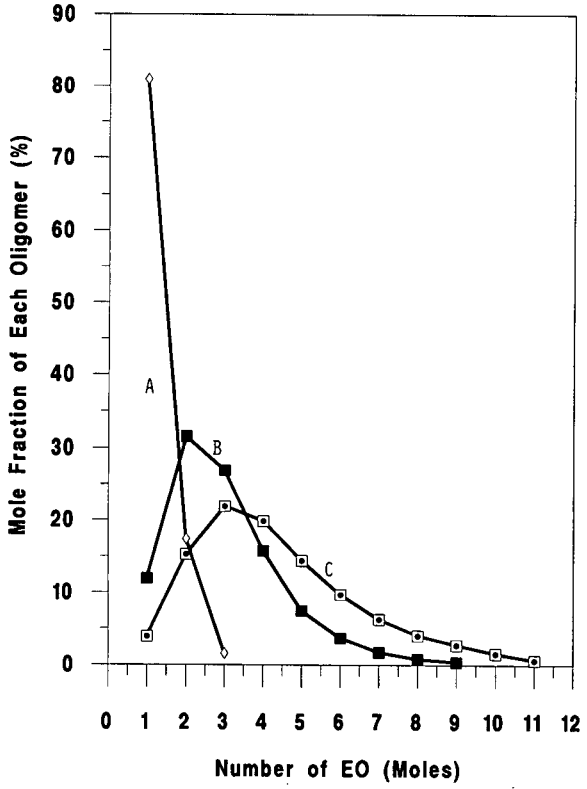

Fig. 2. Oligomer distribution curves for (A) Triton X-15, (B) Triton X-35 and (C) Triton X-45.

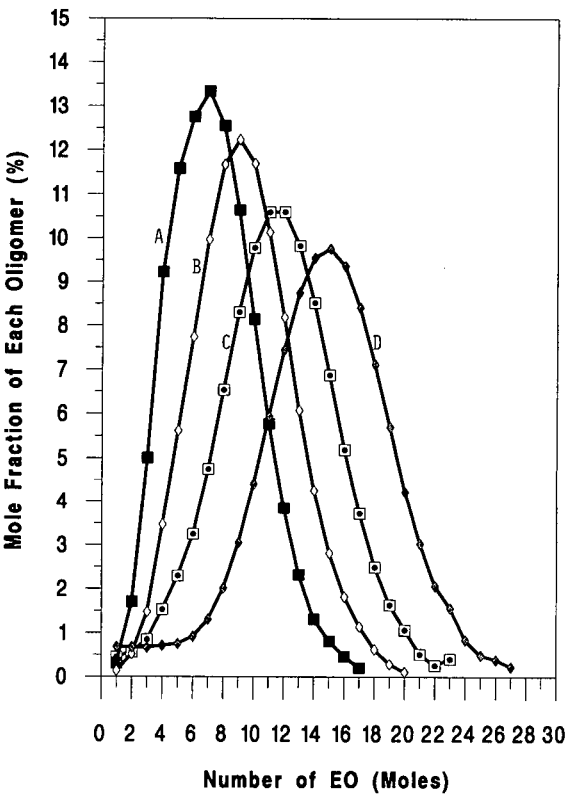

Fig. 3. Oligomer distribution curves for (A) Triton X-114, (B) Triton X-100, (C) Triton X-102 and (D) Triton X-165.

Effect of mobile phase on separation of oligomers

Methanol and acetonitrile were tested as components of the mobile phase. A methanol–water mobile phase produced good separations for all of the surfactant oligomers studied. Acetonitrile–water, however, gave poor separations. Therefore, methanol–water was used as the mobile phase throughout this study.

The experimental results demonstrated that the composition of the mobile phase has a great effect on the separation of ethoxylate adducts. Figs. 5 and 6 show chromatograms of Triton X-114 and X-35 recorded using different mobile

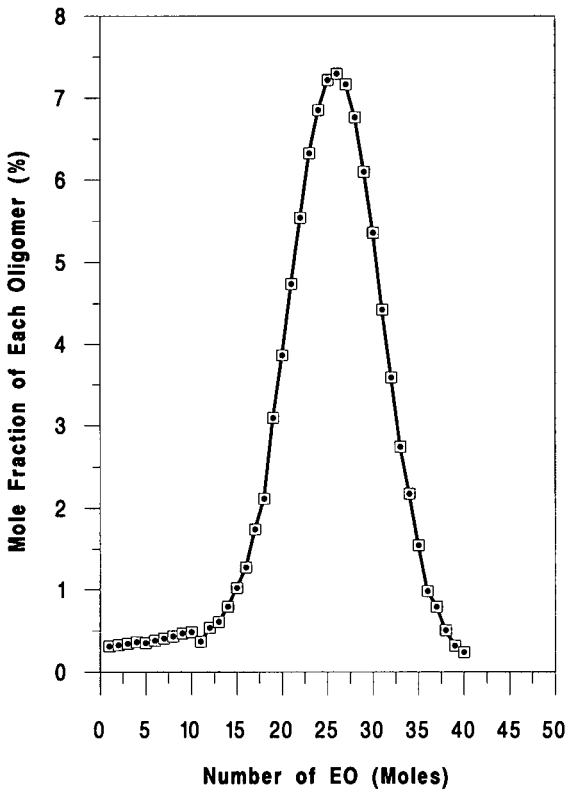

Fig. 4. Oligomer distribution curve for POE (30) octylphenol.

phase compositions. Table V summarizes the retention times for peaks 1, 5, 10 and 15, the total peak numbers identified, the total times needed for complete elution of all components and total integrated peak areas at different mobile phase compositions. The average EO numbers determined for different mobile phase compositions for Triton X-114 are also given in the last column of Table V. When the polarity of the mobile phase was decreased (that is, with a larger proportion of methanol), a shorter elution time was observed. For example, it took 53 min for peak 15 of Triton X-114 to be eluted when the ratio of methanol to water in mobile phase was set at 52:48. It took only 10 min for the same component peak to be eluted when the proportion of methanol in the mobile phase was increased from 52% to 62%. Obviously, the more ethoxylate adducts the sample contains, the more significant is the decrease with time.

It should be noted that for those samples which consisted of shorter chain oligomers and which were dissolved in methanol, poorer separation was observed as the proportion of methanol in mobile phase was increased. No separation between peaks 1 and 2 was observed for Triton X-15, X-35 and X-45 as the methanol proportion increased from 52% to 60%.

In contrast, for the samples which consisted of

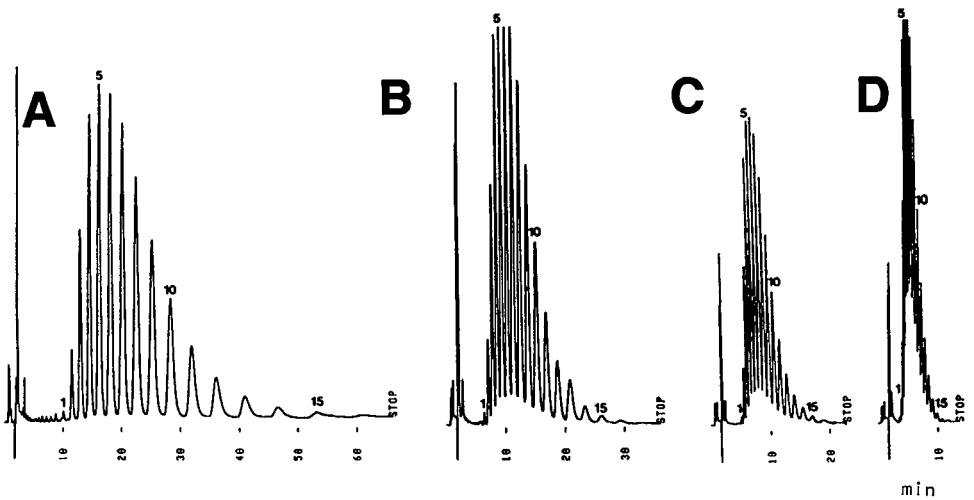

Fig. 5. Chromatograms of Triton X-114 using different methanol–water mobile phase compositions: (A) 53:47; (B) 55:45; (C) 57.3:42.7; (D) 62:38. Other conditions as in Fig. 1.

TABLE V

EFFECT OF MOBILE PHASE COMPOSITION ON THE ANALYSIS OF TRITON X-114

Mobile phase (CH_3OH–H_2O)	N [a]	Retention time (min)				Total peak number	Elution time (min)	Total area counts	Average EO number (n)
		Peak 1	Peak 5	Peak 10	Peak 15				
52:47	4	10.1	16.1	28.3	53.1	16	65	3 666 487	7.37
55:45	2	6.4	9.5	15.3	26.1	17	36	3 592 992	7.44
57.3:42.7	1	5.2	7.3	10.9	17.3	17	23	3 638 398	7.45
60:40	4	4.6	6.2	8.9	13.4	17	17	3 695 434	7.43
62:38	1	4.0	5.1	7.0	10.1	17	13	3 624 514	7.41

[a] N = number of measurements.

longer chain oligomers and which were dissolved in water, such as Triton X-114, X-100, X-102 and X-165, the effect of the composition of the mobile phase on peak resolution was much smaller. When the proportion of methanol in the mobile phase was increased from 52% to 60%, very little resolution was sacrificed, but good separation with much sharper peaks was achieved in a much shorter run time.

Effect of solvent on separation of oligomers

Three solvents, methanol, water and the mobile phase, were used to prepare solutions of PEAP surfactant Triton X-114, X-100, X-102 and X-165. The HLB values of all these surfactants are >12, and therefore they can be easily dissolved in water, methanol and the mobile phase. It is interesting that the sample solutions of the same surfactant, but prepared with different solvents at the same concentration, gave very different chromatograms (the sample volumes injected were all 20 μl). If the sample was an aqueous solution, the oligomers were completely separated. An identical chromatogram was obtained for the sample solution prepared with the mobile phase. However, if the sample was prepared in methanol, the oligomers were very poorly separated, especially for the shorter chain oligomers.

Typical chromatograms of Triton X-114 in methanol solution with methanol–water mobile phases of 60:40 and 55:45 are shown in Fig. 7.

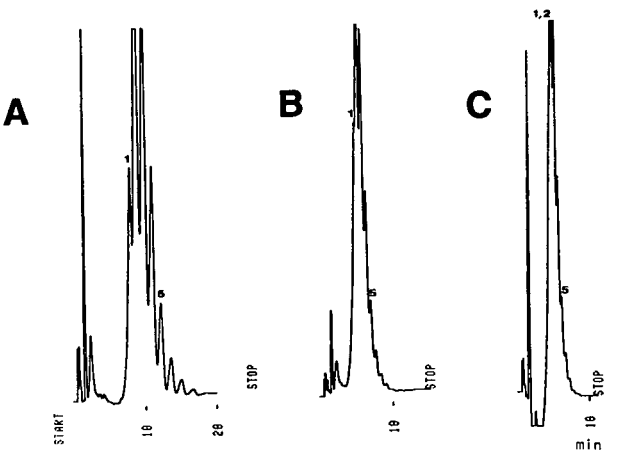

Fig. 6. Chromatograms of Triton X-35 using different methanol–water mobile phase compositions: (A) 55:45; (B) 57.3:42.7; (C) 60:40. Other conditions as in Fig. 1.

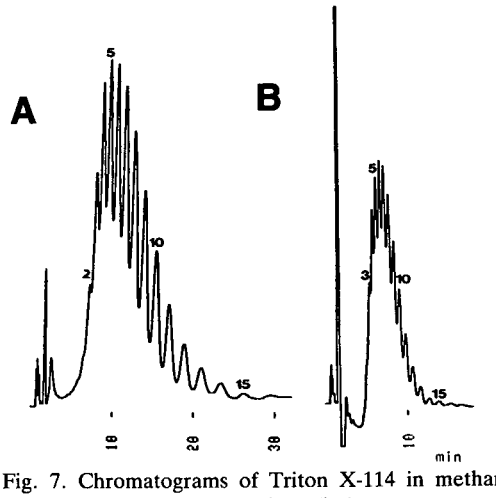

Fig. 7. Chromatograms of Triton X-114 in methanol solutions. (A) Methanol–water (55:45); integrator attenuation 4; (B) methanol–water (60:40); integrator attenuation 5. Other conditions as in Fig. 1.

TABLE VI

EFFECT OF SOLVENT ON SEPARATION OF TRITON X-114 AT VARIOUS MOBILE PHASE COMPOSITIONS

Values given are retention times (min).

Methanol–water mobile phase	Dissolved in	Peak No.																
		1	2	3	4	5	6	7	8	9	10	11	12	13	14	15	16	17
60:40	Water[a]	4.75	5.14	5.55	5.96	6.40	6.88	7.38	7.94	8.55	9.22	9.97	10.81	11.73	12.76	13.89	15.14	16.54
	Methanol[b]	–	–	5.51	5.91	6.34	6.82	7.31	7.85	8.48	9.12	9.86	10.69	11.61	12.66	13.75	15.04	16.38
55:45	Water[c]	6.35	7.05	7.78	8.55	9.37	10.31	11.32	12.45	13.72	15.16	16.80	18.65	20.75	23.20	25.99	29.18	32.80
	Mobile phase[d]	6.31	7.00	7.73	8.50	9.33	10.26	11.27	12.40	13.67	15.11	16.78	18.61	20.71	23.12	25.83	28.96	32.57
	Methanol[e]	–	–	7.75	8.52	9.34	10.28	11.28	12.41	13.68	15.12	16.78	18.66	20.75	23.17	26.02	29.17	32.70

[a] Total integrated area = 3 695 434 counts.
[b] Total integrated area = 3 747 324 counts.
[c] Total integrated area = 3 592 992 counts.
[d] Total integrated area = 3 584 481 counts.
[e] Total integrated area = 3 760 714 counts.

Comparison of Figs. 1D and 7 shows the differences in peak shape and component resolution. Table VI gives a detailed comparison of the retention times and total integration peak areas for Triton X-114 samples prepared with three different solvents. Fig. 7 and Table VI show that the retention times and total peak areas are almost identical, regardless of the solvent used. Obviously, it is not a surfactant solubility problem; if it were, the total peak areas would not be the same. Hence the question remains as to the cause of the separation difference between the aqueous and methanol solutions, and why different solvents have such a great effect on the separation of oligomers with identical injection volumes under identical HPLC conditions.

The non-aqueous surfactant solution is a very complex system. A detailed discussion and explanation of the phenomena noted above is beyond the scope of this paper, and requires more experimental work emphasizing physical chemistry studies. However, the general explanation for this phenomenon could possibly be as follows: it is well known that surfactants form micelles if their concentrations are higher than the critical micellar concentration (CMC), and that the CMC of the same surfactant is different in different solvents; hence the microstructure of micelles so formed can also be different [26]. Methanol is less polar than water. The Snyder polarity index of methanol is 5.1, only half that of water, 10.2 [27]. Another factor that should be considered is that the surfactants studied here are not pure compounds, but are a series of oligomers with varying hydrophilic EO chain lengths, and therefore the micelles may consist of varying oligomers. The combination of these factors results in physical chemical properties of surfactants in methanol that are different from those in water, and in different behaviours on the stationary phase of the HPLC column for the surfactants in methanol solution. As a result, the separation of oligomers is incomplete.

CONCLUSIONS

A method employing C1 column reversed-phase liquid chromatography has been developed for the rapid separation of non-ionic surfactants of polyethoxylated alkylphenols and the determination of their ethoxylate oligomer distribution. As a chromatographic technique, it offers several advantages for the analysis of ethoxylated non-ionic surfactants, such as the separation of oligomers, simplicity and economy with respect to time, while still having precision and accuracy. With this technique, complex distributions can be resolved and individual oligomers containing up to 40 or more EO units can be detected, allowing differences in molecular mass and mole fraction to be qualitatively and quantitatively determined. It is possible to apply this technique to the separation and identi-

fication of many other non-ionic surfactant oligomers. More studies are being conducted in this laboratory to apply HPLC and other chromatographic techniques to identify and characterize surfactants in environmental samples.

REFERENCES

1 P.L. Layman, *Chem. Eng. News*, January (1984) 17.
2 P.L. Layman, *Chem. Eng. News*, January (1986) 21.
3 M. Ahel and W. Giger, *Anal. Chem.*, 57 (1985) 1577.
4 J. Cross, *Nonionic Surfactants: Chemical Analysis*, Marcel Dekker, New York, 1987.
5 H.G. Nadeau, D.M. Oaks, Jr., W.A. Nichols and L.P. Carr, *Anal. Chem.*, 36 (1964) 1914.
6 F.J. Ludwig, Sr., *Anal. Chem.*, 40 (1968) 1620.
7 S.R. Lipsky and M.L. Duffy, *LC · GC*, 4 (1986) 898.
8 E. Stephanou, *Chemosphere*, 13 (1984) 43.
9 E. Stephanou, *Int. J. Environ. Anal. Chem.*, 27 (1985) 41.
10 P. Rudewicz and B. Munson, *Anal. Chem.*, 58 (1986) 674.
11 F.P.B. Van der Maeden, M.E.F. Biemond and P.C.G.M. Janssen, *J. Chromatogr.*, 149 (1978) 539.
12 M.S. Holt, E.H. McKerrell, J. Perry and R.J. Watkinson, *J. Chromatogr.*, 362 (1986) 419.
13 J.A. Pilc and P.A. Sermon, *J. Chromatogr.*, 398 (1987) 375.
14 *Separating Homologs and Polymers by HPLC (HPLC Bulletin 796D)*, Supelco, Bellefonte, PA, 1988.
15 M.C. Allen and D.E. Linder, *J. Am. Oil Chem. Soc.*, 58 (1981) 950.
16 J.F.K. Huber, F.F.M. Kolder and J.M. Miller, *Anal. Chem.*, 44 (1972) 105.
17 A. Marcomini and W. Giger, *Anal. Chem.*, 59 (1987) 1709.
18 A. Marcomini, S. Capri and W. Giger, *J. Chromatogr.*, 403 (1987) 243.
19 M. Ahel and W. Giger, *Anal. Chem.*, 57 (1985) 1577.
20 M. Ahel and W. Giger, *Anal. Chem.*, 57 (1985) 2584.
21 C.F. Allen and L.I. Rice, *J. Chromatogr.*, 110 (1975) 151.
22 R.E.A. Escott and D.W. Chandler, *J. Chromatogr. Sci.*, 27 (1989) 134.
23 J. Kelly and H.L. Greenwald, *J. Phys. Chem.*, 62 (1958) 1096.
24 N.T. Crabb and H.E. Persinger, *J. Am. Oil Chem. Soc.*, 45 (1968) 611.
25 S. Hayano, T. Nihongi and T. Asahara, *Tenside*, 5, Nos. 3/4 (1968) 80.
26 K.L. Mittal (Editor), *Solution Chemistry of Surfactants*, Vols. 1 and 2, Plenum Press, New York, 1979.
27 A.F.M. Barton, *CRC Handbook of Solubility Parameters and Other Cohesion Parameters*, CRC Press, Boca Raton, FL, 1983, pp. 198–199.

Journal of Chromatography, 637 (1993) 157–165
Elsevier Science Publishers B.V., Amsterdam

CHROM. 24 890

Peroxides

XII.[☆] Gas–liquid and high-performance liquid chromatographic analysis of aliphatic hydroperoxides and dialkyl peroxides

Thomas A. Foglia*, Leonard S. Silbert[☆☆] and Peter D. Vail

Eastern Regional Research Center, US Department of Agriculture, Agricultural Research Service, 600 East Mermaid Lane, Philadelphia, PA 19118 (USA)

(First received September 29th, 1992; revised manuscript received January 19th, 1993)

ABSTRACT

The chromatographic resolution of 1-alkyl hydroperoxides and di-1-alkyl peroxides by either gas–liquid chromatography and/or high-performance liquid chromatography (HPLC) was investigated. The chromatographic methods developed were applied to the compositional analysis of hydroperoxides and dialkyl peroxides in reaction mixtures and to purity determinations. The effect of aliphatic peroxide structure based on the conformations imposed by the dihedral angle of the peroxide bond has strong implications for peroxide resolutions in HPLC compared to their non-peroxy analogues. Comparison of the chromatographic data for peroxide content with that obtained by iodometry show that the methods developed are suitable for peroxide determinations.

INTRODUCTION

Numerous methods of peroxide determination have been devised to cover the range of reactivities shown by diverse peroxide structures. For an aliphatic series of derivatives, the order of increasing O–O bond strength parallels the following decreasing order of reactivity [2,3]: peroxy acid [R–C(O)–O–O–H]; diacyl peroxide [R–C(O)–O–O–C(O)–R]; hydroperoxide (R–O–O–H); perester [R–C(O)–O–O–R]; dialkyl peroxide (R–O–O–R). This peroxide sequence depicts a decreasing reactivity in liberating iodine from iodide ion [4], and increasing stability based on polarographic half-wave potential ($-E_{1/2}$) and energy of activation (E_a) for decomposition [3]. Because of this wide difference in reactivity, no general analytical method for all peroxide classes has appeared in the literature.

Gas–liquid chromatography (GLC) has been a sensitive method of peroxide determination [5], although the relatively low thermal stability of the peroxygen bond has limited the utility of GLC analysis of peroxides to members of low molecular mass, generally below 10 carbon atoms [5–11] and at column temperatures below 100°C. Hydroperoxides are stable to about 90°C [12] but readily decompose to alkyl alcohols and carbonyl compounds (aldehydes from primary alkyl hydroperoxides and ketones from secondary and tertiary alkyl hydroperoxides). This sensitivity of hydroperoxides to thermal de-

* Corresponding author.
☆ For Part XI, see ref. 1.
☆☆ Retired: 7800-C Stenton Avenue, Philadelphia, PA 19118, USA.

composition has been used in their analyses by pyrolysis GLC [13]. Alternatively, hydroperoxide decomposition has been avoided by reduction to alcohol prior to GLC determination. On the other hand, dialkyl peroxides are the most stable to thermal effects as illustrated by the GLC elution of 2,5-dimethyl-2,5-di(*tert.*-butylperoxy)hexyne-3 and 2,5-dimethyl-2,5-di(*tert.*-butylperoxy)hexane [14] at 138°C. Like hydroperoxides, dialkyl peroxides undergo thermal decomposition at elevated temperatures which permit their analysis by pyrolytic GLC [15,16].

High-performance liquid chromatography (HPLC) is a mild method usually conducted at room temperature that assures the peroxide's structural integrity. Because of this major advantage over GLC in the analysis of thermally sensitive, non-volatile and higher-molecular-mass compounds, HPLC has been actively studied for peroxide structures [17–21] and, most importantly, has been accepted as the method of choice for lipid peroxide analysis.

In the course of our recent developments of alkyl hydroperoxide [22] and dialkyl peroxide [23] syntheses, we found limited published literature on chromatographic analyses of homologous series of long chain aliphatic peroxides. This void may have resulted from the compounds' unavailability or by the failure or inadequacies of earlier synthetic methods [24–26] of preparation. The success of our peroxide syntheses was dependent on instituting concurrent GLC and HPLC examinations of reaction products to assess their relative advantages and limitations. The suitability of these chromatographic methods for quantitating hydroperoxides could be independently confirmed by iodometry whereas their accuracy for dialkyl peroxides lacked this independent verification.

The initial goal of this study was to update GLC and HPLC methods using high-resolution columns for the direct determination of hydroperoxides and dialkyl peroxides in complex reaction mixtures. Because of thermal and surface sensitivities of hydroperoxides, GLC and HPLC can give unreliable quantitation that necessitate an independent method of analytical verification. Iodometry has been well established for hydroperoxide determinations [5] but it measures total hydroperoxide content whereas chromatographic methods measure the separated components.

By contrast, dialkyl peroxides have been difficult to analyze iodometrically [5,27]. However, the reverse option of using GLC and HPLC methods would provide a criterion that would validate the results of iodometry. In fact, the results of the current study has made possible the development of a newly modified iodometric method [1].

As this study progressed, we observed unexpected effects of peroxide structure on the chromatographic separation of peroxides from their oxy-analogues. Accordingly, this paper composites the details of our chromatographic results on the even-membered homologous series of primary hydroperoxides (hexyl to hexadecyl) and primary dialkyl peroxides (dihexyl to dihexadecyl), a comparison of the chromatographic and iodometric results, and the correlation of the separation of peroxides and their oxy-analogues that together provide new insights on peroxide separations and analyses.

EXPERIMENTAL[a]

Materials

Hydroperoxides were prepared by either of two methods [22]: (a) the perhydrolysis of alkyl triflates or (b) the perhydrolysis of alkyl mercuric tetrafluoroborates. The crude preparations were analyzed directly and pure hydroperoxides isolated by semi-preparative HPLC. Primary dialkyl peroxides were obtained by phase transfer reaction of potassium superoxide with primary alkyl bromides [23] and the peroxides purified as described. *tert.*-Butyl myristate [2] and *tert.*-butyl permyristate [28] were prepared and purified as described. Di-*tert.*-butyl peroxide, 98% (Aldrich, Milwaukee, WI, USA) and dicumenyl peroxide, 98% (Akzo, Chicago, IL, USA) were used as received. HPLC-grade solvents (Burdick & Jackson, Muskegon, MI, USA) were used throughout the investigations.

[a] Reference to a brand or firm name does not constitute an endorsement by the US Department of Agriculture over others of a similar nature not mentioned.

Methods

Gas–liquid chromatography. The instrument was a Hewlett-Packard (Avondale, PA, USA) Model 5830A gas chromatograph equipped with a capillary inlet system and a flame ionization detector (200°C). The quartz capillary columns were 12 m × 0.2 mm coated with 0.33-μm methyl silicone fluid (HP-101) and a 4 m × 0.2 mm coated with 0.33-μm 5% cross-linked phenyl methyl silicone fluid (HP-5). Initial column temperature for the 12-m column was 50°C for hexyl hydroperoxide and 80°C for octyl hydroperoxide, decyl hydroperoxide, and dodecyl hydroperoxide (injector port, 140°C). The carrier gas was helium with a linear velocity of 22.5 cm s^{-1} at a split ratio of 60:1. Dodecyl hydroperoxide was also analyzed on a 4-m column at 40°C (injector port, 140°C) tetradecyl and hexadecyl hydroperoxides at 110°C (injector port, 160°C) with helium at linear velocity of 12 cm s^{-1}. All components in reaction mixtures were resolved by temperature programming at 2°C min^{-1} except for hexadecyl hydroperoxide at 5°C min^{-1} to a final temperature of 150°C, and the important components were identified by comparison with available standards. For differentiation of dialkyl ethers from dialkyl peroxides, the former were prepared by the alcohol alkylation method of Barluenga *et al.* [29].

High-performance liquid chromatography. The HPLC solvent delivery systems used were a Beckman (San Ramo, CA, USA) Model 110A solvent delivery module equipped with an Altex 210 loop injector with either a 20-μl or 100-μl sample loop and a Waters differential refractometer detector, Model R401 (Waters Assoc., Milford, MA, USA) and a Hewlett-Packard Model 1090 solvent delivery module equipped with a Rheodyne Model 7125 loop injector with a 20-μl loop and a Tracor (Austin, TX, USA) Model 945 flame ionization detector operated at 80°C. The HPLC columns used were a 25 cm × 4.6 mm I.D. stainless-steel column prepacked with 5-μm silica (Zorbax SIL, DuPont, Wilmington, DE, USA) or 5-μm ODS (Altex Ultrasphere, Deerfield, IL, USA) for analytical HPLC. Semipreparative isolation of 1-alkyl hydroperoxides was made on a Dynamax (Rainin, Woburn, MA, USA) prepacked 8-μm silica column, 25 cm × 10 mm I.D. The integrator/recorder was a Hewlett-Packard Model 3396A. Samples were dissolved in mobile phase at 5 mg ml^{-1} for analytical HPLC and 100 mg ml^{-1} for semi-preparative HPLC. Response factors to the refractive index and flame ionization detectors were obtained on the purified peroxides over the range of 0.05–0.5 mg. Hydroperoxides were eluted isocratically from the silica columns with hexane–isopropanol (98:2, v/v) at a flow-rate of 1 ml min^{-1} (analytical) or 3 ml min^{-1} (semi-preparative HPLC). Dialkyl peroxides were analyzed isocratically on the ODS column with acetone–acetonitrile (70:30, v/v) at a flow-rate of 0.8 ml min^{-1}.

Iodometry. Iodometric analysis of hydroperoxides by the Wheeler method [4] is the liberation of iodine by iodide reduction of easily reducible peroxides in acetic acid–chloroform solution. The method was recently modified for its application to dialkyl peroxides by incorporating catalysis with perchloric acid or ferric ion in acetic acid at 80–100°C [1].

RESULTS AND DISCUSSION

Hydroperoxides

We have recently developed two new methods of preparing alkyl hydroperoxides, each of which has its advantages [22]. In one method, 1-alkyl hydroperoxides were obtained by perhydrolysis of primary alkyl mercuric tetrafluoroborate which produced primary hydroperoxide with minor amounts of positional hydroperoxide isomers (3%), dialkyl ether and dialkyl peroxide in addition to aldehyde and alkanol. In these studies GLC analysis of the reaction products on a 12-m capillary column was found to be highly efficient for the resolution of hydroperoxides from their reaction co-products. For example, Fig. 1 illustrates the resolution of 1-, 2- and 3-hexyl hydroperoxide isomers and the longer retention time co-products, dihexyl ether and dihexyl peroxide. Alternatively, perhydrolysis of a primary alkyl triflate (trifluoromethanesulfonate) forms the primary hydroperoxide with no formation of positional isomers. Although triflate and hydroperoxide have similar GLC reten-

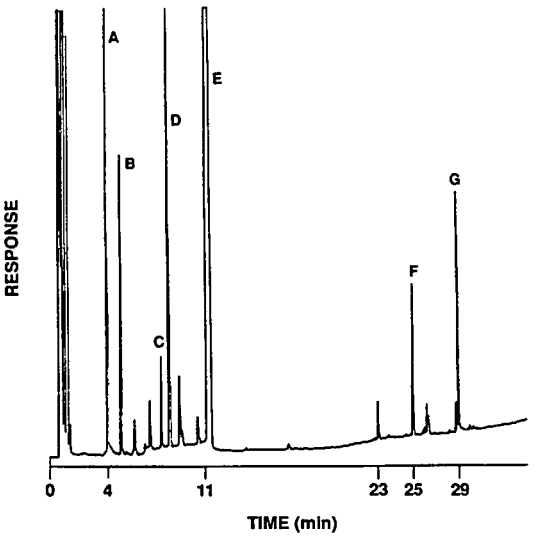

Fig. 1. Reaction products from hexyl hydroperoxide synthesis via perhydrolysis of alkyl mercuric tetrafluoroborate as separated by GLC, 12-m HP-101 capillary column. Conditions as in text. Peaks: A = R_6OH; B = R_6Br; C = 3-R_6OOH; D = 2-R_6OOH; E = 1-R_6OOH; F = R_6OR_6; G = R_6OOR_6.

tion times they are resolvable with triflate having the longer retention time.

Chromatographic determinations of the homologous hydroperoxide series up to 12 carbon atoms at column temperatures not exceeding 90°C established 10 carbon atoms to be the limit in chain size of hydroperoxides for which there is little or no decomposition. Brief contact at higher temperatures volatilizes samples onto the column but injection port temperatures should not exceed 130°C. The effect of temperature on peroxide content was observed on two dodecyl hydroperoxide preparations using a short column (4 m) having the following parameters and giving the results shown in parentheses (injection port temperature, column temperature, peroxide eluate temperature) (% peroxide by iodometry, % peroxide by GLC, % peroxide decomposed): (1) (160°C, 60°C, 91°C) (97%, 20%, 77%), and (2) (140°C, 40°C, 61°C) (75%, 67%, 8%). The milder temperature conditions in No. 2 resulted in mild decomposition compared to No. 1, indicating the injection port temperature should be lower than 140°C.

The hydroperoxide preparations for syntheses up to decyl hydroperoxide were conveniently monitored by GLC to determine reaction completeness. The isolated hydroperoxide products were then analyzed by GLC and iodometry for comparison. Since iodometry measures the sum of all isomeric peroxides present and GLC resolves hydroperoxide isomers, the isomer correction to be added to the GLC value of primary hydroperoxides amounts to about 2–3%. The GLC values for primary hydroperoxides and the

TABLE I

ANALYSIS OF 1-ALKYL HYDROPEROXIDES BY IODOMETRY, GLC AND HPLC

Primary 1-alkyl	% Hydroperoxide				
	Iodometric value[a]	GLC[b]	HPLC[c]		
			RP/FID	NP/FID	NP/RID
Hexyl	79	81			
Octyl	81	79	51		
Decyl	81	78		66	87
Dodecyl	82	67	56	60	
Tetradecyl	80	48	77		72
Hexadecyl	81	18[d]	80	58	75

[a] Ref. 22, values based on % (w/w) active oxygen.
[b] 12-m HP-101 capillary column, see Experimental.
[c] RP = Reversed phase; NP = normal phase; FID = flame ionization detection; RID = refractive index detection; results based on % (w/w) from calibration curves of purified hydroperoxides.
[d] 4-m HP-5 capillary column, see Experimental.

iodometric data for the series up to decyl (Table I) were in reasonable agreement to within 3% average. For longer chain hydroperoxides, dodecyl and larger, significant thermal decomposition was observed for each GLC value compared to the corresponding iodometric value (Table I).

Since hydroperoxide reaction products beyond decyl could not be quantified by GLC, the longer-chain hydroperoxides were determined by HPLC in two instruments separately equipped with refractive index (RID) or flame ionization (FID) detection systems and interchangeable reversed-phase (RP) or normal-phase (NP) columns. The hydroperoxides also were determined iodometrically for comparison with the HPLC chromatographic quantitations. The selected data presented in Table I are typical for the series of hydroperoxide preparations. RP/FID was effective only for non-volatile compounds which were not thermally evaporated on the heated evaporative belt that functions for solvent removal prior to sample entry into the detector. The RP/FID values were low compared to the iodometric results but the former increased in value with increasing chain length which indicated their relative degree of volatility. The iodometric and reversed-phase HPLC values for hexadecyl hydroperoxide were in good agreement.

The homologous series of alkyl hydroperoxides and their corresponding alcohols were chromatographed isocratically in reversed-phase HPLC. The two series are graphically presented in Fig. 2 where log k' (capacity factor) *vs.* carbon number of alkyl residues depict the linearity in their order of elution. In this series, the alcohol has the longer retention time for each hydroperoxide–alcohol analogue pair. The alcohol and hydroperoxide series were obtained under identical conditions for comparison whereas literature data reported for the alcohols [30–32] were unusable for this purpose.

An example of a normal-phase HPLC separation of a hydroperoxide preparation is given in Fig. 3A showing alcohol as more strongly retained than hydroperoxide. Normal-phase hydroperoxide values with either FID or RID were low for all examples examined, although RID

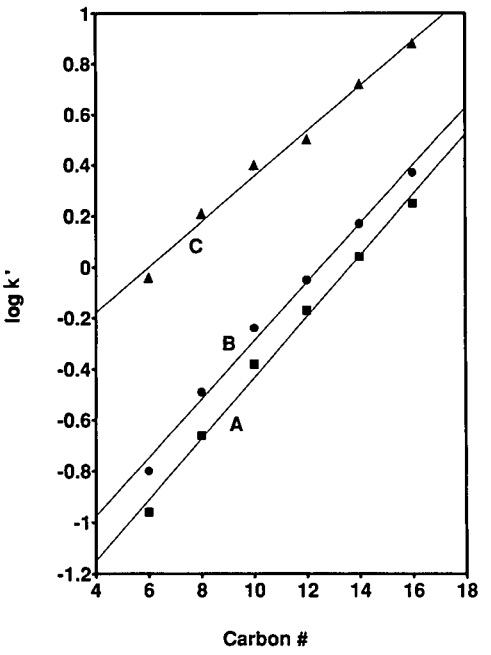

Fig. 2. Plot of log k' *vs.* carbon No. (#) of alkyl chain separated by RP-HPLC. A = Alkyl hydroperoxide; B = alkyl alcohols; C = dialkyl peroxides, where carbon No. is half total carbons of dialkyl peroxide.

gave the higher values. The NP/RID method introduced a large negative peak [33,34] with a corresponding uncertainty in the quantitation. This negative peak arises from solvent and pressure effects. Assuming the negative peak contained no overlapping component of identical retention time, the peroxide results could be

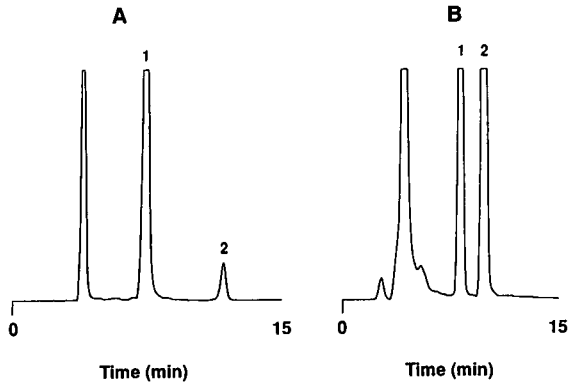

Fig. 3. HPLC–FID: (A) normal-phase (decyl hydroperoxide and decyl alcohol); (B) reversed-phase (didecyl peroxide and didecyl ether). Peaks: (A) 1 = $R_{10}OOH$, 2 = $R_{10}OH$; (B) 1 = $R_{10}OOR_{10}$, 2 = $R_{10}OR_{10}$.

adjusted proportionally. The measured values were within an average 8% of the iodometric values for the few determinations obtained. Consequently, RP/FID offered the best set of determinations for non-volatile hydroperoxides beyond C_{12} chain length and is the method of choice for chromatographic analysis. However, the NP/RID system was useful for isolating pure long-chain hydroperoxides on a semi-preparative scale: for example, a sample of hexadecyl hydroperoxide (70%, 1 g) was purified to 99% (0.5 g).

Dialkyl peroxides

A summary of the analyses of dialkyl peroxide preparations by iodometry, GLC and reversed phase HPLC is presented in Table II. Primary dialkyl peroxides are readily prepared from alkyl bromides by reaction with superoxide anion under phase transfer conditions [23]. In these reactions the major co-products are the dialkyl ether analogues. Quantitation of volatile dialkyl peroxides up to eight carbon atoms per alkyl chain was obtained by GLC (12-m column). The isomeric pair, dihexyl and butyl octyl peroxides, were resolved with the latter unsymmetrical peroxide having the longer retention time (Fig. 4). Dialkyl peroxides and reaction products exceeding eight carbon atoms per chain, although chromatographable by GLC, gave variable results because of the peroxides' thermal decomposition associated with the higher column temperatures needed for the analysis.

TABLE II

ANALYSIS OF DIALKYL PEROXIDES BY IODOMETRY, GLC AND HPLC

Carbon No. per alkyl	% Dialkyl peroxides		
	Iodometric[a]	GLC[b]	HPLC[c]
6	93.8	93.9	
8	89.1	90.1	
10	94.6		95.4
12	32		95.6
14	40		98.8
16	26		99.1
Supplementary dialkyl peroxides			
tert.-Butyl 1-octyl	91.2	90.6	
Dicumenyl	99.4		99.6
Di-*tert.*-butyl	97.2	99.9	

[a] Ref. 1, values based on % (w/w) active oxygen.
[b] 12-m HP-101 capillary column, see Experimental.
[c] By reversed-phase/flame ionization detection: values based on % (w/w) from calibration curves of purified dialkyl peroxides.

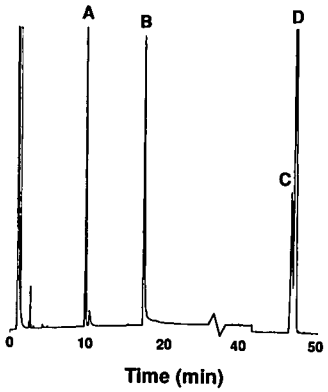

Fig. 4. Reaction products from 1-butyl 1-octyl peroxide synthesis. Peaks: A = 1-hexyl hydroperoxide (R_6OOH); B = 1-octyl hydroperoxide (R_8OOH); C = dihexyl peroxide (R_6OOR_6); D = 1-butyl 1-octyl peroxide (R_4OOR_6). GLC conditions as in text.

Dialkyl peroxide homologues were not resolvable using normal-phase HPLC. The medium- and long-chain homologues were chromatographed by HPLC in the RP/FID system with good resolution using acetonitrile–acetone cosolvents. The homologous even-carbon alkyl chain C_6–C_{16} series, which was chromatographed in reversed-phase HPLC, gave the linear relationship shown in Fig. 2. The nonperoxy analogue, dialkyl ether, similar to alcohol in the hydroperoxide series, was more strongly retained as demonstrated in Fig. 3B.

The synthetic availability of the dialkyl peroxides offered the opportunity to examine them iodometrically [1]. Dialkyl peroxides are unreactive with iodide ion at room temperature but were induced to liberate iodine thermally under complex conditions [27]. A new simplified method using perchloric acid or ferric ion catalysis achieved rapid, quantitative liberation of iodine whose values could be accepted with confidence by comparison with the chromatographic values serving as the standards (Table II) [1]. This

represents the inverse of the hydroperoxide analyses whereby iodometry functioned as the criterion for the chromatographic values.

Table II summarizes these results for which there is good agreement for all the compounds listed except the C_{12}–C_{16} members. The latter failed to achieve quantitation in the heated acetic acid solution because of poor solubility and decomposition within the melted sample globules. The table includes additional representations of dialkyl peroxide structures analyzed iodometrically. Each class of normal to tertiary alkyl peroxide required specific analytical conditions which permitted the arrangement of an order of increasing stability and decreasing reactivity as follows:

increasing stability →

n-dialkyl → *tert*-butyl *n*-alkyl → dicumenyl → di-*tert*.-butyl

← decreasing reactivity

Peroxide structural effects

Peroxides have a dihedral angle as a characteristic structural feature that twists the O–O bond into opposing planes that is aptly described as an open book model (Fig. 5A). The dihedral angle leads to conformations in different peroxide structures in which this angle is enlarged or compressed [35].

Peroxides and their non-peroxy analogues were resolved in GLC with the former having the longer retention time in accordance with the peroxide's higher molecular mass. Both the alkyl hydroperoxide and dialkyl peroxide were eluted at longer retention times than their corresponding alcohols and dialkyl ethers, respectively. Resolution of the isomeric di-1-hexyl and 1-butyl 1-octyl peroxides, the latter having the longer retention time, may be explained in terms of the dihedral angle inducing the longer octyl chain into conformations engaging Van der Waals interactions more extensively than the hexyl chain, *i.e.*, the longer the chain, the greater the degree of interaction and the longer the retention time.

By contrast in HPLC, alkyl hydroperoxides elute earlier (less retained) than their corresponding alkyl alcohol analogues in both reversed-phase (Fig. 2) and normal-phase (Fig. 3A) chromatography. Primary hydroperoxides dimerize to an intermolecular hydrogen-bonded cyclic structure (Fig. 5B) in contrast to their alcohol counterpart (dimers and polymers) [36] presumably arising from the greater acidity of the hydroperoxide and the increased stability of the pseudo six-membered ring structure. Accordingly, for normal-phase HPLC, the free terminal hydroxyl group of alcohol hydrogen bonds more strongly to silica leading to increased elution volumes.

In the case of dialkyl peroxides, the dihedral angle about the peroxy bond (Fig. 5A), which exceeds 100°, projects the two alkyl chains at approximately right angles to each other. The alkyl chains are thereby skewed into conformations that diminish their Van der Waals interactions with the octadecyl groups of the bonded stationary phase. The conformations are expressed as a foreshortening of chain length [2] compared to the more linear extension of the non-peroxide analogue. Hence, dialkyl peroxides in HPLC have shorter retention times than their non-peroxide analogues.

The generality of the foregoing relationship may be applied to peroxides of all classes as is further illustrated by the *tert*.-butyl permyristate/*tert*.-butyl myristate pair (Fig. 6) for which the ester was more strongly retained in reversed-phase HPLC. This same relationship would be

A

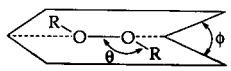

B

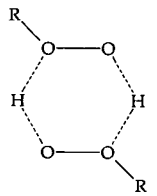

Fig. 5. (A) Structure of peroxides (R=H, alkyl, acyl); ϕ = dihedral angle; θ = R–O–O angle. (B) Cyclic dimer of alkyl hydroperoxide in solution.

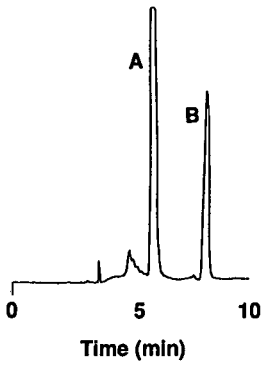

Fig. 6. Reversed-phase HPLC: (A) *tert.*-butyl permyristate; (B) *tert.*-butyl myristate. HPLC conditions as in text.

predicted by extension to diacyl peroxides relative to anhydrides for which peroxide there was foreshortening via the O–O bond skew [2].

Peroxy acids would also be expected to follow this rule. However, peroxy acids are monomeric, intramolecular hydrogen-bonded species [35,37,38] (dihedral angle, 72°) in the liquid and vapor states compared to intermolecular hydrogen-bonded dimers for carboxylic acids so that peroxy acids would be more volatile and less strongly retained in chromatographic separations than their carboxylic acid analogues.

CONCLUSIONS

Alkyl hydroperoxides for chain-size up to C_{10} were analyzable by GLC in 3% average deviation which is of moderate accuracy compared to their iodometric values. Although GLC could be used qualitatively to detect longer chain hydroperoxides, up to C_{16}, thermal decomposition precluded their quantitative analysis. Longer-chain hydroperoxides, C_{10} to C_{16}, were determined by NP-HPLC–RID with 7% average deviation, a fair accuracy which is attributed to the quantitative uncertainties associated with RID. RP-HPLC–FID requires the hydroperoxide to be non-volatile and that the FID thermal evaporative belt be operated below the hydroperoxide's decomposition temperature. Nevertheless, as hydroperoxide chain length increases and volatility decreases, there is a concomitant increase in quantitation so as to provide an excellent determination for hexadecyl hydroperoxide. Among these methods, NP-HPLC–FID was the least useful analytically being consistently low by 15–20%. NP-HPLC–RID, however, provided a useful semi-preparative method for obtaining alkyl hydroperoxides in pure form.

Dialkyl peroxides are more stable than the hydroperoxides. The dialkyl peroxides with average carbon number per alkyl chain up to 8 carbon atoms were accurately determined by GLC whereas the longer chain members were best determined by RP-HPLC–FID. Since previous iodometric methods could not be easily applied as a standard analytical method for dialkyl peroxides, the reverse approach of applying the chromatographic determinations derived in this study to establish accurate peroxide values facilitated the recent development of a new modification of iodometry.

The resolution of long chain dialkyl peroxides is based on chain size and the inherent property of skewness derived from the dihedral angle of the O–O bond. Between two dialkyl peroxide isomers, the one having one chain longer than the longest chain in the other isomer has the longer retention time in GLC. In HPLC, it is proposed that the peroxygen dihedral angle imposes a conformation to the dialkyl peroxide that foreshortens the overall chain length leading to diminished column interactions that shortens its retention time relative to the more extended ether analogue.

REFERENCES

1 L.S. Silbert, *Analyst*, 117 (1992) 745.
2 L.S. Silbert, L.P. Witnauer, D. Swern and C. Ricciuti, *J. Am. Chem. Soc.*, 81 (1959) 3244.
3 L.S. Silbert, *J. Am. Oil Chem. Soc.*, 39 (1962) 480.
4 D.H. Wheeler, *Oil Soap*, 9 (1932) 89.
5 R. Mair and R.T. Hall, in D. Swern (Editor), *Organic Peroxides*, Vol. 2, Wiley-Interscience, New York, 1971, p. 535.
6 H. Ewold, G. Öhlemann and W. Schirmer, *Z. Phys. Chem. Leipzig*, 234 (1967) 104.
7 L. Červený, A. Marhoul and V. Růžička, *J. Chromatogr.*, 74 (1972) 118.
8 L.G. Tsypysheva, É.A. Kruglov, Yu.N. Popov and A. S. Ziganshin, *J. Anal. Chem. (USSR)*, (1984) 141.
9 P. Hudec, B. Novotná and J. Petrúj, *Analyst*, 101 (1976) 379.
10 A.F. Shushunova, *J. Chromatogr.*, 365 (1986) 417.

11 P. Schieberie, W. Maier, J. Firi and W. Grosch, *J. High Resolut. Chromatogr. Chromatogr. Commun.*, 10 (1987) 588.
12 C.F. Cullis and E. Fersht, *Combustion Flame*, 7 (1963) 185.
13 A.F. Shuskunova, *J. Chromatogr.*, 365 (1986) 417.
14 S. Bukata, L. Zabrocki and M. McLaughlin, *Anal. Chem.*, 35 (1963) 885.
15 S. Hyden, *Anal. Chem.*, 35 (1963) 113.
16 G.A. Blondin, B.D. Kulkarni, J.P. John, R.T. van Allen, P.T. Russell and W.R. Nes, *Anal. Chem.*, 39 (1967) 36.
17 W.J.M. van Tilborg, *J. Chromatogr.*, 115 (1975) 616.
18 L.A. Cornish, R. Ferris and J.E. Paterson, *J. Chromatogr. Sci.*, 19 (1981) 85.
19 P. Jonvel and G. Andermann, *J. Chromatogr.*, 298 (1984) 193.
20 M.O. Funk, Jr. and W.J. Baker, *J. Liquid Chromatogr.*, 8 (1985) 663.
21 C. P. Patel and S. Lilly, *LC · GC*, 6 (1988) 425.
22 T.A. Foglia and L.S. Silbert, *J. Am. Oil Chem. Soc.*, 69 (1992) 151.
23 T. Foglia and L.S. Silbert, *Synthesis*, (1992) 545.
24 O.L. Magelli and C.S. Sheppard, in D. Swern (Editor), *Organic Peroxides*, Vol. 1, Wiley-Interscience, New York, 1970, Ch. 1, p. 1.
25 R. Hiatt, in D. Swern (Editor), *Organic Peroxides*, Vol. 2, Wiley-Interscience, New York, 1971, Ch. 1, p. 1.
26 R. Hiatt, in D. Swern (Editor), *Organic Peroxides*, Vol. 3, Wiley-Interscience, New York, 1972, Ch. 3, p. 1.
27 R.D. Mair and A.J. Graupner, *Anal. Chem.*, 36 (1964) 194.
28 L.S. Silbert and D. Swern, *J. Am. Chem. Soc.*, 81 (1959) 2364.
29 J. Barluenga, L. Alonso-Cures and G. Asensia, *Synthesis*, (1979) 962.
30 F.E. Lockwood, L.J. Matienzo and B. Sprissler, *J. Chromatogr.*, 262 (1983) 397.
31 J.E. Parkin, *J. Chromatogr.*, 287 (1984) 457.
32 J.E. Parkin, *J. Chromatogr.*, 314 (1984) 488.
33 K. Šlais and M. Krejči, *J. Chromatogr.*, 91 (1974) 161.
34 L.R. Snyder and J.J. Kirkland, *Introduction to Modern Chromatography*, Wiley, New York, 2nd ed., 1979, p. 810.
35 L.S. Silbert, in D. Swern (Editor), *Organic Peroxides*, Vol. 2, Wiley-Interscience, New York, 1971, Ch. 7, p. 637.
36 L.S. Silbert, in D. Swern (Editor), *Organic Peroxides*, Vol. 2, Wiley-Interscience, New York, 1971, Ch. 7, pp. 742 and 778.
37 W.H.T. Davison, *J. Chem. Soc.*, (1951) 2456.
38 P.A. Giguire and A.W. Olmos, *Can. J. Chem.*, 30 (1952) 821.

Journal of Chromatography, 637 (1993) 167–173
Elsevier Science Publishers B.V., Amsterdam

CHROM. 24 937

Simultaneous determination of the herbicides glyphosate, glufosinate and bialaphos and their metabolites by capillary gas chromatography–ion-trap mass spectrometry

N. Tsunoda

National Research Institute of Police Science, 6, Sanban-cho, Chiyoda-ku, Tokyo 102 (Japan)

(First received September 25th, 1992; revised manuscript received January 2nd, 1993)

ABSTRACT

A sensitive gas chromatographic (GC)–ion-trap mass spectrometric (IT-MS) method has been developed to determine simultaneously the herbicides glyphosate, glufosinate and bialaphos and their major metabolites. A single-step derivatization is achieved at 80°C for 30 min with the reagent N-methyl-N-(*tert.*-butyldimethylsilyl)trifluoroacetamide in dimethylformamide, which introduces the *tert.*-butyldimethylsilyl group at active hydrogens and gives only a single peak for each compound. The derivatives of three herbicides, their metabolites and nineteen amino acids were simultaneously chromatographed and well separated in a single run on a DB-1 fused-silica capillary column. Each *tert.*-butyldimethylsilylated derivative produces an easily interpretable mass spectrum dominated by unique M − 15, M − 57, M − 85 and M − 159 fragment ions. The limits of detection were estimated to be 10–20 ng for glyphosate and glufosinate and their metabolites, and 500 ng for bialaphos, by GC–IT-MS. On the other hand, using GC analysis with flame ionization detection, glyphosate and glufosinate and their metabolites were detectable at levels of approximately 100 ng, but bialaphos could not be detected at a level of 5000 ng.

INTRODUCTION

Glyphosate [N-(phosphonomethyl)glycine] (GLYP), glufosinate [DL-homoalanine-4-yl-(methyl) phosphinic acid] (GLUF) and bialaphos [L-2-amino-4-(hydroxy)(methyl) phosphonoyl]butyryl-L-alanine (BIAL) are broad-spectrum, non-selective herbicides with an increasing number of international users, including in Japan. And there is great interest in the need to determine these herbicides and their major metabolites, aminomethyl phosphonic acid (AMPA), 3-methylphosphinico propionic acid (MPPA) and L-2-amino-4-[(hydroxy)(methyl) phosphinoyl] butyric acid (AMPB, enantiomer of DL-GLUF), in physiological, food, plant, water and soil samples. Their chemical structures and proposed metabolic pathways are shown in Fig. 1.

Various approaches to the analyses of GLYP, GLUF and BIAL and their metabolites have been taken. These include gas chromatography (GC) after chemical derivatization [1–7], high-performance liquid chromatography (HPLC) utilizing pre- or post-column fluorogenic labelling [8–14] and thin-layer chromatography [7, 15–19]. However, these methods are not suitable for simultaneous determination. Recently, the simultaneous detection of the herbicides by paper chromatography [20] has been demonstrated.

This paper describes the simultaneous preparation and analysis of *tert.*-butyldimethylsilyl (*t*BDMS) derivatives of the herbicides and their

0021-9673/93/$06.00

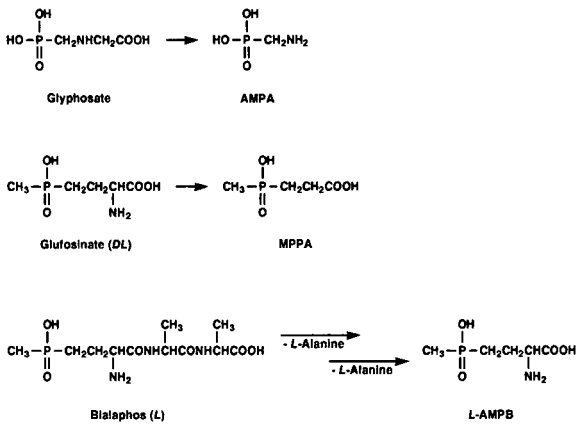

Fig. 1. Proposed metabolic pathways of glyphosate, glufosinate and bialaphos.

metabolites by GC–ion-trap mass spectrometry (IT-MS). The *t*BDMS derivatives are more stable than the trimethylsilyl ones upon storage [21], easily gas chromatographed and give more informative mass spectra in both electron impact (EI) and chemical ionization (CI) mode under moderate conditions without the need for the removal or destruction of the reagent, N-methyl-N-(*tert.*-butyldimethylsilyl)trifluoroacetamide (MTBSTFA) [22–26]. In earlier studies, this reagent has been shown to be a very powerful *t*BDMS donor capable of *tert.*-butyldimethylsilylating active protic functions (*i.e.*, hydroxyl, amino, carboxylic and thiol moieties) [27]. This reagent has been used for the derivatization of sulphate, phosphate and other oxyanions [27], and introduces *t*BDMS groups to inorganic acids [28], amino acids [22–25] and dipeptides [26] at sites having active hydrogens. Furthermore, this reagent allows *t*BDMS derivatization of dicarboxylic acids [29], alkylphosphonic and alkyl methylphosphonic acids [30] and organic sulphonates [31].

MTBSTFA has also been shown to be a useful reagent in the GC analysis of GLYP and its metabolite, AMPA [4], which include hydroxy, amino, carboxylic and methylphosphonic functions in their structures. Also, gas chromatographic analysis of GLUF has been reported to convert into aminoacetyl and methyl derivatives by employing acetic acid–trimethyl orthoacetate [7]. On the other hand, since it has been difficult to detect BIAL as an intact molecule by GC analysis, AMPB, which is the L-isomer of GLUF (Fig. 1), can be indirectly determined using the same GC method for GLUF as described above after acid hydrolysis of BIAL.

The present investigation reports on a simultaneous analytical method that employs the *t*BDMS derivatives of the phosphorus-containing amino acid-type herbicides, GLUF and BIAL, and their metabolites, including GLYP and AMPA, and keeps them intact.

IT-MS is capable of providing full-scan mass spectra on 1 ng of material or less. This enhanced sensitivity, coupled with GC retention indices (*I*), provides the analytical chemist with a powerful means for unambiguous identification and quantitation of trace levels of organic compounds. In this paper, the application of IT-MS to the analyses of the phosphorus-containing amino acid-type herbicides and their metabolites is described.

EXPERIMENTAL

Chemicals

GLYP was supplied by Monsanto Japan (Tokyo, Japan), and AMPA was purchased from Sigma (St. Louis, MO, USA), GLUF and MPPA were donated by Hoechst Japan (Tokyo, Japan), and BIAL and L-AMPB by Meiji Seika Kaisha (Tokyo, Japan). MTBSFTA was purchased from Pierce (Rockford, IL, USA). Nineteen amino acids were obtained from Ajinomoto (Tokyo, Japan). All other compounds were of analytical-reagent grade obtained from Wako (Osaka, Japan).

Gas chromatography–mass spectrometry

GC–MS analyses were performed on a Perkin-Elmer Model 8420 capillary gas chromatograph equipped with an ion trap detector. Chromatographic conditions for these analyses were: a DB-1 fused-silica capillary column (30 m × 0.24 mm I.D., 0.25 μm film thickness; J & W Scientific, Folsom, CA, USA); helium carrier gas at 1 ml/min; GC oven temperature programme, 8°C/min from 100 to 300°C, held for 5 min; injector and transfer line temperature, 320°C; split/splitless injector, split mode, split ratio

1:30, and injection volume, 1 μl. The mass spectrometer was operated in the EI mode or in the CI mode using isobutane as reagent gas at a pressure that has a 3:2 ratio for *m/z* 43 to *m/z* 57. The scan range of the EI mode was from 45 to 650 u at 1 s/scan, and that of the CI mode from 70 to 650 u. Manifold temperature was 220°C. The data system was an IBM PC/AT computer with the automatic gain control software version 4.00.

Straight-chain hydrocarbons were used for the calculation of retention indices.

Gas chromatography

GC analyses were carried out with a Hewlett-Packard (Palo Alto, CA, USA) Model 5890 gas chromatograph equipped with a split/splitless capillary injector port, a flame ionization detector and an HP 3396 integrator. The capillary column used was the same as that for GC–IT-MS. The operating conditions for the chromatograph were: helium carrier gas at 1 ml/min; oven temperature, 160 to 320°C at 8°C/min; injector and detector temperature, 320°C; split ratio 1:50 and injection volume 1 μl.

Derivatization

Solutions (1 mg/ml) of GLYP, GLUF, BIAL and their metabolites and nineteen amino acids in distilled water were prepared. Aliquots (20 μl) of these solutions were transferred into 1-ml PTFE-lined screw-capped derivatization vials. The solvent was evaporated under a gentle stream of nitrogen at 40°C. To the dry residue were added 50 μl of MTBSFTA and 50 μl of dimethylformamide. The mixture was sonicated for 2 min at room temperature, then heated at 80°C for 30 min. After cooling to room temperature, aliquots of the solution containing the derivatives were used directly for GC–IT-MS.

In some experiments the reaction time was varied from 30 to 120 min, and *n*-docosane for quantitative analysis was used as an internal standard. A Pierce Reacti-Thermo block heater was used to heat samples during derivative preparation.

RESULTS AND DISCUSSION

Derivatization reactions

As the reagent employed for *t*BDMS derivative synthesis of amino acids was a mixture of MTBSTFA and acetonitrile, dimethylformamide or tetrahydrofuran [23], a mixture of MTBSTFA and dimethylformamide (1:1) was used for *t*BDMS derivatives of those herbicides and their metabolites in this study. The time courses for the derivatization of GLYP, GLUF and BIAL and their metabolites at 80°C are shown in Fig. 2. For three herbicides and their metabolites, as would be expected, the incubation time of 30–60 min produced almost the highest yields of *t*BDMS derivatives. Sonication of the reaction mixtures for 2 min at room temperature before incubation has an enhancing effect on the responses, reaction rate and reproducibility of *t*BDMS derivatives as compared with those that were not sonicated. In some cases, no peak or fewer peaks of *t*BDMS derivatives were unexpectedly detected without sonication. The resulting derivatives were found to be stable at least for a few days in a refrigerator (data not shown).

Gas chromatographic separation

The *t*BDMS derivatives of GLYP, AMPA, GLUF, MPPA and BIAL eluted as single chro-

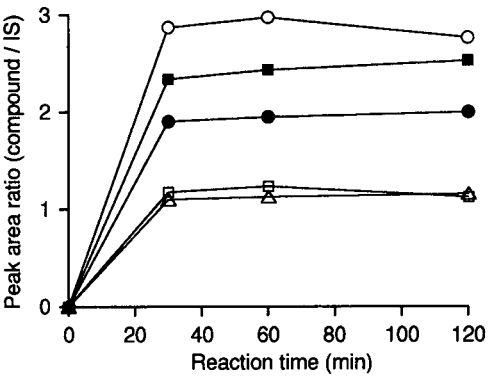

Fig. 2. Kinetics curves for glyphosate, glufosinate and bialaphos and their metabolites at 80°C. The reaction mixture consisted of glyphosate (8 μg, ○), AMPA (5 μg, ●), glufosinate (10 μg, □), MPPA (10 μg, ■), bialaphos (250 μg, △) and *n*-docosane [internal standard (IS), 10 μg] in 100 μl of MTBSTFA–dimethylformamide (1:1). A 1-μl aliquot was injected into the GC–IT-MS system. For GC–IT-MS conditions, see the Experimental section.

matographic peaks, and all peaks showed almost complete baseline separation using a DB-1 fused-silica capillary column. The GC separation of the *t*BDMS derivatives of an amino acid standard mixture presented the same good results. Fig. 3 shows the typical reconstructed total ion chromatograms of the mixture of the herbicides and their metabolites (top) and the mixture of nineteen amino acids (bottom). Of the herbicides studied, each peak showed chromatographic separation and also could be distinguished from all the amino acids studied. The retention data of the *t*BDMS derivatives of the herbicides and amino acids studied on a DB-1 fused-silica capillary column is given in Table I in ascending order of retention index.

The herbicides and their metabolites emerged from the non-polar SE-30 capillary column in order of increasing molecular mass of their derivatives, the same as those of amino acid derivatives [23]. MPPA, the metabolite of GLUF that has the smallest derivatized molecular mass ($M_r = 380$), has the shortest retention time ($I = 2031$), followed by threonine ($I = 2041$), BIAL, the largest derivative ($M_r = 665$) of the herbicides studied, was observed to have the longest retention time ($I = 2642$), followed by tyrosine ($I = 2649$). In these experimental conditions, sufficient resolution was achieved when the I differences between two adjacent peaks was 5

TABLE I

RETENTION INDICES OF GLYPHOSATE, GLUFOSINATE, BIALAPHOS AND THEIR METABOLITES AND NINETEEN AMINO ACIDS AS THEIR *tert.*-BUTYLDIMETHYLSILYL DERIVATIVES

For GC–IT-MS conditions, see the Experimental section.

Compound	Retention index
MPPA	2031
AMPA	2100
Glyphosate	2436
Glufosinate (=AMPB)	2550
Bialaphos	2642
Alanine	1537
Glycine	1553
Valine	1684
Leucine	1726
Isoleucine	1756
Proline	1783
Methionine	1960
Serine	2000
Threonine	2041
Phenylalanine	2094
Aspartic acid	2164
Hydroxyproline	2196
Glutamic acid	2282
Lysine	2389
Arginine	2498
Histidine	2593
Tyrosine	2649
Tryptophan	2938
Cystine	3208

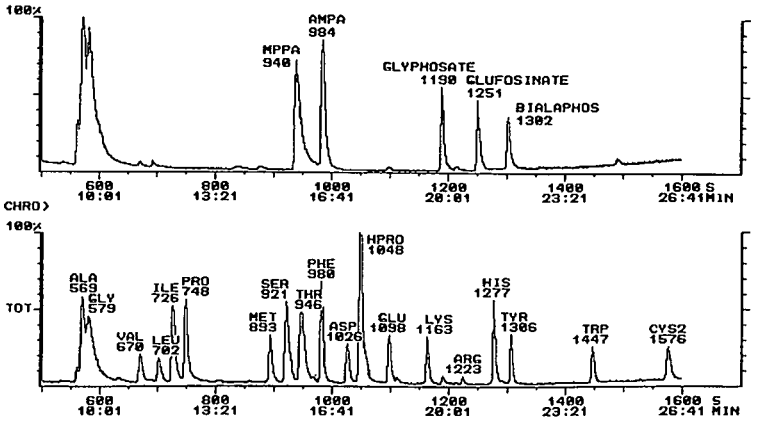

Fig. 3. Total ion chromatograms of the mixture of the herbicides (top) and nineteen amino acids (bottom) as *tert.*-butyldimethylsilyl derivatives. Amino acids: ALA = alanine; GLY = glycine; VAL = valine; LEU = leucine; ILE = isoleucine; PRO = proline; MET = methionine; SER = serine; THR = threonine; PHE = phenylalanine; ASP = aspartic acid; HPRO = hydroxyproline; GLU = glutamic acid; LYS = lysine; ARG = arginine; HIS = histidine; TYR = tyrosine; TRP = tryptophan; CYS2 = cystine. Numbers of peaks are retention times (s). For GC–IT-MS conditions, see the Experimental section.

units or more. Therefore, MPPA, AMPA and BIAL could be distinguished from threonine, phenylalanine and tyrosine by their retention times and mass spectra.

Minimum detectable amounts

The minimum detectable amounts were determined until a signal-to-noise ratio of 3 was reached by GC–MS and GC or a full mass spectrum was measured by GC–MS (Table II). In this way, the minimum detectable amounts obtained were 10–20 ng for GLYP and GLUF and their metabolites and 500 ng for BIAL using their peaks or full mass spectra on GC–IT-MS analyses. On the other hand, the detection limits of gas chromatographic analysis were 60–300 ng for GLYP, GLUF and their metabolites, but 5000 ng of bialaphos gave no peak by the GC method. The sensitivity of the GC–IT-MS method was about ten-fold greater than that of the GC method.

Canned tomato juice submitted to forensic examination was diluted with four volumes of water, and centrifuged. An aliquot of the supernatant was dried *in vacuo*, and the residue after washing with acetone was subjected to GC–MS according to this method. GLYP was identified and confirmed by GC–IT-MS as the *t*BDMS derivative. Glyphosate was adulterated in the specimen at the level of 13.7 ± 0.5 mg/ml ($n = 3$) by GC using peak area *versus* detector response. The calibration curve was plotted for concentration of 1–100 μg per vial.

TABLE II

LOWER DETECTION LIMITS OF GLYPHOSATE, GLUFOSINATE, BIALAPHOS AND THEIR METABOLITES AS THEIR *tert.*-BUTYLDIMETHYLSILYL DERIVATIVES BY GC–IT-MS (ng)

GC–IT-MS and GC conditions as in the Experimental section. ++ = Detected easily; + = detected; − = not detected.

Compound	GC–IT-MS		GC
	Peak	Full mass spectrum	
Glyphosate	10 (+)	10 (−)	100 (++)
AMPA	10 (++)	10 (+)	60 (++)
Glufosinate	20 (+)	20 (+)	300 (++)
MPPA	20 (+)	20 (+)	100 (++)
Bialaphos	500 (+)	500 (+)	5000 (−)

Mass spectra

Although few ion-trap mass spectra of organic compounds have been published, the fragmentation patterns obtained are, in most respects, very similar to those obtained on conventional quadrupole and magnetic-sector instruments. By obtaining both EI and CI ion-trap mass spectra, the expected structures of *t*BDMS derivatives were confirmed for the herbicides and their metabolites.

In the CI mode, quasi-molecular ions (MH^+) of *t*BDMS-derivatized GLYP and GLUF and their metabolites were revealed as the base peaks. The EI mass spectra of GLYP, AMPA, GLUF, MPPA and BIAL as *t*BDMS derivatives are shown in Fig. 4 and their diagnostic ions are compiled in Table III. Ionization in the EI mode produced for these derivatives two strong [M − 57 as the base peak; loss of $C(CH_3)_3$, m/z 73; $Si(CH_3)_3$] and less intense (M − 15; loss of CH_3) ions, as was observed for the derivatives of the oxyanions and amino acids [23–25,27]. No molecular ion was observed for any derivative except GLYP. The molecular or quasi-molecular ion of *t*BDMS-derivatized BIAL (m/z 665 or 666) could not be confirmed because the scan range of the IT-MS system is from m/z 45 to 650.

M − 15 and M − 57 ions for GLYP, AMPA and GLUF indicated that three *t*BDMS groups were introduced into their molecules, and two *t*BDMS groups were introduced into the metabolite of GLUF, MPPA. An m/z 364 ion of GLUF, due to [M − 156(COO*t*BDMS)], suggests that the secondary amino group after introducing one *t*BDMS group into the primary amino moiety is not silylated in the same manner as GLYP and AMPA.

The mass spectrum of the derivatized BIAL, a kind of dipeptide, in the EI mode showed two characteristic fragment ions, m/z 364 and 324. These dominant ions in the EI spectrum of *t*BDMS-derivatized dipeptides originate from the N-terminal amino acid. The base peak ion m/z

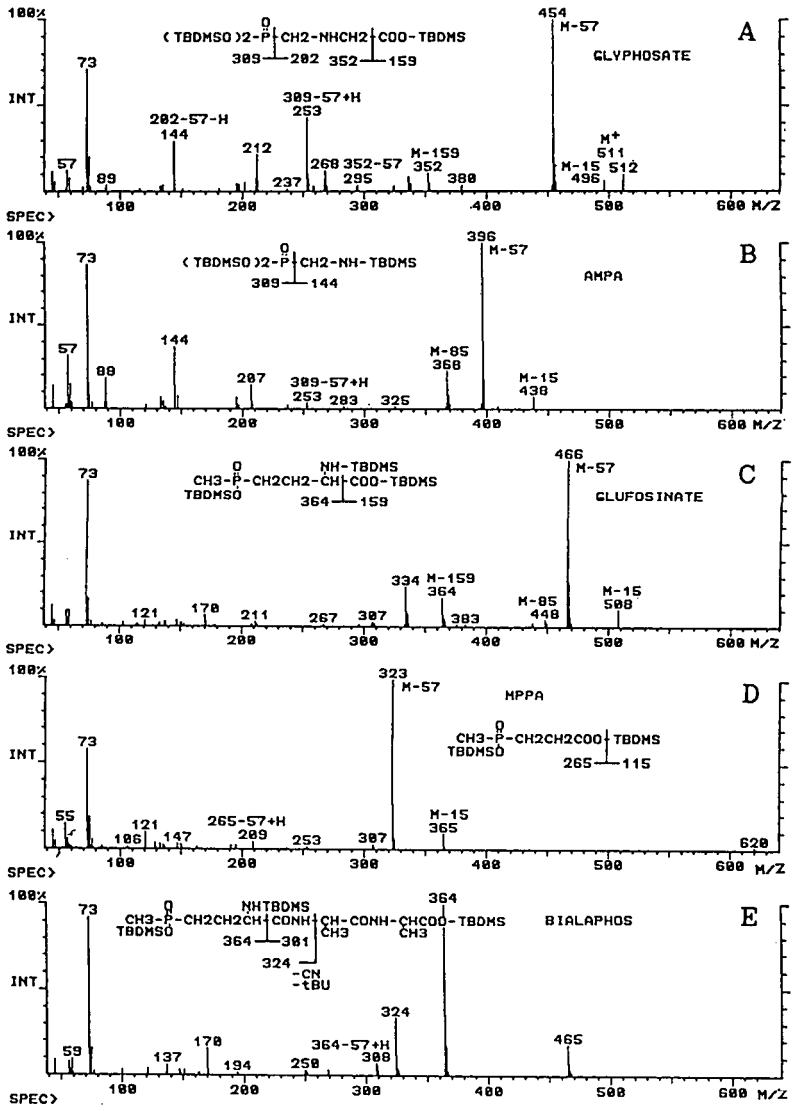

Fig. 4. EI mass spectra of *tert.*-butyldimethylsilyl derivatives of (A) glyphosate, (B) AMPA, (C) glufosinate, (D) MPPA and (E) bialaphos.

364 results from cleavage of the CH–CO bond to the N-terminal acid. This fragment ion is also found in the *t*BDMS derivatives of the corresponding amino acid, but at a lower intensity. A further peak, m/z 324, is observed at an m/z 40 less than this fragment. This fragment may arise from cleavage of the central NH–CH bond followed by loss of *tert.*-butyl and a cyanide radical. The distinctive pair of ions separated by m/z 40 clearly distinguishes the spectra of amino acid and dipeptide *t*BDMS derivatives [26].

CONCLUSIONS

A selective and sensitive GC–MS method using IT-MS as a mass detection system has been developed for the determination of GLYP, GLUF and BIAL and their metabolites. The sample preparation method is simple by derivatization with MTBSTFA and dimethylformamide. This procedure allows the determination of these herbicides and their metabolites simultaneously.

The GC–IT-MS method offers more sensitivi-

TABLE III

DIAGNOSTIC IONS IN THE EI MASS SPECTRA OF THE *tert.*-BUTYLDIMETHYLSILYL DERIVATIVES OF GLYPHOSATE, GLUFOSINATE, BIALAPHOS AND THEIR METABOLITES OBTAINED IN GC–IT-MS

BP, base peak; –, not detected.

Compound (M_r)	M^+	M – 15	M – 57	M – 85	M – 159	Others
Glyphosate (511)	511	496	454(BP)	–	352	73, 144, 212, 253
AMPA (453)	–	438	396(BP)	368	–	73, 144, 207, 253
Glufosinate (523)	–	508	466(BP)	438	364	73, 334
MPPA (380)	–	365	323(BP)	–	–	73, 121, 209
Bialaphos (665)	–	–	–	–	–	73, 170, 308, 324, 364(BP), 465

ty than the GC method. Monitoring several ions at m/z M – 15, M – 57 and M – 159 for *t*BDMS derivatives affords additional structural confirmation beyond retention time matching with a reference standard. This was found to be useful in the determination of the herbicides and discriminating them from amino acids typically found in physiological and food samples.

ACKNOWLEDGEMENTS

The author thanks Monsanto Japan, Hoechst Japan and Meiji Seika Kaisha Ltd. for the donation of the herbicides and their metabolites.

REFERENCES

1 M.L. Rueppel, L.A. Suba and J.T. Marvel, *Biomed. Mass Spectrom.*, 3 (1976) 28.
2 M.L. Rueppel, B.B. Brightwell, J. Schaefer and J.T. Marvel, *J. Agric. Food Chem.*, 25 (1977) 517.
3 R.A. Guinivan, N.P. Thompson and W.B. Wheeler, *J. Assoc. Off. Anal. Chem.*, 65 (1982) 35.
4 H.A. Moye and C.L. Deyrup, *J. Agric. Food Chem.*, 32 (1984) 192.
5 C.L. Deyrup, S-M. Chang, R.A. Weintraub and H.A. Moye, *J. Agric. Food Chem.*, 33 (1985) 944.
6 D.N. Roy and S.K. Konar, *J. Agric. Food Chem.*, 37 (1989) 441.
7 A.E. Smith, *J. Agric. Food Chem.*, 37 (1989) 267.
8 A.J. Burns and D.F. Tomkins, *J. Chromatogr. Sci.*, 17 (1979) 333.
9 H. Roseboom and C.J. Berkhoff, *Anal. Chim. Acta*, 135 (1982) 373.
10 R.L. Glass, *J. Agric. Food Chem.*, 31 (1983) 280.
11 H.A. Moye, C.J. Miles and S.J. Scherer, *J. Agric. Food Chem.*, 31 (1983) 69.
12 L.N. Lundgren, *J. Agric. Food Chem.*, 34 (1986) 535.
13 D.G. Thompson, J.E. Cowell, R.J. Daniels, B. Staznik and L.M. MacDonald, *J. Assoc. Off. Anal. Chem.*, 72 (1989) 355.
14 Y.Y. Wigfiels and M. Lanouette, *Anal. Chim. Acta*, 233 (1990) 311.
15 O. Gottrup, P.A. Sullivan, R.J. Schraa and W.H. Vanden Born, *Weed Res.*, 16 (1976) 197.
16 J.C. Young, S.U. Khan and P.B. Marriage, *J. Agric. Food Chem.*, 25 (1977) 918.
17 M.T.H. Ragab, *Chemosphere*, 2 (1978) 143.
18 A. Suzuki, K. Nishida, M. Shimura and I. Yamamoto, *J. Pesticide Sci.*, 12 (1987) 105.
19 A.E. Smith, *J. Agric. Food Chem.*, 36 (1988) 393.
20 A. Suzuki and M. Kawana, *Bull. Environ. Contam. Toxicol.*, 43 (1989) 17.
21 E.J. Corey and A. Venkateswarlu, *J. Am. Chem. Soc.*, 94 (1972) 6190.
22 S.L. MacKenzie and D. Tenaschuk, *J. Chromatogr.*, 322 (1985) 228.
23 T.P. Mawhinney, R.S.R. Robinett, A. Atalay and M.A. Madson, *J. Chromatogr.*, 358 (1986) 231.
24 S.L. MacKenzie, D. Tenashuk and G. Fortier, *J. Chromatogr.*, 387 (1987) 241.
25 H.J. Chaves das Nevas and A.M.P. Vacsoncelos, *J. Chromatogr.*, 392 (1987) 249.
26 M.E. Corbett, C.M. Scrimgeour and P.W. Watt, *J. Chromatogr.*, 419 (1987) 263.
27 T.P. Mawhinney and M.A. Madson, *J. Org. Chem.*, 47 (1982) 3336.
28 T. Mawhinney, *J. Chromatogr.*, 257 (1983) 37.
29 T.P. Mawhinney, R.S.R. Robinett, A. Atalay and M.A. Madson, *J. Chromatogr.*, 361 (1986) 117.
30 J.G. Purdon, J.G. Pagotto and R.K. Miller, *J. Chromatogr.*, 475 (1989) 261.
31 L.-K. Ng and M. Hupe, *J. Chromatogr.*, 513 (1990) 61.

Journal of Chromatography, 637 (1993) 175–179
Elsevier Science Publishers B.V., Amsterdam

CHROM. 24 935

Extraction and analysis of diesel fuel by supercritical fluid extraction and microbore supercritical fluid chromatography

Matthew W. Brooks* and Peter C. Uden

Department of Chemistry, University of Massachusetts, Amherst, MA 01003 (USA)

(First received October 2nd, 1992; revised manuscript received February 2nd, 1993)

ABSTRACT

Supercritical fluid extraction was used to extract diesel fuel from soil. Extraction efficiency was greater than 90% regardless of the organic content of the soil and even after the soil had been aged for five days before analysis. Analysis of extracts by microbore supercritical fluid chromatography provided rapid characterization while GC–MS was used for analysis of residue levels.

INTRODUCTION

As environmental concerns grow, so does the need for rapid and reliable analytical methodology. One area of concern is contamination from underground storage tanks. In Massachusetts, where 80% of its municipalities rely on groundwater for their community drinking water [1], stringent penalties for polluters have been adopted under general law 21E [2].

Analytical methodology for extraction and analysis of soil for diesel fuel has largely been confined to extraction with dichloromethane [3], or alkalized methanol [4]. Both these techniques illustrate the problems associated with present environmental methods; (a) they are slow, requiring a minimum of two or more hours, and (b) they generate their own hazardous waste.

Further, the sample preparation step makes it virtually impossible to carry out the analytical procedure "on site". The increasing utilization of mobile laboratories has enhanced the demand for methods which require little or no sample clean-up.

Supercritical fluid extraction (SFE) is increasingly becoming the technique of first choice for new environmental methodology. A general rule is that by increasing the pressure of the supercritical fluid, the solvating power of the fluid is increased [5]. This is a highly simplistic view of the dynamics of SFE and only appropriate for compounds sharing similar degrees of polarity to the fluid. For example carbon dioxide has a dipole moment of zero; increasing its density increases its ability to solubilize apolar analytes. This makes supercritical carbon dioxide an ideal vehicle for extraction of alkanes in fossil fuels from environmental matrices.

Supercritical fluid chromatography (SFC) has been recently somewhat overshadowed by SFE. Since the same equipment can often be used for both SFC and SFE, this technique combination presents an excellent tool for mobile laboratories where space is a premium.

Microbore column SFC presents several advantages over both capillary SFC and conventional packed column SFC [6]. Microbore offers

* Corresponding author.

0021-9673/93/$06.00

the same advantages of packed column SFC over capillary column SFC [7], namely (a) a wide choice of stationary phases, (b) use of modifier gradients with organic solvents, and (c) use of less expensive grade carbon dioxide. However, microbore columns also boast advantages of capillary SFC, *i.e.*, being mobile phase linear velocities closer to optimum and less fluid consumption compared to standard packed SFC. Microbore SFC allows a simple 0.53 μm O.D. fused-silica capillary to act as a restrictor and still maintain flow-rates between 0.5 and 1.5 ml/min, consequently not extinguishing the flame in the flame ionization detector at higher pressures. Microbore SFC has been used previously for analysis of pesticides [8].

This paper considers extraction of diesel fuel from soil, followed by analysis with either SFC or GC–MS. The extraction requires only a brief concentration step. SFC allows rapid on site analysis of soil contaminated by diesel spills while GC–MS analysis can be used for trace analysis. The effects of organic materials and water on the extraction efficiency are also explored.

EXPERIMENTAL

Reagents

Organic soil was potting soil purchased from Frank's Florist (Hadley, MA, USA). Low organic soil was collected at the University of Massachusetts (Amherst, MA, USA). Diesel fuel was automobile grade and purchased from Pride service station (Hadley, MA, USA). Dichloromethane was HPLC grade (Fisher Scientific, Springfield, NJ, USA) and liquid carbon dioxide was from Scott Specialty Gases (Plumsteadville, PA, USA).

Supercritical fluid extractions

Aliquots of 1 to 2 g of 40/60 mesh sieved soil were spiked with various amounts of diesel fuel. The fuel spikes were delivered in 50 μl of dichloromethane, the solvent was allowed to evaporate and the samples were placed in an empty 15 cm × 4 mm I.D. liquid chromatography column for extraction. The apparatus (Fig. 1), was a Suprex Model 200A supercritical fluid chromatograph which had been modified so that extractions could alternately be carried out with chromatographic separations [9]. Samples were extracted for 10 min at 290 atm CO_2 (1 atm = $1.01 \cdot 10^5$ Pa) and ambient temperature (23–25°C) and collected in 10 ml dichloromethane. The dichloromethane extract was then reduced to 0.5 ml for analysis. Since the extraction was carried out below the critical temperature for carbon dioxide (31°C), it did not utilize a true supercritical fluid but rather a material in a dynamic gas–liquid equilibrium (*i.e.*, a "supercritical-like" fluid).

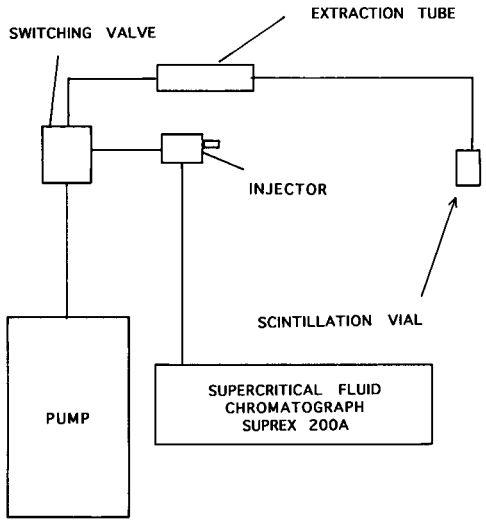

Fig. 1. Block diagram of SFE–SFC apparatus. A switching valve diverted the mobile phase to either the extraction vessel or the chromatograph.

In some cases the soils were extracted moments after spiking while in others the spikes were aged for 5 days in the dark under ambient conditions.

Supercritical fluid chromatography

A Suprex Model 200A supercritical fluid chromatograph equipped with a flame ionization detector was used. The unmodified carbon dioxide mobile phase was pressure programmed from 80 atm (3 min) to 165 atm at 5.7 atm/min then to 200 atm at 11.7 atm/min. The carbon dioxide effluent was restricted with 0.53 mm O.D. inert fused silica tubing to give a flow-rate of approximately 200 ml/min at ambient pressure for a pump head pressure of 80 atm. The oven con-

tained a 250 mm × 1 mm I.D. microbore Hypersil ENV column (Keystone Scientific, Bellefonte, PA, USA) and was maintained at 100°C. The flame ionization detector was operated at 250°C with hydrogen at 30 ml/min and air at 180 ml/min. Diesel fuel recoveries were quantitated by peak height against a one-point standard corresponding to 100% recovery. Comparison of random samples against a three-point curve gave equivalent recovery values to those obtained against the single standard.

Gas chromatography–mass spectrometry

Extracts analyzed by GC–MS utilized an HP 5890 equipped with an HP 5970A mass selective detector (Hewlett-Packard, Avondale, PA, USA). The 60-m DB-1 column (J & W Scientific, Folsom, CA, USA) was temperature programmed from 100°C (1) to 250°C (2) at 10°C/min. The injector and interface zones were maintained at 50°C and 280°C, respectively. Data acquisition was by single ion monitoring (SIM) for ion masses 57, 71, 85, 99, 113, 127, 140 and 155. Quantitation was by peak area against a reference standard equal to 100% recovery.

RESULTS

The soil utilized was arbitrarily classified as either 'high organic' or 'low organic' for the purpose of these experiments. High organic soil contained approximately 11% organic carbon while low organic soil was determined to contain about 3% organic carbon (Table I). All soil was dried at 100°C for 24 hr before use. SFE provided an effective means for extraction with recoveries greater than 90% (Table I). The presence of organic matter did not appreciably affect diesel fuel recoveries, not did aging the spikes for one week. Addition of water, however, reduced recoveries.

Microbore SFC provided rapid and reproducible diesel fuel chromatograms (Fig. 2A) and gives an excellent means for spill identification. The unmodified carbon dioxide eluent did not extract extraneous materials from either type of soil (Fig. 2B). Sensitivity limitations of the FID and SFC capacity limitations (low injection volumes) limit the technique to ppt (w/w) detection limits. However with spills where concentrations of this magnitude exist, identification is simple and rapid even after sample aging (Fig. 3).

TABLE I

RECOVERY OF DIESEL FUEL FROM VARIOUS MATRICES

Soil type[a]	Aging period (days)	% Recovery ± S.D.[b]
Low organic	0	97 ± 10
High organic	0	108 ± 4
Low organic	5	96 ± 10
High organic	5	108 ± 1
Low organic + water[c]	0	61 ± 2
High organic[d]	0	102 ± 3
High organic[d]	5	92 ± 10

[a] As defined in text, low organic soil contains 3% organic carbon while high organic soil contains 11% organic carbon.
[b] Recoveries are an average of 2 spikes with standard deviation. Unless otherwise specified, spikes were 43 mg total diesel fuel per 2 g soil (roughly 2%, w/w) and were determined by SFC.
[c] Soil was adjusted to be 10% (w/w) aqueous.
[d] These values were obtained by GC–MS for 30 ppm (w/w) soil spikes.

GC–MS analysis of diesel fuel gives a typical

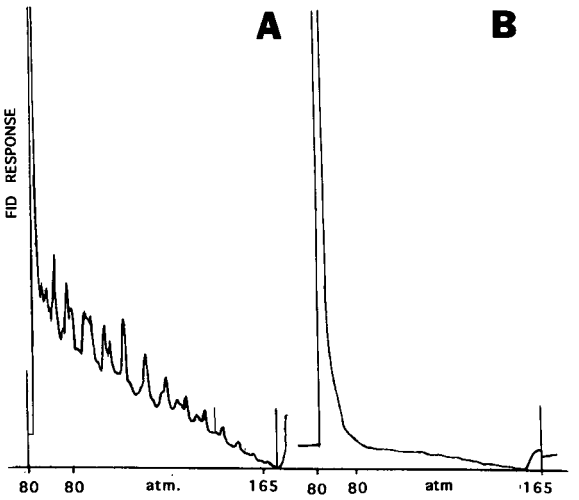

Fig. 2. Analysis of diesel fuel by SFC. (A) A 100-nl injection of an 86 mg/ml diesel fuel standard. SFC conditions as given in text. (B) A 100-nl injection of blank high organic soil extract. The 10-ml extraction was reduced to 0.5 ml for analysis.

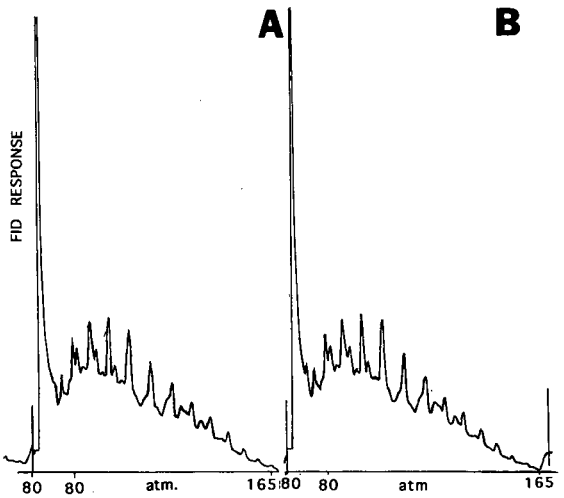

Fig. 3. Analysis of soil spikes by SFC. (A) A 100-nl injection of high organic soil spike. Sample was extracted within minutes of spiking. A 2-g soil sample was spiked with 43 mg diesel fuel. The 10-ml extract was reduced to 0.5 ml for analysis. (B) A 100-nl injection of high organic spike aged 5 days before analysis. Concentrations the same as those for A.

hydrocarbon profile (Fig. 4) and this technique enhanced detection significantly compared to SFC, with limits of 1–10 ppm being easily obtainable. Fig. 5 is an example of a SIM-GC–MS analysis of a 30-ppm soil spike extract. Mass spectrometry showed that analyte recoveries of residue level diesel contamination were similar to values obtained from spill level recoveries.

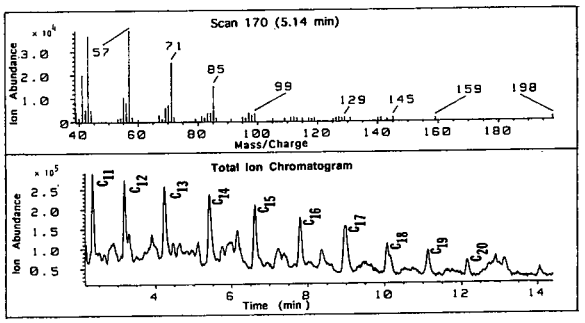

Fig. 4. Total ion chromatogram of 1 mg/ml diesel fuel standard. Chromatographic conditions as given in text, 2 μl injected in the splitless mode. Peaks are identified by carbon number on chromatogram.

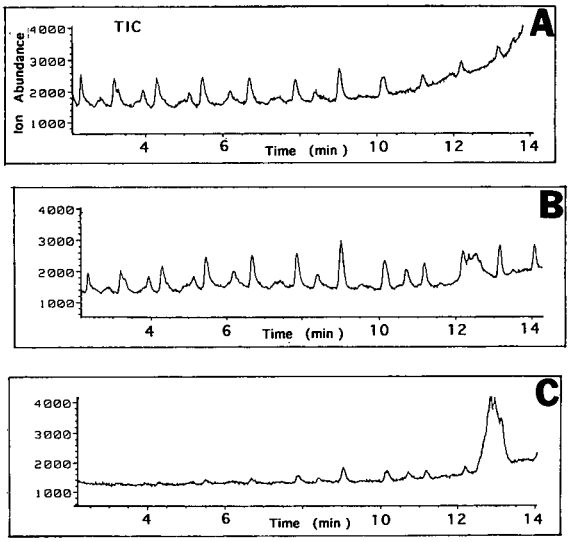

Fig. 5. Single ion monitoring chromatograms of 30 ppm soil spikes. Ions monitored are listed in text. (A) Extracted ion profile of a 2-μl injection of a 120 μg/ml standard. (B) Ion profile of a 30-ppm high organic soil spike recovery which was extracted moments after spiking. Final extract volume was 0.5 ml to give an expected concentration of 60 μg/0.5 ml. An aliquot of 2 μl was injected. (C) Ion profile of 2 g high organic soil which was not spiked with diesel fuel.

DISCUSSION

SFE is a simple yet powerful tool for extraction of diesel fuel from soils. The selectivity of unmodified supercritical carbon dioxide for apolar compounds provides an excellent medium for extraction of the alkane series from petroleum fuels. The fact that effectiveness is not diminished as organic content is increased shows that even high levels of polar or slightly polar materials are not easily swept into the supercritical effluent. This dimension provides exciting prospects for designing clean-up steps with modified and unmodified carbon dioxide. The decrease in efficiency in the presence of water has been previously noted [10]. In solid phase extraction, large aqueous samples eventually form a hydrophobic envelope about the absorbing surface [11]; an analogous situation may be occurring here. Since water has such a dramatic effect of supercritical recoveries, addition of drying agents

such as Celite or sodium sulfate may enhance recoveries.

The utilization of SFC provides the analyst with a rapid (less than 1 hour from receipt of sample) and efficient means of on-site analyses. The use of microbore columns allows the chemist more flexibility with restrictors *vs.* standard packed columns and greater column capacity and ruggedness *vs.* capillary columns, which tend to become brittle in the presence of cold supercritical carbon dioxide.

ACKNOWLEDGEMENTS

The support of the Union Carbide Corporation and Merck, Sharp and Dohme Research Laboratories is gratefully acknowledged.

REFERENCES

1 M. Sheehan, *Boston Bar J.*, Jan./Feb. (1987) 177.
2 J. Shotwell, *Boston Bar J.*, Jan./Feb. (1988) 203.
3 M. Hiatt and T. Jones, *J. High Resolut. Chromatogr. Chromatogr. Commun.*, 8 (1985) 4.
4 J. Albaiges and J. Grimalt, *Int. J. Environ. Anal. Chem.*, 31 (1987) 281.
5 S. Hawthorne, *Anal. Chem.*, 62 (1990) 633A.
6 F. Onuska and K. Terry, *J. High Resolut. Chromatogr.*, 13 (1990) 317.
7 F. Verillon, D. Heems, B. Pichon, K. Coleman and J. Robert, *Am. Lab.*, June (1992) 45.
8 J. Wheeler and M. McNally, *J. Chromatogr. Sci.*, 27 (1989) 534.
9 M. Davis, *Ph.D. Dissertation*, University of Massachusetts, Amherst, MA, 1991.
10 A. Emery, S. Chesler and W. MacCrehan, *J. Chromatogr.*, 606 (1992) 221.
11 M. Brooks, J. Jenkins, M. Jimenez, T. Quinn and J. Clark, *Analyst*, 114 (1989) 405.

Journal of Chromatography, 637 (1993) 181–186
Elsevier Science Publishers B.V., Amsterdam

CHROM. 24 926

Validation of the aromatic ring distribution in diesel fuel refinery streams by supercritical fluid chromatography and mass spectrometry

Evan N. Chen, Jr.*, Patrice D. Cusatis and Edward J. Popiel

Texaco Research & Development, P.O. Box 509, Beacon, NY 12508 (USA)

(Received November 5th, 1992)

ABSTRACT

In anticipation of stricter environmental mandates, a new supercritical fluid chromatographic (SFC) method has been developed to determine the aromatic ring distribution in various diesel fuel refinery streams. Although preparative open column liquid chromatography (OCLC) followed by mass spectral (MS) quantitation is often used to determine the individual aromatic ring types, this procedure is quite time consuming and labor intensive. The SFC technique described here provides rapid, quantitative hydrocarbon analysis of the aromatic ring species without prior OCLC separation. Nearly fifty test diesel fuels, ranging from 6.0 to 48.0% (w/w) total aromatics, originating from separate refineries, have been analyzed. Excellent correlation has been established between the OCLC–MS data and the SFC results confirming the validity of this new SFC method.

INTRODUCTION

Various state and local environmental laws have stipulated that drastic reductions in the level of aromatic hydrocarbons in diesel fuels must be made in order to decrease harmful exhaust emissions which can lead to smog. Anticipating this to be federal regulation, appropriate analytical methods are needed to insure that diesel fuels meet these restrictions.

In the petroleum industry, classical liquid chromatography (LC) is widely used for determination of aromatics in light and middle distillate fuels. Unfortunately, the fluorescence indicator adsorption method (ASTM D1319) [1] and preparative open column liquid chromatography (OCLC) (modified ASTM D2549) [2] are labor intensive, time consuming, and cannot be automated. In addition, the precision of the fluorescence indicator adsorption method is poor since diesel fuels are beyond the scope of this method.

Hydrocarbon analysis by high-performance liquid chromatography (HPLC) has been successful [3–6], but this technique lacks a universal detector which can respond uniformly to the hydrocarbons typically found in petroleum fractions. Nuclear magnetic resonance (NMR) and mass spectrometry (MS) are effective in providing detailed structural information compositional analysis. Unfortunately, NMR results are usually reported in terms of aromatic carbon [7,8] and prior sample preparation is often required for MS [9] rendering these techniques less desirable for routine analysis.

Supercritical fluid chromatography (SFC) with flame ionization detection (FID) has proven to be quite effective for the analysis of total aromatics in diesel fuels [10–14]. In addition, the American Society for Testing and Materials (ASTM) has recently approved a new standard test method to determine the aromatic content in diesel fuels (ASTM D5186) [15]. Unfortunately,

* Corresponding author.

0021-9673/93/$06.00

these techniques do not describe the separation and quantitation of the aromatic ring distribution. Although the total aromatic content is generally considered the parameter responsible for hazardous emissions, recent studies suggest that diaromatics and triaromatics have a stronger influence on diesel particulates than monoaromatics [16].

Aromatic types in middle distillates are typically determined by separating the saturate components from the aromatics by OCLC with subsequent MS quantitation [17] of the individual ring species. The precision and accuracy of the data are good, however, this procedure is quite time consuming. In addition, running the OCLC–MS requires a large amount of solvent, tedious evaporation step, and the high cost of specialty glassware and mass spectral instrumentation.

This paper reports the development of an improved, automated SFC method which is time and cost efficient, not as labor intensive, and applicable to different diesel refinery streams. More importantly, this technique covers the hydrocarbon analysis and quantitation of the aromatic ring distribution without the need for prior OCLC separation.

EXPERIMENTAL

Apparatus

A Computer Chemical Systems 7000 controller/fluid delivery system (CCS, Avondale, PA, USA) was used to convert a 5890 gas chromatograph (Hewlett-Packard, Paramus, NJ, USA) into a fully functional SFC system. The system was equipped with a 50-ml syringe pump, a 0.1-μl injection valve, and a FID system. The chromatographic data were processed using the Hewlett-Packard HP-3350 laboratory automation system with C-PLOT software.

Materials

Hexane and carbon disulfide (CS_2) (Aldrich, Milwaukee, WI, USA) were of HPLC grade. The carbon dioxide mobile phase (Scott Specialty Gases, South Plainfield, NJ, USA) was of SFC grade and contained a 1500 p.s.i. (1 p.s.i. = 6894.76 Pa) cylinder head pressure. The performance mixture consisted of hexane, hexadecane (Aldrich) benzene, toluene, indane, phenyldecane, naphthalene, 2,3,6-trimethylnaphthalene, fluorene, dibenzothiophene, anthracene, fluoranthene and pyrene (ChemService, West Chester, PA, USA).

Validation of SFC system

Total aromatic content. To verify the accuracy of the SFC system, each test diesel fuel was first separated into their actual saturate and aromatic fractions by OCLC. The actual aromatic fraction was then compared to the total aromatic FID response of the original diesel fuel as shown in Fig. 1. Excellent correlation was obtained for diesel fuels ranging from 6.0 to 48.0% (w/w) total aromatics and was consistent with different refinery streams.

Aromatic ring distribution. Initially, the aromatic fraction obtained by OCLC of each standard sample was further quantitated for the individual ring species by MS and SFC. The separation scheme used to validate the SFC system for aromatic types is given in Fig. 2. It should be noted that the OCLC procedure [2] was modified for middle distillates in order to achieve the highest possible recovery of the individual hydrocarbon fractions. Upon validation, the original diesel fuels were then injected directly into the SFC system for aromatic type analysis, bypassing the OCLC separation and the need for solvent evaporation.

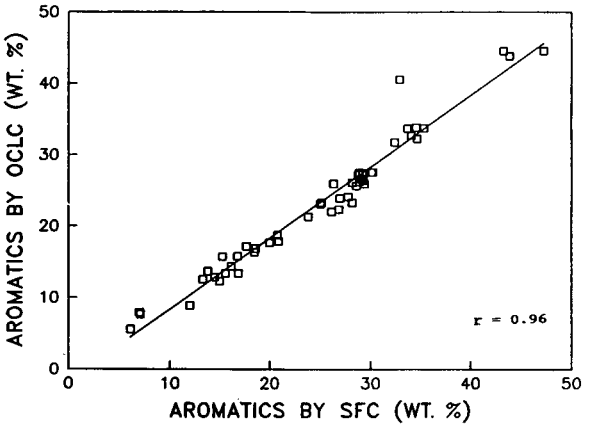

Fig. 1. Analysis of total aromatics in diesel fuels by OCLC *versus* SFC.

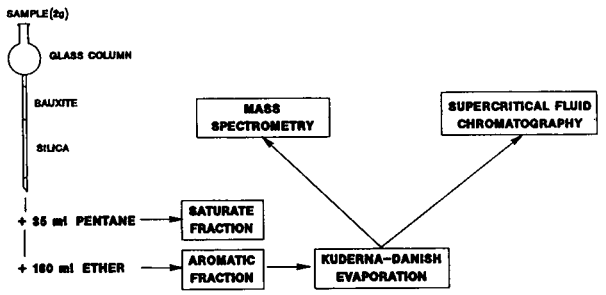

Fig. 2. Separation scheme for the validation of the aromatic ring distribution in diesel fuels.

Chromatographic procedure

The hydrocarbon group separation was accomplished with a Chromegabond cyano column (25 cm × 2.0 mm I.D., 5 μm spherical particle size) connected in series with a Chromegasphere SI-60 silica column (25 cm × 2.0 mm I.D., 5 μm spherical particle size) (ES Industries, Marlton, NJ, USA). The columns were maintained at a constant temperature (40°C) and pressure (4500 p.s.i.) throughout the entire analysis.

The CO_2 flow-rate exiting the tapered stainless-steel post-column restrictor was 45 ml/min. The FID system was operated at 350°C and the air and hydrogen flows were 300 and 47 ml/min, respectively. These parameters represent the most optimal conditions for separating the saturate and aromatic ring fractions on this SFC system.

The performance mixture was prepared by making a 0.2% (w/w) solution of each component in hexane. Upon equilibration, 0.1 μl of original diesel fuel was injected into the SFC system and the entire analysis was accomplished in less than 45 min.

RESULTS AND DISCUSSION

For aromatic type analysis, the performance mixture was injected and the retention time regions according to aromatic ring number were recorded as shown in Fig. 3a. A corresponding SFC chromatogram of a diesel fuel is shown in Fig. 3b. The first peak of the model compounds consisted entirely of hexane and hexadecane, while all the monoaromatics eluted in the region between benzene and just before naphthalene;

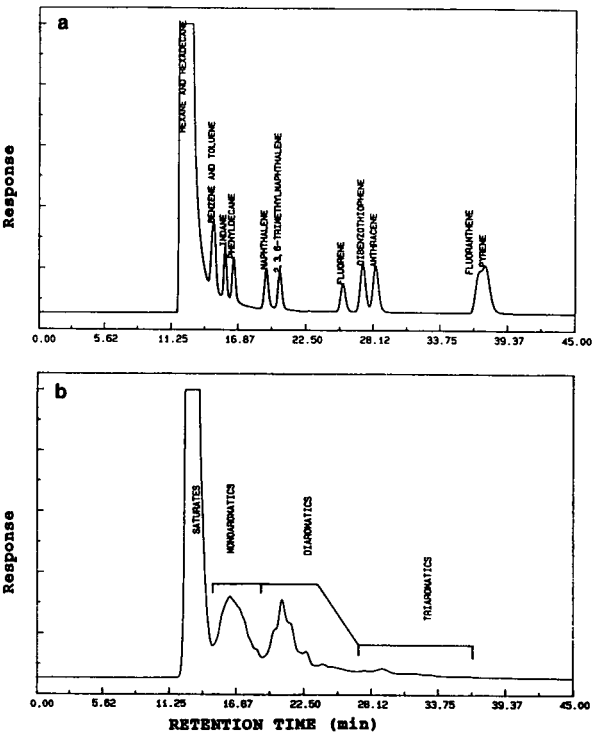

Fig. 3. SFC chromatogram of (a) performance mixture and (b) original diesel fuel employing the same chromatographic conditions.

all the diaromatics between naphthalene and just before dibenzothiophene; and all the triaromatics and higher between dibenzothiophene and the final return to the baseline at the end of the chromatogram. For the fuels analyzed, we did not find any aromatic components containing more than three rings. The aromatic retention time ranges of the performance mixture were recorded before every set of five diesel fuels. This accounted for any fluctuations in the retention time of the sample caused by the plugging of the restrictor or column degradation.

Using the validation procedure shown in Fig. 2, the OCLC aromatic fraction of each fuel was analyzed by both MS and SFC techniques. Fig. 4 shows the comparison between the OCLC–MS and OCLC–SFC data for the aromatic ring distribution of nearly fifty test diesel fuels. There was a slight bias towards higher SFC results for the monoaromatics as shown in Fig. 4a. On the other hand, Fig. 4b shows that the diaromatics resulted in higher values by MS. Both the

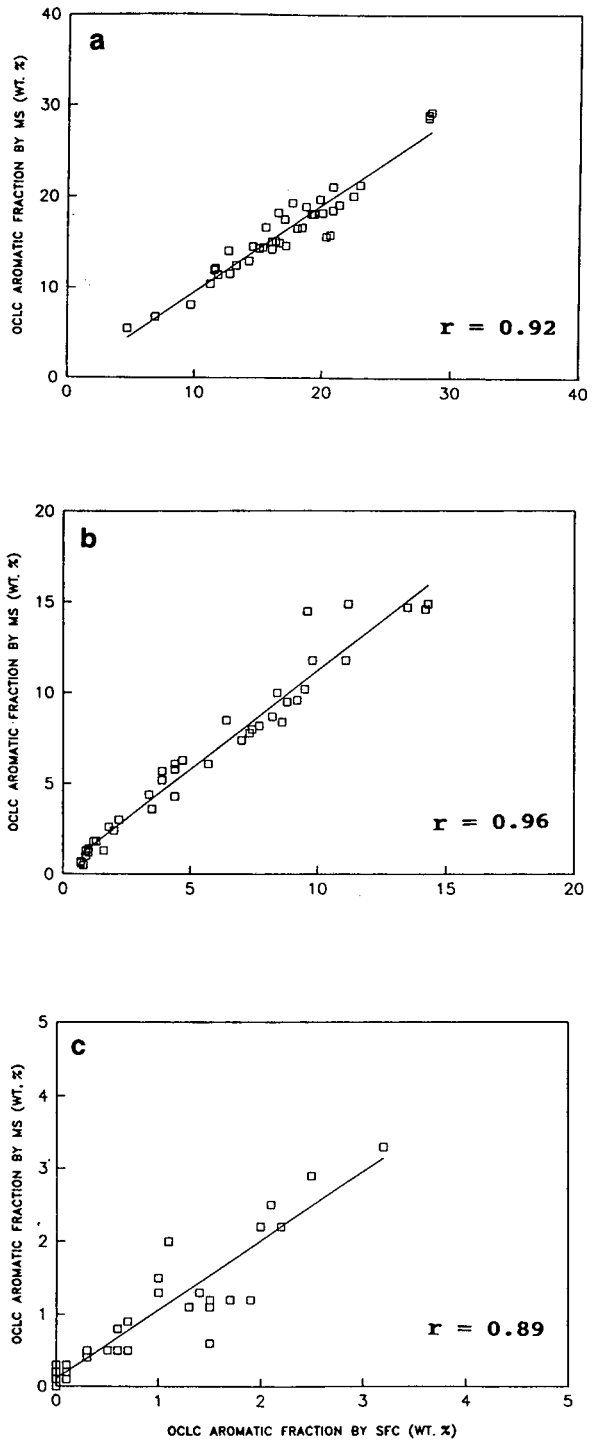

Fig. 4. Analysis of the OCLC aromatic fraction by MS *versus* SFC for (a) monoaromatics, (b) diaromatics and (c) triaromatics in diesel fuels. Note the different scales for each ring type.

monoaromatic and diaromatic type analyses gave correlation coefficients greater than 0.90. In spite of the incomplete resolution among the hydrocarbon fractions in Fig. 3b, a good correlation was established between the results obtained by this SFC method and the mass spectrometry data.

Although the correlation coefficient for the triaromatics was 0.89, a good comparison of the MS and SFC was achieved as shown in Fig. 4c. A typical summary of the mass spectral quantitation of the individual ring types is shown in Table I. In general, the diesel fuels analyzed contained low concentrations of three ring aromatics, thus, peak areas were more difficult to integrate due to lower resolution. Also, nitrogen and sulphur containing materials may have contributed to some SFC–FID response differences.

One of the goals of this SFC method was to analyze diesel fuels routinely and efficiently. Since the OCLC–SFC data in Fig. 4 were favorable and have been validate by MS, our intent was to determine the individual ring species without prior OCLC separation and solvent evaporation. An excellent comparison of the

TABLE I

MASS SPECTRAL QUANTITATION OF THE AROMATIC RING TYPES IN A DIESEL FUEL

ASTM test D2425: Hydrocarbon type analysis of middle distillates by mass spectrometry.

Hydrocarbon type	% (w/w)
Paraffins	42.3
Monocycloalkanes	10.1
Dicycloalkanes	11.3
Tricycloalkanes	3.9
Total saturates	67.6
Alkylbenzenes	8.8
Indanes/tetralins	9.1
Dinaphthenebenzenes	2.7
Naphthalenes	4.2
Biphenyls	4.5
Fluorenes	2.1
Phenanthrenes	1.0
Total aromatics	32.4
Total	100.0

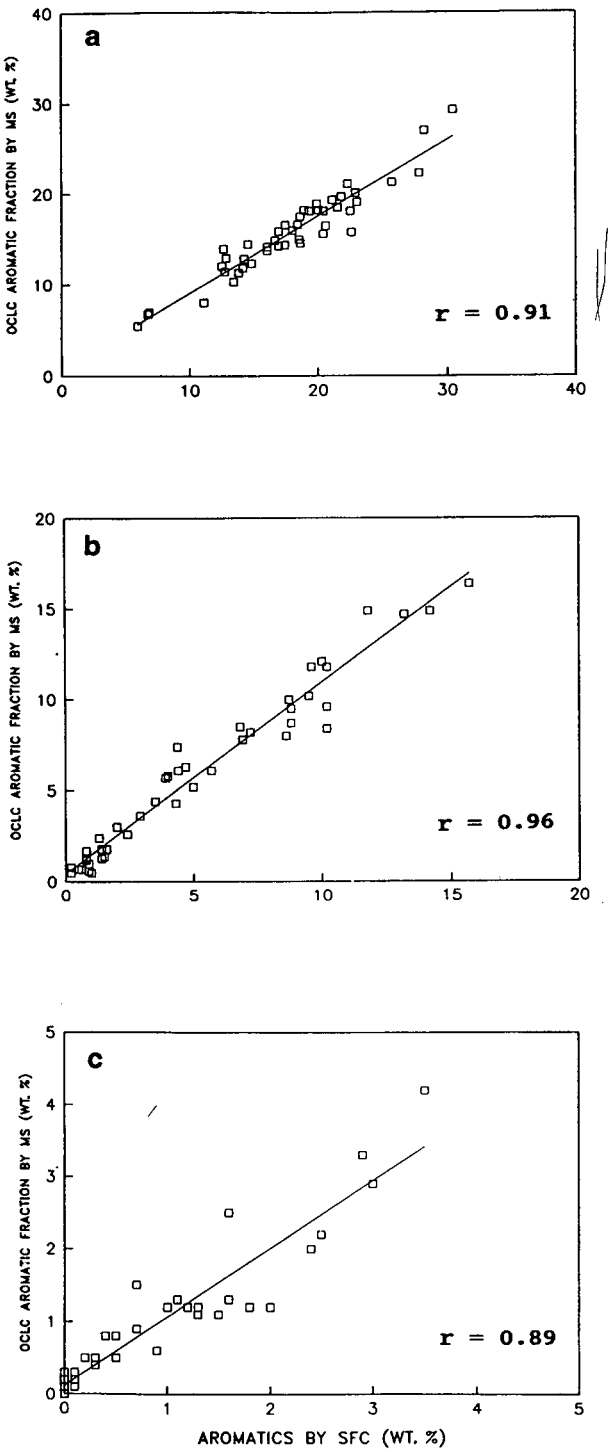

Fig. 5. Analysis of the OCLC aromatic fraction by MS *versus* the original diesel fuel (without prior OCLC separation) for (a) monoaromatics, (b) diaromatics and (c) triaromatics. Note the different scales for each ring type.

TABLE II

REPEATABILITY OF SFC–FID FOR AROMATIC TYPE ANALYSIS OF A DIESEL FUEL

Injection	Aromatic types (%, w/w)		
	Monoaromatic	Diaromatic	Triaromatic
1	15.7	13.3	2.2
2	15.5	12.8	2.1
3	15.0	13.0	2.1
4	15.0	13.0	1.5
5	15.4	14.1	2.0
6	15.8	13.8	2.2
7	15.7	13.1	1.4
8	15.1	13.6	1.9
9	15.4	13.3	1.4
10	15.6	13.2	1.9
11	15.5	13.6	1.9
Mean	15.4	13.3	1.9
Standard deviation	±0.3	±0.4	±0.3

OCLC–MS results and the original diesel fuel (without prior OCLC separation) quantitated by SFC is shown in Fig. 5. Similar correlation coefficients were obtained for each ring type as previously discussed in Fig. 4. The repeatability of this SFC method is shown in Table II. Excellent precision was obtained for eleven injections of the original diesel fuel in Fig. 3b over a 36-day period.

CONCLUSIONS

An improved SFC technique was developed to provide rapid hydrocarbon analysis of the aromatic ring distribution in diesel fuels ranging from 6.0 to 48.0% (w/w) total aromatics. The method is routine, not operator intensive, and applicable to different refinery streams without prior OCLC separation and solvent evaporation. The precision of the SFC data was excellent. Work is currently underway to improve the resolution between each hydrocarbon fraction and to analyze other petroleum fuels.

ACKNOWLEDGEMENTS

We would like to gratefully thank Greg Marsh and Vincent Nero for implementing and developing the MS procedure.

REFERENCES

1 *Annual Book of ASTM Standards*, Vol. 05.02, American Society for Testing and Materials, Philadelphia, PA, 1991, method ASTM D1319.
2 *Annual Book of ASTM Standards*, Vol. 05.02, American Society for Testing and Materials, Philadelphia, PA, 1991, method ASTM D2549.
3 J.M. Colin and G. Vion, *J. Chromatogr.*, 280 (1983) 152.
4 J.C. Suatoni, H.R. Garber and B.E. Davis, *J. Chromatogr. Sci.*, 13 (1967) 367.
5 P.C. Hayes and S.D. Anderson, *Anal. Chem.*, 58 (1986) 2384.
6 P.C. Hayes and S.D. Anderson, *J. Chromatogr. Sci.*, 26 (1988) 210.
7 D.K. Calling, B.K. Bailey and R.J. Pugmire, *NASA Contract Report 174761*, 1984.
8 *Aromatic Hydrogen and Aromatic Carbon Contents of Hydrocarbon Oils by High Resolution Nuclear Magnetic Resonance Spectrocopy*, proposed ASTM method, ASTM Committee D-2, American Society for Testing and Materials, Philadelphia, PA, 1991.
9 R.S. Ozubko, D.M. Clugston and E. Furimsky, *Anal. Chem.*, 53 (1981) 183.
10 F.P. DiSanzo and R.E. Yoder, *J. Chromatogr. Sci.*, 29 (1991) 4.
11 R.M. Campbell, N.M. Djordjevic, K.E. Markides and M.L. Lee, *Anal. Chem.*, 60 (1988) 356.
12 S.W. Lee, B.J. Fuhr, L.R. Holloway and C. Reichert, *J. Energy Fuels*, 3 (1989) 80.
13 T.A. Norris and M.G. Rawdon, *Anal. Chem.*, 56 (1984) 1767.
14 B.W. Wright, H.R. Udseth, E.K. Chess and R.D. Smith, *J. Chromatogr. Sci.*, 26 (1988) 228.
15 *Annual Book of ASTM Standards*, Vol. 05.03, American Society for Testing and Materials, Philadelphia, PA, 1991, method ASTM D5186.
16 V.P. Nero, C.S. MacMahon, E.J. Popiel, G.L. Chapman and S.H. Chao, *Prepr. Am. Chem. Soc. Div. Pet. Chem.*, 36 (1991) 265.
17 *Annual Book of ASTM Standards*, Vol. 05.02, American Society for Testing and Materials, Philadelphia, PA, 1991, method ASTM D2425.

Journal of Chromatography, 637 (1993) 187–194
Elsevier Science Publishers B.V., Amsterdam

CHROM. 24 977

Supercritical fluid extraction of metal-containing selective sorbents

Thomas J. Wenzel*, Karen J. Townsend, Daphney E. Frederique and Andrew G. Baker

Department of Chemistry, Bates College, Lewiston, ME 04240 (USA)

(First received November 9th, 1992; revised manuscript received February 15th, 1993)

ABSTRACT

Nickel(II), copper(II), zinc(II) and lanthanum(III) complexes with bis-β-diketonate ligands form polymeric materials that function as selective sorbents for use as gas chromatographic precolumns. Supercritical fluid extraction was evaluated as a method of desorbing compounds retained by these sorbents. Alcohols, ketones, esters and sulfur-containing compounds were effectively extracted using carbon dioxide at 80 atm (1 atm = 101 325 Pa) and 50°C. The blanks observed with supercritical fluid extraction were often better than those obtained with thermal desorption. The applicability of supercritical fluid extraction is demonstrated on the constituents of cigarette smoke retained on a copper-containing sorbent. Two other sorbents employing metal complexes of either a β-diketone derivative of polystyrene or a β-ketoamide derivative of silica gel were evaluated. The blanks with these materials were not found to be suitable using either thermal desorption or supercritical fluid extraction.

INTRODUCTION

Gas chromatography is the method of choice for analyzing volatile constituents of samples. The large number of volatile compounds in many samples, however, often results in complex chromatograms with overlapping peaks. One approach to reducing the complexity of gas chromatograms is to employ selective detectors. Another is to use selective sorbents in the sample collection or workup prior to analysis. Selective sorbents are designed to retain only specific compounds from a sample mixture. In most instances it is desirable to be able to remove the compounds retained by the sorbent for analysis. This has usually been accomplished by thermal desorption, however, the technique of supercritical fluid extraction has increasingly been applied as a desorption method [1–9].

Carbon dioxide is usually employed in the supercritical fluid extraction of sorbent materials. Supercritical carbon dioxide is relatively inert, a property which facilitates the design of extraction devices, the handling of the effluent, and reduces the likelihood of degradation of the sorbent polymer. The low critical point conditions of carbon dioxide [73 atm (1 atm = 101 325 Pa), 31°C] contribute to the ease of construction of an extraction apparatus, and reduce the possibility of thermal degradation of the sorbent polymer. Supercritical carbon dioxide is nonpolar, which may limit its use in applications when highly polar molecules are to be extracted. Its polarity can be raised by elevating the pressure and decreasing the temperature of the system [10]. At temperatures of approximately 50°C and pressures of approximately 2200 atm the Hildebrand solubility parameter is similar to that of methylene chloride [10]. It is also possible to add polar modifiers such as methanol, acetonitrile, or water to the carbon dioxide to increase

* Corresponding author.

0021-9673/93/$06.00

the polarity [9,11]. Supercritical fluid extraction of sorbents can be performed in either an off- or on-line [11–15] mode.

We have developed a series of metal-containing selective sorbents based on complexes with bis-β-diketone ligands of structure **I** [16,17].

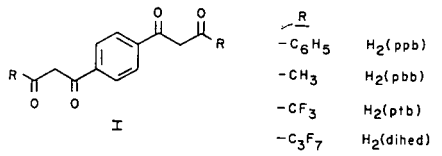

I

The orientation of the β-diketone groups is such that metal complexes of **I** form polymers, an example of which is shown in Fig. 1. Nickel(II), zinc(II), copper(II) and lanthanum(III) were chosen for study because β-diketonate complexes of these metals are coordinatively unsaturated, and these metals span a range of Lewis acidities. Metal complexes of **I** are therefore effective sorbents for Lewis bases such as oxygen-, nitrogen- and sulfur-containing compounds [16,17]. The selectivity of the sorbents varies depending on the metal and the substituent group of the β-diketone ligand. Electron-withdrawing moieties such as trifluoromethyl and heptafluoropropyl groups enhance the Lewis acidity of the metal and increase the association constants with Lewis bases. Electron-donating moieties such as phenyl and methyl groups do the opposite. A series of four sorbents that provide the optimum range of selectivity has been described [17].

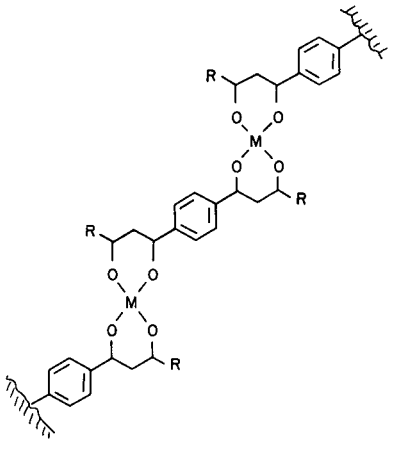

Fig. 1. Structure of the β-diketonate polymer for a metal in the 2+ oxidation state.

Previous work on metal-containing sorbents utilized thermal desorption [16–20]. We now describe the use of supercritical fluid extraction with these sorbents. Supercritical fluid extraction with carbon dioxide will be shown to be an effective means of removing compounds retained by these sorbents. Supercritical fluid extraction was also tested with Eu(III) and Cu(II) complexes of a β-diketone-derivatized polystyrene described by Williams and Sievers [20]. Repeated clogging of the restrictor on the extraction device seemed to indicate that these polystyrene derivatives were slightly soluble in supercritical carbon dioxide. The Cu(II) complex of a β-ketoamide derivative of silica gel was also evaluated as a selective sorbent, however, adequate blanks could not be obtained using either thermal desorption or supercritical fluid extraction.

EXPERIMENTAL

Reagents

Chemicals employed in the synthetic preparations were reagent grade and were used as received. Solvents were dried prior to use. Tenax GC (20–35 mesh) and Chromosorb 102 (60–80 mesh) were obtained from Alltech (Deerfield, IL, USA). Supercritical fluid-grade carbon dioxide was obtained from Scott Specialty Gases (Plumsteadville, PA, USA).

Preparation of polymer sorbents

Metal polymers of **I** were prepared as previously described [16]. The 4,4,4-trifluoro-1,3-butanedionyl derivative of Chromosorb 102 (**II**), and europium(III) complex of **II** were prepared as reported by Williams and Sievers [20]. Spectral and elemental analysis confirmed the identity of the desired products. The copper(II) complex of **II** was prepared by filtering a hot solution of cupric acetate (1.68 g) in 60 ml of water through a fine-pore sintered glass crucible into an Erlenmeyer flask containing a stirred suspension of **II** (2.0 g) in 60 ml of ethanol. The polymer immediately turned green upon the addition of the copper solution. The flask was stoppered and

shaken on an orbital shaker for 5 h, after which the solid was collected by suction filtration and washed with copious amounts of water and 95% aqueous ethanol. The product was dried under vacuum in a desiccator for 12 h. Elemental analysis (Galbraith Labs., Knoxville, TN, USA) showed the product to contain 2.97% copper. This value is reasonable assuming that 8–10% of the styrene rings are derivatized with the β-diketone group [20].

The synthesis of the 4,4,5,5,6,6,6-heptafluoro-1,3-hexanedionyl derivative of Chromosorb 102 was attempted by a procedure analogous to that used to prepare the trifluoro derivative. A spot test using a solution of iron(III) chloride failed to show much incorporation of β-diketone moieties onto the polymer. Similar attempts to prepare the 1,3-butanedionyl derivative also failed to produce the desired product as evidenced by testing with iron(III) chloride.

A β-ketoamide derivative of silica gel (**III**) was prepared by reacting diketene with aminopropyl-derivatized silica according to previous methods [21]. The Cu(II) complex was prepared by a procedure analogous to that described above for the polystyrene except that the copper(II) acetate was added in hot methanol. Elemental analysis (Galbraith Labs.) showed the product to contain 1.00% copper.

Precolumns

Precolumns [10 × 1/8 in. I.D. (1 in. = 2.54 cm) rapid heating/cooling, Valco, Houston, TX, USA] containing La(dihed), Ni(dihed), Cu(dihed), and Zn(ppb) were prepared and conditioned as previously described [16]. The Cu(II) and Eu(III) complexes of **II** were packed by plugging one end of the precolumn with glass wool and attaching that end to a vacuum pump. The polymer was added under suction, the other end plugged with glass wool, and then the trap was conditioned either thermally or by repeated extraction with supercritical carbon dioxide. The Cu(II) and complex of **III** was packed by procedures similar to complexes of **I** [16] and conditioned thermally at 100°C for repeated intervals, or by repeated extraction with supercritical fluid carbon dioxide.

Apparatus and procedures

The valve system with sorbent precolumns was as previously described [16]. Chromatograms were obtained on either a Hewlett-Packard 5880 gas chromatograph with flame ionization detector or Hewlett-Packard 5890 gas chromatograph with mass-selective detector. The column was a 25-m cross-linked 5% phenyl methyl silicone fused-silica capillary column (Hewlett-Packard), and the flow-rate was 1 ml/min. Helium or nitrogen was employed as the carrier gas.

A diagram of the apparatus used for supercritical fluid extraction is shown in Fig. 2. A syringe pump (Model 260D; ISCO, Lincoln, NE, USA) was fitted with a carbon dioxide-delivery system and shut off valves both before and after the syringe. The metal-containing trap was connected to the outlet valve of the syringe pump via a 30 in. length of 1/16 in. O.D. stainless-steel tubing. Supercritical conditions were maintained in the metal-containing trap by connecting an uncoated 4 in. length of 20 μm I.D. fused-silica restrictor (Polymicro Technologies, Phoenix, AZ, USA) to the end of the trap. The end of the restrictor was either immersed in 2 ml of methylene chloride or connected to a trap containing Tenax GC, either of which were maintained at ambient temperatures.

The chamber was filled with carbon dioxide, the valves closed, and the chamber then pressurized to the desired value. The outlet valve was then opened and when the flow-rate had

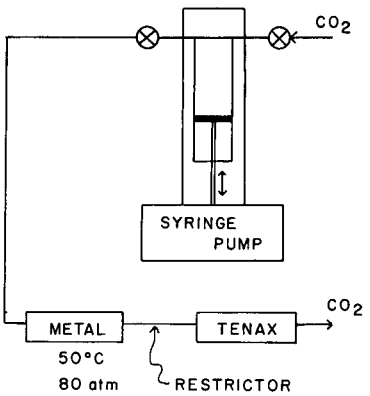

Fig. 2. Diagram of the apparatus for supercritical fluid extraction.

stabilized, which required only several seconds, the metal-containing sorbent trap was heated above the critical temperature for the desired length of time. After completion of the extraction step, the contents of the methylene chloride or Tenax trap were analyzed. Samples of ketones, esters, alcohols and sulfur-containing compounds were prepared by dissolving 1 μl of each compound in 5 ml of methanol. A 1-μl sample of the methanol solution was used for evaluating the sorbent properties as previously described [16].

Samples of cigarette smoke were obtained by drawing smoke for a set period of time (usually 5 s) from the end of a cigarette through a trap containing Tenax GC.

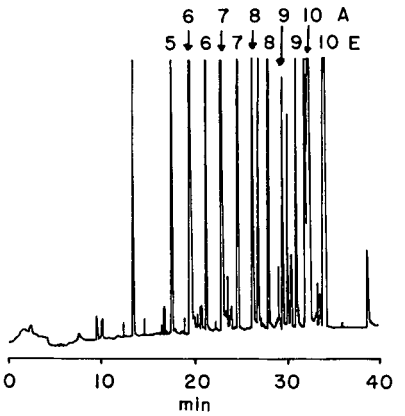

Fig. 3. Chromatograms of *n*-alcohols (6–10A = C_6–C_{10}) and methyl esters (5–10E = C_5–C_{10}) retained by La(dihed) at 100°C and desorbed via supercritical fluid extraction (80 atm, 50°C, 10 min).

RESULTS AND DISCUSSION

Preliminary investigation of the efficacy of using supercritical fluid extraction with metal-containing polymer sorbents was investigated using homologous series of 2-ketones, *n*-alcohols, and methyl esters with sorbent traps containing La(dihed), Cu(dihed) or Zn(ppb). In previous work with metal-containing sorbents with **I**, it was shown that oxygenated donor compounds associated most strongly with La(dihed) [16,17]. At temperatures of 100°C, the test ketones (C_5–C_{10}), esters (C_4–C_{10}) and alcohols (C_6–C_{10}) were fully retained by La(dihed). In Fig. 3 is shown the chromatogram of a sample of methyl esters and alcohols retained by La(dihed) and extracted in 10 min at 50°C and 80 atm. Even under these relatively mild conditions, the retained compounds are extracted. Comparison of the integrated areas of the peaks to those of the same sample when thermally desorbed directly from Tenax into the gas chromatograph indicate that the extraction and recovery of the compounds from the La(dihed) sorbent was complete. After completion of the supercritical fluid extraction, the La(dihed) was subjected to a 5 min thermal desorption at 150°C. The resulting chromatogram showed no peaks for any of the alcohols or methyl esters, confirming the efficiency of removal by supercritical fluid extraction. Similar efficiencies of removal were noted for the ketones, esters and alcohols on Cu(dihed) and Zn(ppb).

Two reasons might be proposed for the efficiency of extraction of these compounds from the metal-containing sorbents under the relatively mild conditions. The first is that all of the test solutes have aliphatic moieties that ought to enhance their solubility in the non-polar supercritical carbon dioxide. The second is that carbon dioxide may adsorb to the metal ions in the sorbents, thereby facilitating the desorption of the adsorbed solutes.

The volatile constituents of cigarette smoke were used to further evaluate supercritical fluid extraction of these sorbents. Portions of the chromatograms for total smoke, and the retained and unretained components of smoke after passage through Cu(dihed) are shown in Fig. 4. Only that portion in which peaks were observed in the chromatogram of the compounds retained by Cu(dihed) is shown. The chromatogram of the total smoke and those constituents unretained by Cu(dihed) are identical in many respects. The variations in relative intensity of several of the peaks was typical of the reproducibility of smoke from one analysis to the next. The major constituents in the chromatogram of the unretained compounds were identified as aromatic hydrocarbons. The peaks ob-

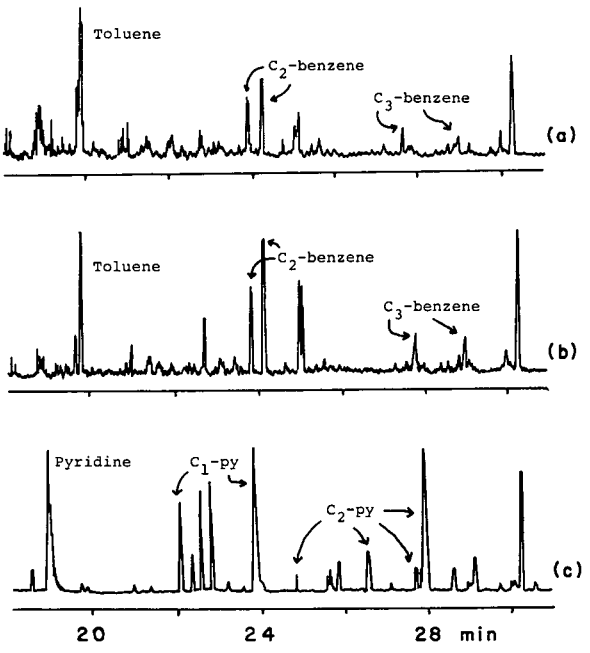

Fig. 4. Chromatograms of the volatile constituents of cigarette smoke: (a) total smoke, (b) unretained by Cu(dihed) at 100°C and (c) retained by Cu(dihed) at 100°C with desorption via supercritical fluid extraction (200 atm, 100°C, 20 min). py = Pyridine.

served in the chromatogram of those compounds retained by Cu(dihed) represent minor constituents in the total smoke, and primarily correspond to pyridine-containing compounds. Those compounds that were identified by mass spectral data are labelled in the chromatograms.

Removal of the pyridine-containing compounds from Cu(dihed) using supercritical fluid extraction was not complete at 80 atm and 50°C. Increasing the temperature, pressure, and extraction time were all observed to improve the extraction efficiency, as shown by the data in Table I. The efficiency of extraction was better for methyl pyridines than for pyridine. Complete removal of all of the adsorbed compounds except pyridine was effected at conditions of 200 atm, 100°C and 20 min extraction time.

An advantage of supercritical fluid extraction over thermal adsorption can be seen by comparing the blanks obtained using the two methods. The series of chromatograms shown in Fig. 5 for *n*-alcohols retained on Cu(dihed) illustrate this point. The chromatogram in Fig. 5a is that of the unretained alcohols. The C_6 alcohol is partially retained at 100°C; all of the other alcohols are fully retained at the conditions employed (100°C, 5 min). The chromatogram in Fig. 5b is that of the retained *n*-alcohols removed by supercritical fluid extraction. The extra peaks occurring in the latter portion of the chromatogram were noted when the sample was directly injected into the gas chromatograph and are therefore impurities in the alcohols. The chromatogram in Fig. 5c was obtained by thermal desorption of the polymer at 150°C immediately after completion of the supercritical fluid extraction. Of particular interest in this chromatogram are the five peaks at 8, 10, 16, 18 and 24 min. The intensity of these peaks increased with desorption temperature. They are believed to be thermal degradation products of the sorbent. These peaks were not observed to any significant extent in the chromatogram obtained after supercritical fluid extraction. The metal polymers of **I** also exhibit long-term stability under the conditions employed for the supercritical fluid extraction. One particular

TABLE I

EXTRACTION OF PYRIDINES FROM Cu(dihed)

Pressure (atm)	Temperature (°C)	Time (min)	Extraction (%)		
			Pyridine	C_1-pyridine	C_2-pyridine
120	50	10	29	96	77
120	50	20	33	99	98
120	100	20	53	100	100
200	100	20	89	100	100

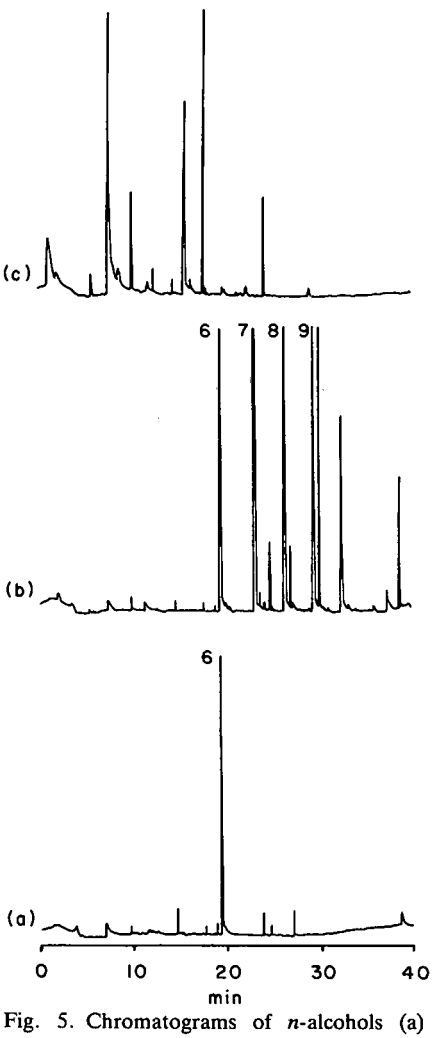

Fig. 5. Chromatograms of *n*-alcohols (a) unretained by Cu(dihed) at 100°C (6 = C_6), (b) retained by Cu(dihed) at 100°C with desorption via supercritical fluid extraction (6–9 = C_6–C_9) and (c) thermal desorption of Cu(dihed) at 150°C after the supercritical fluid extraction.

trap containing Cu(dihed) was used for over twenty analyses with no noticeable change in performance.

Another comparison of the difference in blanks between supercritical fluid extraction and thermal desorption can be seen for a sorbent consisting of Zn(ppb) that had undergone repeated heating cycles. The blank obtained by thermal desorption at 150°C (Fig. 6a) was no longer acceptable for use. The chromatogram in Fig. 6b is that of a sample of *n*-alcohols retained

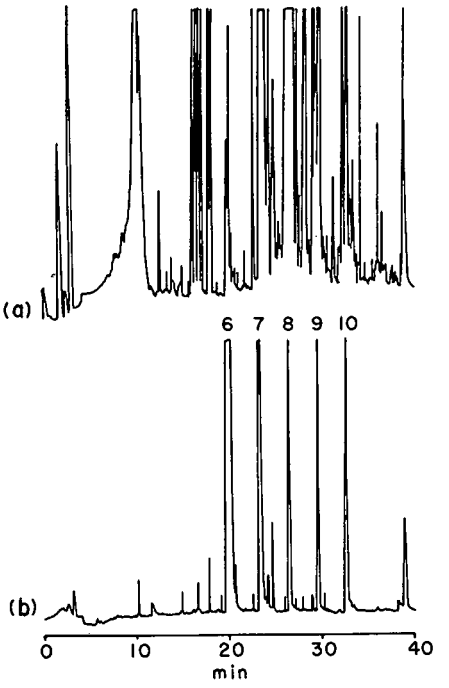

Fig. 6. Chromatograms of (a) Zn(ppb) desorbed thermally at 150°C and (b) *n*-alcohols (6–10 = C_6–C_{10}) retained at 100°C by Zn(ppb) and desorbed via supercritical fluid extraction.

on the sorbent and removed by supercritical fluid extraction. This chromatogram exhibits only a few small peaks that might be attributed to degradation of the sorbent.

We have previously shown that nickel(II) chelates of I are effective sorbents for sulfur-containing compounds [17]. Tetrahydrothiophene and di-*n*-butylsulfide were fully retained by Ni(dihed) at 100°C. Supercritical fluid extraction at 50°C and 80 atm for 10 min completely removed the di-*n*-butylsulfide, but only removed about half of the tetrahydrothiophene. A subsequent thermal desorption or supercritical fluid extraction led to removal of the remainder of the tetrahydrothiophene. The association between tetrahydrothiophene and nickel(II) complexes with I is expected to be greater than that with di-*n*-butylsulfide because of reduced steric encumbrance in the ring compound [22]. Complete removal of the tetrahydrothiophene in one extraction was accomplished by using a longer extraction time.

Williams and Sievers [20] reported the use of

a Eu(III) complex of a 4,4,4-trifluoro-1,3-butanedionyl derivative of Chromosorb 102 as a sorbent for oxygenated compounds in air. We prepared a Cu(II) complex in addition to the Eu(III) complex and investigated the suitability of applying supercritical fluid extraction for removal of retained compounds. With both sorbents we experienced difficulty in obtaining suitable blanks following thermal conditioning or repeated supercritical fluid extraction. The blanks observed after thermal conditioning at 150°C improved for the first 30 min, then notably degraded with further heating. After 45 min at 150°C, the polymers exhibited significant darkening. At temperatures of 100°C, which are necessary for selective retention studies, we were able to obtain a suitable blank (5 min thermal desorption at 100°C) after 30 min of conditioning. The polymer was then subjected to repeated 30-min extractions with supercritical carbon dioxide. The blank (10 min extraction at 50°C and 80 atm) improved after each of the first three extractions, however, the restrictor often clogged during this procedure. Further extractions failed to improve the quality of the blank or eliminate the clogging. Since the blanks were never judged acceptable, no attempt was made to eliminate the clogging of the restrictor, and further study of these sorbents was abandoned.

Seshadri and Kettrup [21] have described the synthesis of a β-ketoamide derivative of silica gel. We prepared the Cu(II) complex of this material but were unable to obtain sufficiently clean blanks at temperatures of 100°C to permit its use as a selective sorbent. Repeated extraction with supercritical carbon dioxide also failed to provide suitably clean blanks at temperatures of 100°C needed for adsorption of donor compounds. Further study of the sorbent properties of this material was therefore abandoned.

CONCLUSIONS

Supercritical fluid extraction with carbon dioxide is an effective means of removing compounds adsorbed on metal polymers with bis β-diketonate ligands. The blanks with supercritical fluid extraction were often better than those obtained using thermal desorption. Pyridine-containing compounds were selectively removed from cigarette smoke using a copper-containing sorbent. Extraction conditions of 200 atm, 100°C and 20 min permitted the complete removal of the pyridine-containing compounds from the sorbent.

ACKNOWLEDGEMENTS

We would like to thank The Camille and Henry Dreyfus Foundation (Scholar/Fellow Program), National Science Foundation (College Science Instrumentation Program), and Pfizer Pharmaceutical for supporting this work.

REFERENCES

1 M. Lohleit, R. Hillmann and K. Bachmann, *Fresenius' J. Anal. Chem.*, 339 (1991) 470–474.
2 L.J. Mulcahey, J.L. Hedrick and L.T. Taylor, *Anal. Chem.*, 63 (1991) 2225–2232.
3 J.H. Raymer and E.D. Pellizzari, *Anal. Chem.*, 59 (1987) 1043–1048.
4 S.B. Hawthorne and D.J. Miller, *J. Chromatogr. Sci.*, 24 (1986) 258–264.
5 J.H. Raymer, E.D. Pellizzari and S.D. Cooper, *Anal. Chem.*, 59 (1987) 2069–2073.
6 B.W. Wright, C.W. Wright, R.W. Gale and R.D. Smith, *Anal. Chem.*, 59 (1987) 38–44.
7 S.B. Hawthorne, D.J. Miller and M.S. Krieger, *J. Chromatogr. Sci.*, 27 (1989) 347–354.
8 R.W. van Noort, J.P. Chervet, H. Lingeman, G.J. de Jong and U.A.Th. Brinkman, *J. Chromatogr.*, 505 (1990) 45–77.
9 N. Alexandrou, M.J. Lawrence and J. Pawliszyn, *Anal. Chem.*, 64 (1992) 301–311.
10 S.B. Hawthorne, *Anal. Chem.*, 62 (1990) 633A–642A.
11 P.J. Schoenmakers and L.G.M. Uunk, *Adv. Chromatogr.*, 30 (1989) 1–80.
12 R.J. Houben, H.G.M. Janssen, P.A. Leclercq, J.A. Rijks and C.A. Cramers, *J. High. Resolut. Chromatogr.*, 13 (1990) 669–673.
13 K. Jinno and M. Saito, *Anal. Sci.*, 7 (1991) 361–369.
14 S.B. Hawthorne, D.J. Miller and M.S. Krieger, *J. Chromatogr. Sci.*, 27 (1989) 347–354.
15 J.H. Raymer and G.R. Velez, *J. Chromatogr. Sci.*, 29 (1991) 467–475.
16 T.J. Wenzel, L.W. Yarmaloff, L.Y. St. Cyr, L.J. O'Meara, M. Donatelli and R.W. Bauer, *J. Chromatogr.*, 396 (1987) 51–64.
17 T.J. Wenzel, P.J. Bonasia and T. Brewitt, *J. Chromatogr.*, 463 (1989) 171–176.
18 J.E. Picker and R.E. Sievers, *J. Chromatogr.*, 203 (1981) 29–40.

19 J.E. Picker and R.E. Sievers, *J. Chromatogr.*, 217 (1981) 275–288.
20 E.J. Williams and R.E. Sievers, *Anal. Chem.*, 56 (1984) 2523–2528.
21 T. Seshadri and A. Kettrup, *Z. Fresenius' Z. Anal. Chem.*, 296 (1979) 247–252.
22 D.M. Rackham, *Spectrosc. Lett.*, 14 (1981) 117–121.

Journal of Chromatography, 637 (1993) 195–200
Elsevier Science Publishers B.V., Amsterdam

CHROM. 24 902

Optimization of separation of porphyrins by micellar electrokinetic chromatography using the overlapping resolution mapping scheme

Y.J. Yao, H.K. Lee and S.F.Y. Li*

Department of Chemistry, National University of Singapore, 10 Kent Ridge Crescent, Singapore 0511 (Singapore)

(First received November 12th, 1992; revised manuscript received January 25th, 1993)

ABSTRACT

The capillary electrophoretic separation of nine porphyrins having two to eight carboxylic acid side-chains was optimized by using a systematic optimization scheme based on the overlapping resolution mapping method. Three parameters were considered for the optimization, *viz.*, surfactant (sodium dodecyl sulphate) concentration, amount of organic modifier (N,N-dimethylformamide) and the ionic strength of the buffer. To utilize the scheme, a set of seven preplanned experiments were performed. Optimum separation conditions were determined which provided satisfactory separation of the porphyrins within an analysis time of *ca.* 30 min.

INTRODUCTION

Since its introduction in 1984 by Terabe *et al.* [1], micellar electrokinetic chromatography (MEKC) has been applied to the separation of a wide variety of compounds, both neutral and ionic, such as pharmaceutical drugs [2,3] and biomolecules [4,5]. Although MEKC was originally conceived for the electrokinetic analysis of neutral molecules, its application has been extended to the analysis of ionic compounds. For some applications, MEKC provides a better resolving power than capillary zone electrophoresis (CZE) [6,7], by taking advantage of the interaction or partition of the analytes with the micellar phase. For further enhancement of selectivity, modifiers such as cyclodextrins [8], organic solvents [9] and tetraalkylammonium salts [10] have been added to the electrophoretic media.

As the degree of complexity of the analyte mixture increases, the need for multi-parameter separation systems arises. Usually, optimization of separation conditions is achieved by varying one parameter at a time, while keeping the other parameters constant. Although such a univariate approach has been successful in obtaining satisfactory separations in many investigations, it should be stressed that owing to its trial-and-error nature, the process tends to be time consuming and tedious, and often local rather than global optima would be obtained. To date, there have been few reports on the systematic optimization of capillary electrophoretic (CE) separations. Recently, Little and Foley [11] and Ghowsi *et al.* [12] presented a theory and two fundamental equations for the optimization of resolution and resolution per unit time in MEKC. In another investigation, Vindevogel and Sandra [13] employed the Plackett–Burman statistical design for the optimization of the MEKC of testosterone esters. Five buffer parameters were optimized within eight experiments.

* Corresponding author.

0021-9673/93/$06.00

Although this design is capable of optimizing several factors simultaneously, no fixed rules existed for the selection of the low and high levels and further experiments may have to be carried out based on conclusions from the optimized experimental conditions.

In our laboratory, we have developed several optimization schemes for CE separations, based on the overlapping resolution mapping (ORM) procedure [14]. In one study, two parameters, *i.e.*, buffer pH and β-cyclodextrin concentration, were optimized using a two-dimensional rectangular ORM scheme for the separation of eight sulphonamides [15]. In another investigation, the concentrations of α-, β- and γ-cyclodextrins were optimized for the CE separation of a group of plant growth hormones with a triangular ORM scheme [16]. To date, the use of a systematic optimization scheme for the CE separation of porphyrins has not been reported.

Naturally occurring porphyrins are intermediate metabolites of haem biosynthesis. Disturbances in the biosynthesis, caused by inborn or acquired defects of the corresponding enzymes, give rise to a family of diseases called porphyria. Depending on the break of the metabolic pathway, different intermediate porphyrins are subsequently formed and accumulated in body fluids and tissues. Porphyrins with different numbers of carboxylic acid groups have been conventionally separated by gradient reversed-phase high-performance liquid chromatography (HPLC) owing to their varying polarity [17]. While providing satisfactory results, the gradient HPLC procedures tended to be laborious and time consuming [17]. The ionizable carboxyl groups on these porphyrins, however, provide an advantage for separation in CE. Under appropriate conditions, they can give rise to different electrophoretic mobilities under an applied voltage [18]. Consequently, it was considered worthwhile to investigate systematic approaches which can be employed to obtain the optimum conditions for the separation of porphyrins by CE. In this investigation, the parameters chosen for the optimization study were sodium dodecyl sulphate (SDS) concentration, percentage of N,N-dimethylformamide (DMF) as modifier and the ionic strength of the buffer solution.

EXPERIMENTAL

Equipment

Separations were performed at ambient temperature using a CE system consisting of a Spellman (Plainview, NY, USA) RHR30 high-voltage power supply, capable of delivering up to 30 kV, and a Shimadzu (Kyoto, Japan) RF535 variable-wavelength fluorescence detector. The excitation and emission wavelengths were set at 405 and 615 nm, respectively. Electropherograms were recorded with a Hewlett-Packard (Palo Alto, CA, USA) Model 3394A integrator. Untreated fused-silica capillary tubing (50 μm I.D.) was obtained from Polymicro Technologies (Phoenix, AZ, USA). A separation tube length of 54.8 cm (effective length 51 cm) was used for all experiments. Samples were injected by hydrostatic siphoning at an elevation of 10 cm for 5 s. The amount injected was estimated to be 1.3 nl.

Chemicals and reagents

The structural formulae of the compounds studied are shown in Fig. 1. Mesoporphyrin IX, deuteroporphyrin IX, pentacarboxylporphyrin I, hexacarboxylporphyrin I, heptacarboxylpor-

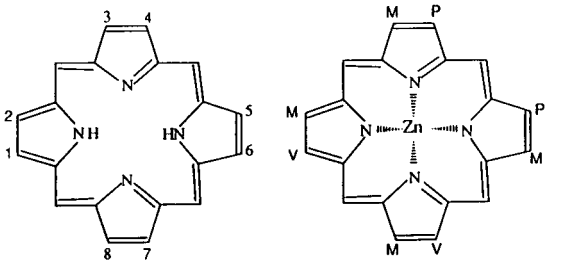

Zinc Protoporphyrin IX (ZP)

Porphyrins	side chain substitution pattern							
	1	2	3	4	5	6	7	8
Deuteroporphyrin IX (DP)	M	H	M	H	M	P	P	M
Mesoporphyrin IX (MP)	M	E	M	E	M	P	P	M
Protoporphyrin IX (PP)	M	V	M	V	M	P	P	M
Coproporhyrin I (CP)	M	P	M	P	M	P	M	P
Pentacarboxylporphyrin I (PeP)	M	P	M	P	A	P	M	P
Hexacarboxylporphyrin I (HxP)	M	P	A	P	A	P	M	P
Heptacarboxylporphyrin I (HtP)	A	P	A	P	A	P	M	P
Uroporphyrin I (UP)	A	P	A	P	A	P	A	P

Abbreviation for substitutions:
M = $-CH_3$, P = $-CH_2CH_2COOH$, E = $-CH_2CH_3$, V = $-CH=CH_2$, A = $-CH_2COOH$

Fig. 1. Structures of the porphyrins studied.

phyrin I and uroporphyrin I were purchased from Porphyrin Products (Logan, UT, USA), zinc protoporphyrin IX and coproporphyrin I from Aldrich (Milwaukee, WI, USA), protoporphyrin IX and 3-cyclohexylamino-1-propanesulphonic acid (CAPS) from Sigma (St. Louis, MO, USA), SDS and diethylene glycol monoethyl ether from Fluka (Buchs, Switzerland) and HPLC-grade N,N-dimethylformamide (DMF) from BDH (Poole, UK). All other reagents were of analytical-reagent grade. All aqueous solutions were prepared with water purified using a Milli-Q system (Millipore, Bedford, MA, USA) and filtered through 0.45-μm pore size filter membranes (Whatman, Arbor Technologies, Ann Arbor, MI, USA).

Porphyrin standards

Stock solutions of each porphyrin (about 100 μM) were prepared by dissolving the appropriate amounts of the porphyrins in DMF. The porphyrins are readily soluble in DMF. When stored at −20°C and protected from light, these stock solutions are stable for about 1 month. The concentrations of the porphyrins were determined spectrophotometrically as described in ref. 19. Further dilutions with methanol were made as required.

Rinsing of capillary tube

A new tube was first flushed with plenty of water, followed by 0.1 *M* NaOH solution. The alkaline solution was left in the tube for a day and was subsequently removed with water. With every new buffer system, the tube was similarly treated with NaOH for 30 min. To ensure a better run-to-run reproducibility, the column was rinsed with the operating buffer for 1 min between runs. With this rinsing procedure, the run-to-run relative standard deviation of the migration times for all the analytes was kept within 1% ($n = 7$).

Flow cell design

Owing to the large amount of light scattering at the cylindrical surface of the fused-silica flow cell, the flow cell design was modified according to Kurosu *et al.*'s immersed flow cell design [20]. The separation capillary with on-column detection window was passed through a conventional rectangular HPLC fluorescence flow cell. The space between the capillary and the rectangular cell was filled with a liquid having refractive index close to that of fused silica. In the present experiment, DMF (refractive index at 20°C = 1.431, refractive index of fused silica at 18°C = 1.459) was chosen as the immersing liquid. The fluorescence emission was collected by a 5.0 mm diameter, 10 mm focal length plano-convex lens (Melles Griot, Irvine, CA, USA). With this design, the minimum detectability of deuteroporphyrin was 4 nmol/ml (=5 fmol) at a signal-to-noise ratio of 4.

RESULTS AND DISCUSSION

Choice of parameters

The porphyrins investigated have two to eight –COOH side-chains which are ionizable at high pH. To utilize fully the electrophoretic mobility differences as a result of this ionization, an alkaline buffer at pH 10.8, using CAPS as the buffering ion, was chosen. Preliminary experiments to separate the porphyrins in the CZE mode revealed some problems. Analytes with different numbers of –COOH groups were well resolved and their migration order was governed by their negative charges. Uroporphyrin, being the most negatively charged, migrated last. However, the four dicarboxylporphyrins migrated close to each other. They also gave comparatively smaller peak heights, probably owing to their poorer solubility in the CZE buffer. In addition, the peak shapes deteriorated with increasing number of runs, accompanied by increasing migration times, both suggestive of possible adsorption of the analytes on the capillary wall.

To overcome these problems, SDS was added, as this anionic surfactant is believed to bind to any electrostatic or hydrophobic sites on the capillary wall, reducing, if not eliminating, interaction of analytes with the bare silica wall through competitive adsorption or repulsion from the wall [18]. Peak shapes were improved slightly in the presence of SDS. SDS also contributes to the separation selectivity by solubilizing the more hydrophobic dicarboxylporphyrins. With 100 m*M* SDS, these compounds co-mi-

grated later, between penta- and hexacarboxylporphyrins. However, SDS alone does not provide sufficient selectivity and solubility and a wider migration range is necessary. To achieve this, DMF was added to the electrophoretic buffer. With increasing amounts of DMF in the buffer system, a lowering of the electroosmotic flow and an expanded migration range were expected [21]. Porphyrins are readily soluble in DMF, hence the presence of DMF in the electrophoretic buffer increased the affinity of the analytes in the aqueous phase, improving the analyte solubility and peak efficiencies. On the other hand, a high percentage of DMF in the operating buffer was found to cause the analysis time to increase substantially. To maintain the total analysis time within reasonable limits without compromising the selectivity, a third variable, the ionic strength of the buffer, was included. It has been shown that the ionic strength of the buffer has significant effects on solute mobilities and separation efficiency [22,23]. With adequate heat dissipation, improvement in resolution and reduction of electroosmotic flow have been observed with increasing buffer concentration [24].

Overlapping resolution mapping scheme

In this study, optimum separation of the porphyrins was accomplished by varying the concentrations of CAPS, SDS and DMF in the run buffer. The triangular ORM scheme was employed to determine the optimum conditions. The first step in the ORM scheme was to define the working range of each parameter. The respective ranges were chosen such that the overall migration times were kept within reasonable limits. Otsuka *et al.* [25] pointed out that migration range is an important factor in determining the final separation of compounds of interest. Although a wider migration range usually improves resolution, longer migration times also generally result in undesirable peak broadening. In this investigation, a maximum analysis time of *ca.* 30 min was chosen as a guide in setting the upper limits of the parameters. Based on these limits, seven preplanned experiments were performed at strategic locations on a triangle. The experimental design and conditions for the seven experiments are as depicted in Fig. 2. From the

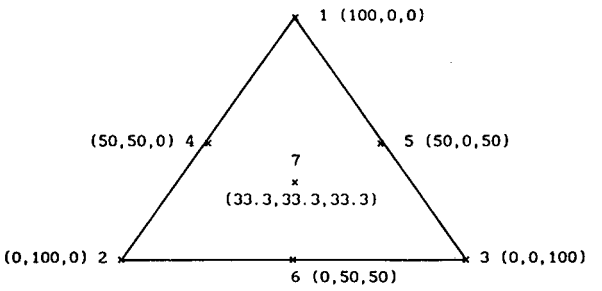

Expt	CAPS, mM	SDS, mM	DMF, %
1	80	20	4
2	20	50	4
3	20	20	10
4	50	35	4
5	50	20	7
6	20	35	7
7	40	30	6

* All experiments were performed at pH 10.8

Fig. 2. Experimental design and conditions for the seven experiments. The coordinates at the points on the triangle (x_1, x_2, x_3) denote the percentages of CAPS, SDS and DMF, respectively.

electropherograms obtained with these experiments, the resolution, R, between adjacent peaks were calculated using the equation

$$R = \frac{2\Delta t}{W_1 + W_2} \quad (1)$$

where Δt is the difference in migration times between adjacent peaks and W_1 and W_2 are peak widths at the baseline. These resolution values were then fitted into the following polynomial equation [16]:

$$R = a_1x_1 + a_2x_2 + a_3x_3 + a_{12}x_1x_2 + a_{13}x_1x_3 + a_{23}x_2x_3 + a_{123}x_1x_2x_3 \quad (2)$$

where a_i are the coefficients and x_i are the percentages of each parameter as defined in Fig. 2. With the aid of a computer program, the coefficients were determined. Once the coefficients were known, the resolutions for every adjacent peak pairs could be calculated at any buffer composition within the triangle. In all seven experiments, hexacarboxylporphyrin, hep-

tacarboxylporphyrin and uroporphyrin were always well separated from each other and from the other porphyrins, hence the resolutions for these compounds were not computed. For the remaining six porphyrins, five resolution maps were generated. By subsequently overlapping all the resolution maps and plotting the lowest resolution amongst all the individual resolution maps, regions defining buffer compositions with which the minimum desired resolution can be achieved for all solutes in the mixture can be identified. In the final overlapped resolution map (Fig. 3), regions denoted by # represent buffer compositions which can give resolutions of at least 1.8 for all peak pairs. To verify the success of the ORM scheme, a point Y was chosen from that region with buffer containing 38 m*M* CAPS, 20 m*M* SDS and 8.2% DMF. The electropherogram obtained is shown in Fig. 4, which indicates that all peaks are baseline-resolved and the overall analysis time is within 30 min. In Fig. 4, three peaks are observed for hexacarboxylporphyrin. The smaller peaks are probably by-products of hexacarboxylporphyrin during its synthesis [18]. The experimentally determined resolutions were compared with those predicted with eqn. 2 (shown in Table I) and the agreement was found to be satisfactory, *i.e.*, all within 10% deviation.

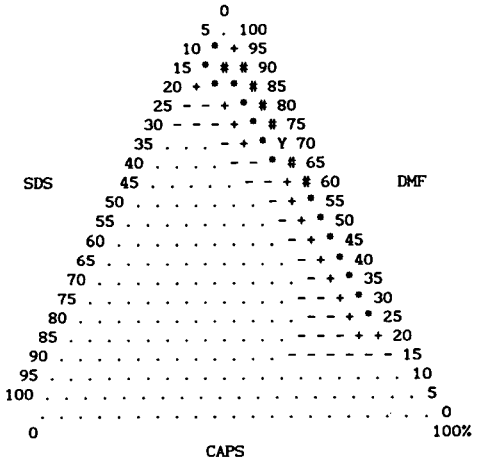

Fig. 3. Overlapped resolution map for the six peak pairs. Notation: •, $R < 0.8$; –, $0.8 \leq R < 1.2$; +, $1.2 \leq R < 1.5$; *, $1.5 \leq R < 1.8$; #, $R \geq 1.8$.

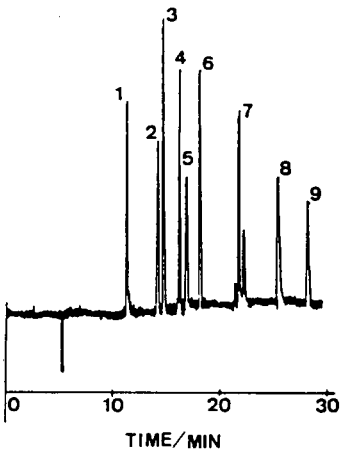

Fig. 4. Electropherogram for the nine porphyrins using the optimum electrophoretic conditions corresponding to point Y within the # region in Fig. 2: 38 m*M* CAPS (pH 10.8), 20 m*M* SDS and 8.2% DMF. Detection, excitation at 405 nm, emission at 615 nm; voltage, 18 kV, current, 18 μA. Peaks: 1 = DP; 2 = ZnPP; 3 = CP; 4 = MP; 5 = PP; 6 = PeP; 7 = HxP; 8 = HtP; 9 = UP. Abbreviations as in Fig. 1.

TABLE I

COMPARISON OF EXPERIMENTAL AND PREDICTED RESOLUTIONS OF ADJACENT PEAK PAIRS UNDER THE OPTIMUM ELECTROPHORETIC CONDITIONS

Experimental conditions as in Fig. 4.

Peak pair	Resolution	
	Experimental	Predicted[a]
1–2	12.47	11.62
2–3	2.53	2.70
3–4	4.62	4.23
4–5	2.18	2.04
5–6	4.16	4.54

[a] Values calculated according to eqn. 2.

CONCLUSIONS

The use of a systematic optimization scheme for the separation of nine porphyrin free acids has been successfully demonstrated. Three buffer parameters, *viz.*, the ionic strength of the buffer and SDS and DMF concentrations, were simultaneously optimized by using a triangular

ORM scheme. The method is straightforward and does not require a theoretical model to describe the migration behaviour, versatile, as it can be readily applied to other experimental parameters, capable of locating the global optimum, rather than a local optimum, and rapid, *i.e.*, with as few as seven preplanned experiments within the preset experimental range, optimum conditions can be determined. The results suggest that there are significant advantages in the use of ORM to optimize CE separations.

ACKNOWLEDGEMENTS

The authors thank Dr. Phillip Marriott of the Royal Melbourne Institute of Technology, Melbourne, Australia, for providing some of the standards. Thanks are also due to the National University of Singapore for financial support.

REFERENCES

1 S. Terabe, K. Otsuka, K. Ichikawa, A. Tsuchiya and T. Ando, *Anal. Chem.*, 56 (1984) 113.
2 M.T. Ackermans, F.M. Everaerts and J.L. Beckers, *J. Chromatogr.*, 585 (1991) 123.
3 J.A. Lux, H.F. Yin and G. Schomburg, *Chromatographia*, 30 (1990) 7.
4 A. Cohen, S. Terabe, J. Smith and B. Karger, *Anal. Chem.*, 59 (1987) 102.
5 H. Kajiwara, *J. Chromatogr.*, 559 (1991) 345.
6 J. Liu, K.A. Cobb and M. Novotny, *J. Chromatogr.*, 468 (1988) 55.
7 T. Lee, E.S. Yeung and M. Sharma, *J. Chromatogr.*, 565 (1991) 197.
8 C.P. Ong, C.L. Ng, H.K. Lee and S.F.Y. Li, *J. Chromatogr.*, 547 (1991) 419.
9 M. Miyake, A. Shibukawa and T. Nakagawa, *J. High Resolut. Chromatogr.*, 14 (1991) 181.
10 H. Nishi, N. Tsumagari and S. Terabe, *Anal. Chem.*, 61 (1989) 2434.
11 E.L. Little and J.P. Foley, *J. Microcol. Sep.*, 4 (1992) 145.
12 K. Ghowsi, J.P. Foley and R.J. Gale, *Anal. Chem.*, 62 (1990) 2714.
13 J. Vindevogel and P. Sandra, *Anal. Chem.*, 63 (1991) 1530.
14 J.L. Glajch, J.J. Kirkland, K.M. Squire and J.M. Minor, *J. Chromatogr.*, 199 (1980) 51.
15 C.L. Ng, H.K. Lee and S.F.Y. Li, *J. Chromatogr.*, 598 (1992) 133.
16 S.K. Yeo, C.P. Ong and S.F.Y. Li, *Anal. Chem.*, 63 (1991) 2222.
17 E. Rossi and D.H. Curnow, in C.K. Lim (Editor), *HPLC of Small Molecules: a Practical Approach*, IRL Press, Oxford, 1986, Ch. 10, p. 261.
18 R. Weinberger, E. Sapp and S. Moring, *J. Chromatogr.*, 516 (1990) 271.
19 *Specifications and Criteria for Biochemical Products*, National Academy of Sciences, Washington DC, 3rd ed., 1972, p. 185.
20 Y. Kurosu, T. Sasaki and M. Saito, *J. High Resolut. Chromatogr.*, 14 (1991) 186.
21 S.F.Y. Li, *Capillary Electrophoresis: Principles, Practice and Applications (Journal of Chromatography Library Series.*, Vol. 52), Elsevier, Amsterdam, 1992, Ch. 5, p. 219.
22 J.S. Green and J.W. Jorgenson, *J. Chromatogr.*, 478 (1989) 63.
23 M.W.F. Nielen, *J. Chromatogr.*, 542 (1991) 173.
24 H.T. Rasmussen and H.M. McNair, *J. Chromatogr.*, 516 (1990) 223.
25 K. Otsuka, S. Terabe and T. Ando, *J. Chromatogr.*, 332 (1985) 219.

Journal of Chromatography, 637 (1993) 201–205
Elsevier Science Publishers B.V., Amsterdam

CHROM. 24 980

Short Communication

Separation of retinoic acid all-*trans*, mono-*cis* and poly-*cis* isomers by reversed-phase high-performance liquid chromatography

Alfred R. Sundquist and Wilhelm Stahl

Institut für Physiologische Chemie I, Universität Düsseldorf, W-4000 Düsseldorf (Germany)

Alois Steigel

Institut für Organische und Makromolekulare Chemie I, Universität Düsseldorf, W-4000 Düsseldorf (Germany)

Helmut Sies*

Institut für Physiologische Chemie I, Universität Düsseldorf, W-4000 Düsseldorf (Germany)

(First received September 8th, 1992; revised manuscript received February 5th, 1993)

ABSTRACT

An HPLC method using a reversed-phase Suplex-pKb-100 column that resolves photoisomerates of retinoic acid into nine peaks of products and the initial all-*trans* isomer is described. This separation is achieved with an isocratic mobile phase and a total elution time of <25 min. Amounts of the five main peaks (which together accounted for *ca.* 95% of the products detected at 350 nm) sufficient for identification by proton NMR spectroscopy as mono-*cis* (9-, 11- and 13-) and di-*cis* (9,13- and 11,13-) isomers of retinoic acid were isolated using a protocol with two chromatographic steps. The methods described in this paper may prove of value in the study of retinoic acid isomer metabolism.

INTRODUCTION

Retinoic acid is involved in cellular processes such as growth promotion and differentiation, and retinoic acid and other retinoids are of interest in cancer prevention and therapy and in the treatment of skin disorders (reviewed in refs. 1–5). Some of the observed effects of retinoic acid may depend on the geometry of its polyene chain (see Fig. 1), *e.g.* all-*trans*- and 13-*cis*-retinoic acid display differential effects on mRNA levels of retinoic acid receptors [6], and a family of retinoic acid receptors that binds 9-*cis*-retinoic acid but not other mono-*cis* isomers or all-*trans*-retinoic acid [7–9] has been characterized. The isomeric composition of these compounds has therefore become a topic of increasing interest.

Study of the metabolism and activities of the

* Corresponding author.

0021-9673/93/$06.00

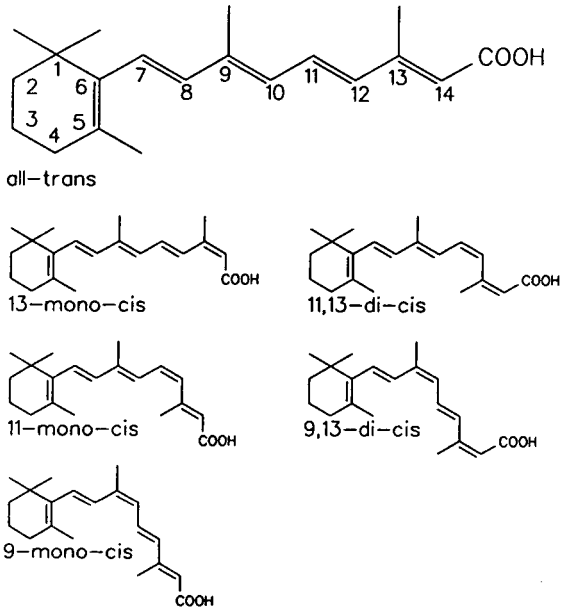

Fig. 1. Isomers isolated from photoisomerates of retinoic acid.

retinoic acid geometric isomers requires analytical methods capable of resolving the closely related compounds. HPLC methods based on reversed-phase octadecylsilane (ODS) columns and normal-phase bonded silica columns have been described and offer good but incomplete separations of the thermodynamically most stable isomers of retinoic acid, *i.e.* the all-*trans* and sterically unhindered mono- and di-*cis* isomers [7,10–13]. Greater success had been achieved with the isomers of methyl retinoate [10,12,14], but the separations are lengthy and would require a derivatization step prior to analysis of biological samples. A method using a small particle size ODS-2 column with an isocratic mobile phase and yielding a superior separation of retinoic acid photoisomerization products has recently been described [15].

In the present report we describe an HPLC methodology based on a reversed-phase Suplex-pKb-100 column that resolves photoisomerates of all-*trans*-retinoic acid into nine peaks of products. The main products, 9-mono-*cis*-, 11-mono-*cis*-, 13-mono-*cis*-, 9,13-di-*cis*- and 11,13-di-*cis*-retinoic acid, were isolated following two chromatographic steps and identified by proton NMR.

MATERIALS AND METHODS

Materials

All-*trans*-retinoic acid (>99% pure by HPLC) was generously provided by Dr. H.E. Keller (F. Hoffmann-La Roche, Basle, Switzerland). Mixtures of mono-*cis*- and poly-*cis*-retinoic acid were generated by photoisomerization of 1 m*M* solutions of all-*trans*-retinoic acid in a Rayonet photochemical reactor (Cat. No. RPR 100; Southern N.E. Ultraviolet, Hamden, CT, USA) fitted with sixteen UV lamps (350 nm emission maximum; Cat. No. RPR 3500A). In experiments to determine the time course of photoisomerization, the incubations were conducted in tightly capped quartz cuvettes (0.5 cm path length), which were chilled between periods of illumination; aliquots were diluted into eluent prior to HPLC analysis. For the purification of retinoic acid isomers, 20 ml of a 1 m*M* methanolic retinoic acid solution was illuminated in a graduated cylinder, into which a smaller cylinder filled with ice had been inserted both to control the temperature and increase light exposure; acetic acid was added to 0.05% prior to the first HPLC step.

HPLC analysis and purification of retinoic acid isomers

HPLC was done on either a Suplex-pKb-100 (5 μm, 250 × 4.6 mm main column 20 and 20 × 2.6 mm precolumn; Supelco, Bellefonte, PA, USA) or a LiChrospher 100 RP-18 end-capped (5 μm, 250 × 4 mm main column and 4 × 4 mm precolumn; Merck, Darmstadt, Germany) column, supported with a pump (L6210), UV–visible detector (L4250) and integrator (D2500) from Merck/Hitachi (Darmstadt, Germany), and a FRAC 100 fraction collector (Pharmacia-LKB, Uppsala, Sweden). Eluents A (acetonitrile–methanol–acetic acid, 95:5:0.6), B (methanol–0.05% acetic acid), and C (acetonitrile–methanol–water–acetic acid, 50:25:25:0.5) were first degassed in a sonicating water bath. A flow-rate of 1 ml min^{-1} was used throughout.

During the isolation, fractions containing iso-

mers were dried in a refrigerated and darkened lyophilizator. Addition of water (20% of final volume) to fractions in eluent B prior to lyophilization greatly diminished the degree of decomposition that can otherwise occur during this step. Purified isomers were stable when stored dry at −70°C.

Characterization of retinoic acid isomers

Proton NMR spectroscopy of the retinoic acid isomers was carried out at room temperature with a Varian VXR-300 instrument and thick-walled tubes containing 0.15–0.4 mg of isomer in 0.15 ml of C^2HCl_3.

RESULTS AND DISCUSSION

Retinoic acid readily undergoes isomerization upon exposure to light, and this represents a convenient method for generating mixtures of retinoic acid geometric isomers. The photoisomerization of all-*trans*-retinoic acid in methanol was followed using a new HPLC method based on a Suplex-pKb-100 column and eluent A. This column, which is composed of a "proprietary" reversed-phase matrix, was recently shown to be effective in resolving β-carotene and lycopene geometric isomers [16].

Significant product formation occurred after only 1 min of illumination, and extending the period to 30 min resulted in nine peaks of products (Fig. 2A). Illumination of the mixture an additional 30 min affected only slightly the relative amounts and yields of products detectable at 350 nm, indicating that a steady-state-like mixture of relatively stable products had been achieved. When the isomerization was repeated in *n*-hexane the same major products formed, but in different amounts, and three additional peaks eluting between 6 and 10 min were detected (Fig. 2B). The influence of solvent polarity on the course of photoisomerization has been previously described for methyl retinoate [14] and retinal [17,18].

The main products, which together accounted for *ca.* 95% of the decrease in the all-*trans* peak at 350 nm (Fig. 2), were isolated by HPLC for identification. Photoisomerates of all-*trans*-retinoic acid prepared in methanol were first

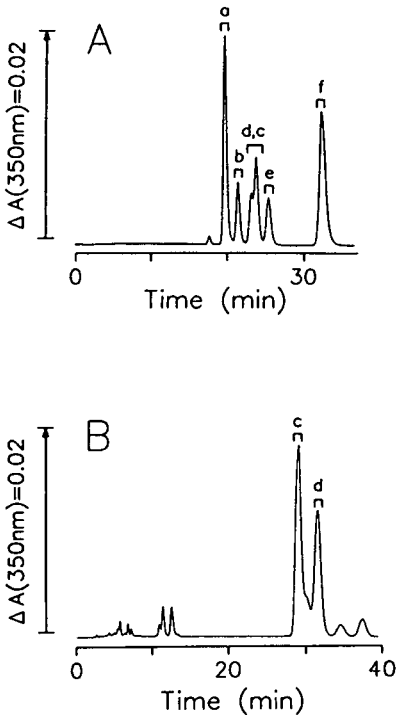

Fig. 2. Reversed-phase HPLC analysis of retinoic acid photoisomerization products. Solutions of all-*trans* retinoic acid in methanol (A) and *n*-hexane (B) were exposed to UV light (350 nm maximum) and analysed after different times of irradiation by HPLC with a Suplex-pKb-100 column and eluent A. The isomeric purity of the all-*trans*-retinoic acid prior to irradiation was *ca.* 99%. The lettered peaks were isolated and identified as follows: a = 13-mono-*cis*-retinoic acid; b = 11-mono-*cis*-retinoic acid; c = 11,13-di-*cis*-retinoic acid; d = 9,13-di-*cis*-retinoic acid; e = 9-mono-*cis*-retinoic acid; f = all-*trans*-retinoic acid (see Fig. 3).

separated with the Suplex column and eluent B (Fig. 3A). Using this eluent, three of the peaks of products (a, b and e) and the all-*trans*-retinoic acid peak (f) could be collected without need for further purification; the other two main peaks (c and d) were pooled and then resolved using a standard ODS column with eluent C (Fig. 3B). The purity of each of the six fractions was estimated by HPLC to be ≥95%.

The products were identified as geometric isomers of retinoic acid based on a comparison of their proton NMR chemical shifts and coupling constants with values reported for isomers of the methyl ester derivative of retinoic acid [14,19] and retinoic acid [15], as follows: a = 13-

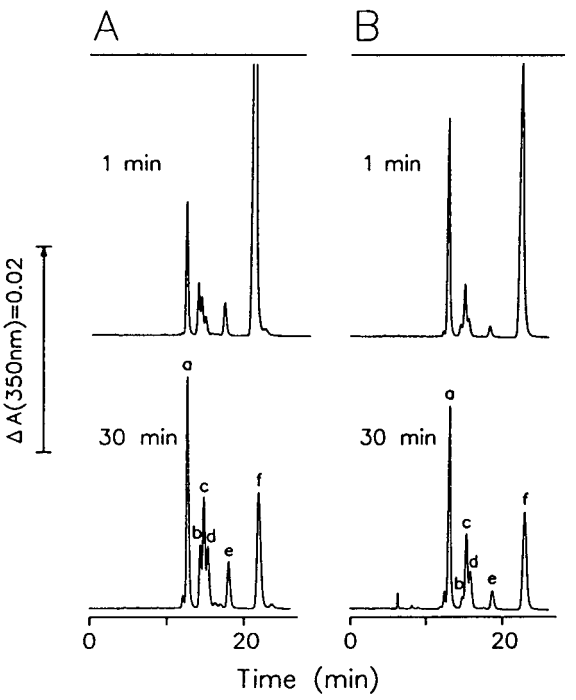

Fig. 3. Isolation of retinoic acid isomers by reversed-phase HPLC. (A) Photoisomerates of retinoic acid in methanol were resolved into five fractions on a Suplex-pKb-100 column with eluent B. Fractions a, b, e and f were not purified further. (B) Fraction d,c was chromatographed on a ODS column with eluent C to yield fractions c and d. The six final fractions were subjected to proton NMR spectroscopy and shown to be geometric isomers of retinoic acid (see Results and Discussion). Peak lettering corresponds to that of Fig. 2.

mono-*cis*-retinoic acid; b = 11-mono-*cis*-retinoic acid; c = 11,13-di-*cis*-retinoic acid; d = 9,13-di-*cis*-retinoic acid; e = 9-mono-*cis*-retinoic acid; f = all-*trans*-retinoic acid [note: the order of elution of the two di-*cis* isomers from the Suplex column is reversed with eluents A (Fig. 2) and B (Fig. 3A)].

The composition of the photoisomerates of retinoic acid in methanol is in agreement with some published values. In a study in which photoisomerates of retinoic acid isomers were generated in buffered ethanol and esterified with diazomethane prior to HPLC analysis, the formation and relative abundance based on detection at 340 nm of the following *cis* isomers were observed: 13-mono (1.00), 11,13-di (0.68), 11-mono (0.42), 9-mono (0.38), 9,13-di (0.37), 9,11,13-tri (0.24) [12]. The yield of the mono- and di-*cis* isomers coincide with those of the photoisomerates in methanol (see Fig. 2A). The reason for the lower level of 9,11,13-tri-*cis*-retinoic acid found in methanol is unclear, but may result from a slight solvent effect.

The structures of the eight or so minor photolysis products of retinoic acid (see Fig. 2) may correspond to some of those found in photoisomerates of methyl retinoate. In addition to the mono-, di- and tri-*cis* isomers seen with retinoic acid, the hindered 7-mono- and 7,13-di-*cis* isomers have been isolated from methyl retinoate photoisomerates [14]. Isomers of (5→10)-cyclized retinoic acid have ben shown to form upon long-term irradiation of retinoic acid [15], but since these products appear to be present in relatively low amounts (<2 mol% each) in photostationary state mixtures of the non-cyclized geometric isomers and to absorb only poorly at 345 nm compared with the non-cyclized isomers [15], they are possibly not among those detected with the present method (see Fig. 2).

To summarize, a rapid and simple HPLC protocol for the analysis of the geometric isomers of retinoic acid has been developed using a Suplex-pKb-100 column. In comparison with this method, a previously described separation based on a small particle size ODS-2 column better resolved the two di-*cis* isomers from 11-mono-*cis* retinoic acid but required significantly longer sample elution times (*i.e.* 40 min *vs.* 25 min). When used in combination with extraction techniques already developed for tissue and plasma [13,20–23], such HPLC methods may prove of use as the research in retinoic acid metabolism and function focuses more closely on the activity and interconversions of the all-*trans* and individual *cis* isomers of retinoic acid.

ACKNOWLEDGEMENTS

The technical assistance of Peter Graf is gratefully acknowledged. Support for this work was received from the Ministerium für Wissenschaft und Forschung Nordrhein-Westfalen and from the Bundesministerium für Forschung und Technologie, Bonn. A.R.S. is a Fellow of the Alexander von Humboldt Foundation, Bonn-Bad Godesberg.

REFERENCES

1 G.L. Peck, in M.B. Sporn, A.B. Roberts and D.S. Goodwin (Editors), *The Retinoids*, Vol. 2, Academic Press, Orlando, CA, 1984, p. 391.
2 W. Friedrich, *Vitamins*, DeGruyter, Berlin, 1988, p. 63.
3 L. Packer (Editor), *Methods Enzymol.*, 190 (1990).
4 M.A. Smith, D.R. Parkinson, B.D. Chesen and M.A. Friedman, *J. Clin. Oncol.*, 10 (1992) 839.
5 R. Blomhoff, M.H. Green and K.R. Norum, *Annu. Rev. Nutr.*, 12 (1992) 37.
6 R.U. Haq, M. Pfahl and F. Chytil, *Biochem. Biophys. Res. Commun.*, 180 (1991) 1137.
7 R.A. Heyman, D.J. Mangelsdorf, J.A. Dyck, R.B. Stein, G. Eichele, R.M. Evans and Ch. Thaller, *Cell*, 68 (1992) 397.
8 A.A. Levin, L.J. Sturzenbecker, S. Kazmer, T. Bosakowski, C. Huselton, G. Allenby, J. Speck, Cl. Kratzeisen, M. Rosenberger, A. Lovey and J.F. Grippo, *Nature (London)*, 355 (1992) 359.
9 D.J. Mangelsdorf, U. Borgmeyer, R.A. Heyman, J.Y. Zhou, E.S. Ong, A.E. Oro, A. Kakizuka and R.M. Evans, *Genes Develop.*, 6 (1992) 329.
10 R.M. McKenzie, D.M. Hellwege, M.L. McGregor, N.L. Rockley, P.J. Riquetti and E.C. Nelson, *J. Chromatogr.*, 155 (1978) 379.
11 P.V. Bhat and A. Lacroix, *Methods Enzymol.*, 123 (1986) 75.
12 R.W. Curley and J.W. Fowble, *Photochem. Photobiol.*, 47 (1988) 831.
13 G. Tang and R.M. Russell, *J. Lipid Res.*, 31 (1990) 175.
14 B.A. Halley and E.C. Nelson, *J. Chromatogr.*, 175 (1979) 113.
15 M.G. Motto, K.L. Facchine, P.F. Hamburg, D.J. Burinsky, R. Dunphy, A.R. Oyler and M.L. Cotter, *J. Chromatogr.*, 481 (1989) 255.
16 W. Stahl, A.R. Sundquist, M. Hanusch, W. Schwarz and H. Sies, *Clin. Chem.*, 39 (1993) in press.
17 W.H. Waddell and D.L. Hopkins, *J. Am. Chem. Soc.*, 99 (1977) 6457.
18 B. Stancher and F. Zonta, *J. Chromatogr.*, 287 (1984) 353.
19 R.W. Curley and J.W. Fowble, *Magn. Reson. Chem.*, 27 (1989) 707.
20 P.R. Sundaresan and P.V. Bhat, *J. Lipid Res.*, 23 (1982) 448.
21 J.L. Napoli, *Methods Enzymol.*, 123 (1986) 112.
22 C. Eckhoff and H. Nau, *J. Lipid Res.*, 31 (1990) 1445.
23 A.P. De Leenheer and H.J. Nelis, *Methods Enzymol.*, 189 (1990) 50.

Journal of Chromatography, 637 (1993) 206–208
Elsevier Science Publishers B.V., Amsterdam

CHROM. 24 987

Short Communication

Determination of ingenol in homoeopathic mother tinctures of *Euphorbia* species by high-performance liquid chromatography

M.A. Girin, S. Paphassarang and Ch. David-Eteve

Laboratoires Boiron, 20 Rue de la Libération, 69110 Sainte-Foy-Les-Lyon (France)

A. Chaboud and J. Raynaud*

Département de Botanique et Biologie Cellulaire, Pharmacognosie (Matière Médicale), Faculté de Pharmacie, Université Claude Bernard, 8 Avenue Rockefeller, 69373 Lyon Cedex 08 (France)

(First received July 8th, 1992; revised manuscript received February 17th, 1993)

ABSTRACT

A high-performance liquid chromatograpic method was developed for the identification and determination of ingenol in homoeopathic mother tinctures of eight *Euphorbia* species. The ingenol esters were hydrolysed with KOH in methanol and the free ingenol was measured using a C_{18} reversed-phase column with methanol–water (60:40, v/v) as the mobile phase. The ingenol content ranged from 0.5 to 16.7 μg/ml. *Euphorbia resinifera* Berg. mother tincture was found to be the richest in ingenol. On the other hand, the ingenol content was not significant in *E. amygdaloides* L. and *E. pilulifera* L. mother tinctures.

INTRODUCTION

The systematic investigation of higher plants for biologically active chemical components has resulted in the discovery of several new classes of secondary metabolites. The ingenanes are a novel group of tetracyclic diterpenes from the genus *Euphorbia* [1]. Interest in these compounds has been centred on two toxicological effects: inflammation produced on application to the skin [2] and tumour-promoting activity demonstrated on continued application to mice following a sub-threshold dose of a carcinogen [3]. Ingenol was the first example of the group, and its esters are those which occurred most widely in the *Euphorbia* species investigated [4]. It was of interest for us to measure ingenol esters in various mother tinctures. However, not all these compounds are commercially available. Therefore, the determination of the ingenol esters is possible only by measuring ingenol (after hydrolysis) in the mother tinctures.

EXPERIMENTAL

Apparatus and conditions

An HP 1050 liquid chromatograph equipped

* Corresponding author.

0021-9673/93/$06.00

with an autosampler, a variable-wavelength UV detector set at 204 nm and an HPLC Chem Station (DOS Series) (Hewlett-Packard, Palo Alto, CA, USA) was used. The column was Spherisorb ODS-2 (5 μm) (25 cm × 4 mm I.D.) (Hewlett-Packard), operated at 30°C, and the mobile phase was methanol–water (60:40, v/v) at a flow-rate of 1.0 ml/min. The sample size was 20 μl.

Chemicals

All reagents were of analytical-reagent grade. Solvents were filtered using a glass Millipore system with a 0.45-μm filter and degassed in an ultrasonic bath for 15 min. Ingenol was purchased from Sigma (St. Louis, MO, USA). Standard solutions were prepared by dissolving ingenol in methanol solution and stored at 20°C.

Plant material

Euphorbia mother tinctures were prepared according to the methods of preparation of the French Pharmacopoeia [5] (see Table I).

Preparation of samples

A 5-ml volume of mother tincture was extracted with 3 × 5 ml of *n*-hexane and the non-polar phase was discarded. The remaining extract, evaporated under reduced pressure (temperature < 40°C) to provide a semi-solid mass, was exhaustively extracted with acetone. The combined acetone extracts were evaporated at 40°C under reduced pressure to yield an extract that was hydrolysed with 0.5 *M* methanolic KOH for 45 min at room temperature according to Upadhyay *et al.* [6]. Neutralization with 1 *M* HCl and then extraction with dichloromethane gave an ingenol-rich fraction. The dichloromethane extract was evaporated to dryness, the residue was dissolved in 100 μl of methanol, and 20 μl of the filtrate were injected into the chromatograph.

RESULTS AND DISCUSSION

Ingenol can be isolated by saponification and extraction from *Euphorbia* mother tinctures. Reversed-phase HPLC with a Spherisorb ODS-2 column and methanol–water (60:40, v/v) as the mobile phase proved suitable for direct determination of free ingenol in *Euphorbia* mother tinctures. The ingenol peak was identified from its retention time (Fig. 1). Sample extracts were also fortified with small amounts of ingenol standard and rechromatographed to see if the peak of interest increased in height.

The ingenol contents in mother tinctures of eight species of *Euphorbia*, determined by the

TABLE I

INGENOL CONTENTS IN MOTHER TINCTURES OF *EUPHORBIA* SPECIES

Mother tinctures were prepared according to the French Pharmacopoeia [5].

Mother tincture	Part used	Alcohol content of the tincture (%, v/v)	Dilution (w/w)	Ingenol content (μg/ml)[a]
E. amygdaloides L.	Whole fresh plant	65	1:10	NS[b]
E. esula L.	Whole fresh plant	65	1:10	0.51
E. helioscopia L.	Whole fresh plant	65	1:10	1.54
E. lathyris L.	Whole fresh plant with fruit	65	1:10	3.02
E. palustris L.	Whole fresh plant	65	1:10	1.27
E. pilosa L.	Whole fresh plant	65	1:10	9.47
E. pilulifera L.	Whole dry plant	65	1:10	NS[b]
E. resinifera Berg.	Latex	90	1:10	16.71

[a] The results are expressed as the mean of triplicate determinations.
[b] NS = Not significant.

TABLE II

REPEATABILITY AND REPRODUCIBILITY DATA

		No. of injections (n)	Peak area		
			Mean	S.D.	R.S.D. (%)
Within-day		$n = 10$	1547.60	7.97	0.51
Between-day	1st day	$n_1 = 3$			
	2nd day	$n_2 = 3$	1536.52	13.56	0.88
	3rd day	$n_3 = 3$			

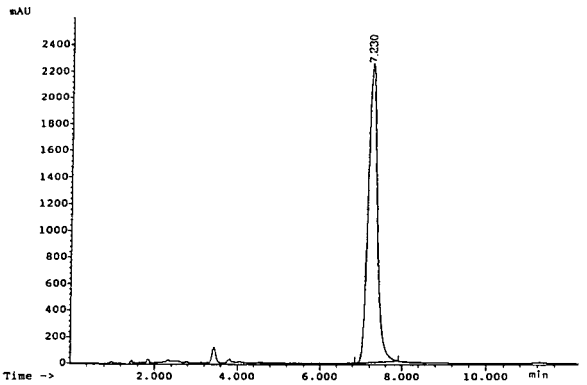

Fig. 1. Chromatogram of ingenol standard solution. For chromatographic conditions, see Experimental.

proposed HPLC method, ranged from 0.5 to 16.7 μg/ml (Table I). *Euphorbia resinifera* mother tincture, prepared from *Euphorbia resinifera* latex, was found to be the richest in ingenol. In contrast, the ingenol content was not significant in *Euphorbia amygdaloides* or *Euphorbia pilulifera* mother tinctures.

Calibration graph

Six standard solutions containing 50–670 μg/ml of ingenol were injected into the column. Linear responses (peak area) were obtained in this range of concentrations, the regression equation being $y = 31.356x + 121.399$ ($r = 0.99$, $n = 6$), where y = peak area, x = ingenol concentration (μg/ml), r = correlation coefficient and n = number of points on the curve (each representing triplicate injections in the range 50–670 μg/ml).

Precision and recovery

Ten replicate injections of a standard solution (50 μg/ml) gave a relative standard deviation (R.S.D.) of 0.51%. The reproducibility of the method was determined by analysing the same solution on three successive days. The R.S.D. was 0.88% (Table II).

To determine the recovery, six samples of ingenol standard solution (100 μg/ml) in a 60% (v/v) alcohol solution were extracted and analysed as described above for the mother tincture sample. The mean recovery of the known ingenol content was 87%.

REFERENCES

1 F.J. Evans and S.E. Taylor, *Prog. Chem. Org. Nat. Prod.*, 44 (1983) 1–99.
2 A.D. Kinghorn and F.J. Evans, *Planta Med.*, 28 (1975) 324–335.
3 E.H. Seip and E. Hecker, *Planta Med.*, 46 (1982) 215–218.
4 E. Hecker, *Cancer Res.*, 28 (1968) 2338–2349.
5 *Pharmacopée Française, Preparations Homéopathiques*, Maisonneuve, Moulins-lès-Metiz, 10th ed., 1983.
6 R.R. Upadhyay, F. Bakhtarar, H. Mohseni, A.M. Sater, N. Saleh, A. Tafazuli, F.N. Dizaji and G. Mohaddes, *Planta Med.*, 38 (1980) 151–154.

Journal of Chromatography, 637 (1993) 209–212
Elsevier Science Publishers B.V., Amsterdam

CHROM. 24 947

Short Communication

Determination of plumbagin by normal-phase high-performance liquid chromatography☆

M.M. Gupta*, R.K. Verma, G.C. Uniyal and S.P. Jain

Central Institute of Medicinal and Aromatic Plants, Lucknow 226016 (India)

(First received August 18th, 1992; revised manuscript received February 3rd, 1993)

ABSTRACT

A simple and rapid normal-phase high-performance liquid chromatographic method for the determination of a pharmacologically important 1,4-naphthoquinone, plumbagin, and a chromene, 2,2-dimethyl-5-hydroxy-6-acetylchromene, in plant extracts was developed. Both compounds were well resolved with maximum recovery (97%) on a μSpherogel column using *n*-hexane–chloroform–2-propanol (30:70:2) as the mobile phase.

INTRODUCTION

Plumbago zeylanica L. is a perennial herb used in Indian medicine for various diseases, *e.g.*, diarrhoea, dyspepsia, piles and anasarea and also in skin diseases including leprotic lesions. The plant is claimed to lead to permanent sterilization [1]. *P. zeylanica* is a rich source of a pharmacologically important 1,4-naphthoquinone, plumbagin. Plumbagin exhibits a wide range of activities, *e.g.*, antifertility [2], mitotic inhibitor [3], antifungal [4], anticoagulant [5] and antibacterial against both Gram-positive and Gram-negative bacteria [4]. In clinical studies plumbagin has been found to be useful in patients with common warts [6]. Owing to the use of *P. zeylanica* in many important Ayurvedic preparations of Indian medicines, a rapid and sensitive method was devised for the determination of its active ingredient plumbagin. The high-performance liquid chromatographic (HPLC) separation of naturally occurring quinones on a cyano-bonded column was reported by Marston and Hostettmann [7], who used *n*-hexane containing 1% acetic acid as the mobile phase.

In this study, we found that the above system [7] is not suitable for the HPLC of *P. zeylanica* as the detection limit of two major constituents of the plant extract, 2,2-dimethyl-5-hydroxy-6-acetylchromene and plumbagin, was very poor. These two constituents have close R_F values in thin-layer chromatography. In this work we developed a method for the determination of plumbagin in *P. zeylanica* roots. To the best of our knowledge, this is the first report of this determination in *P. zeylanica* by HPLC.

* Corresponding author.
☆ CIMAP Communication No. 92-44 J.

0021-9673/93/$06.00

EXPERIMENTAL

Chemicals

The solvents used were of HPLC grade (Spectrochem, Bombay, India) and filtered through a Millipore 0.5-μm filter. Plumbagin and 2,2-dimethyl-5-hydroxy-6-acetylchromene were isolated from the *n*-hexane extract (3.35 g) of *P. zeylanica* roots (500 g) by silica gel column chromatography (400 g, 60–120 mesh; Qualigens Fine Chemicals, Bombay, India) employing *n*-hexane–ethyl acetate (95:5) as mobile phase. Fractions of 50 ml each were collected and monitored by TLC employing benzene (Merck, Bombay, India) as developing solvent and the spots were detected by spraying with 50% H_2SO_4 followed by heating at 80°C. The earlier fractions (28–30) yielded 2,2-dimethyl-5-hydroxy-6-acetylchromene and fractions 31–36 yielded plumbagin. Both compounds yielded crystals in light petroleum (b.p. 60–80°C). The compounds were characterized by ^1H and ^{13}C NMR and mass spectrometry.

The roots of *P. zeylanica* were collected from Ambikapur, Madhya Pradesh, India, in September 1990 and a voucher specimen has been deposited in the Botany Department of this Institute.

Apparatus

A Waters (Milford, MA, USA) modular HPLC system consisting of a U6K injector, M-6000A pump, M-450 variable-wavelength detector and M-730 data system was used. Analysis was performed on μSpherogel column (30 cm × 8.0 mm I.D.; particle size 10 μm) (Altex Scientific, Berkeley, CA, USA).

HPLC conditions

The composition of the mobile phase was optimized by varying the percentage of *n*-hexane, resulting in the following operating conditions: *n*-hexane–chloroform–2-propanol (30:70:2, v/v/v), flow-rate 1 ml/min, column temperature 27°C, detector wavelength 267 nm and detector sensitivity 0.04 a.u.f.s.

Calibration graphs

Known amounts of plumbagin (10 mg in 50 ml) and 2,2-dimethyl-5-hydroxy-6-acetylchromene (10 mg in 50 ml) were prepared in chloroform. Different volumes of these standards were injected using the HPLC conditions described above. The area counts of peaks (y) and the corresponding concentrations (x) were used to plot the calibration graphs. The graphs were linear in the range 0.2–10 μg. The regression equations for plumbagin and 2,2-dimethyl-5-hydroxy-6-acetylchromene were $y = 7.800x + 0.260$ ($r = 0.99$) and $y = 6.600x - 0.000$ ($r = 0.99$), respectively.

Extraction procedure

Four sets of air-dried roots (10 g each) were Soxhlet extracted using *n*-hexane for different time intervals (1, 2, 4 and 6 h). Similarly, another four sets (10 g each) were extracted with chloroform. The extract thus obtained in each extraction was concentrated under vacuum and diluted to 10 ml with chloroform. Samples were filtered through a Millipore sample filtration kit and 1 μl of each extract was injected into the HPLC system under the conditions mentioned above. Three experiments were peformed and average values are reported in Table I. Extraction of plant material with chloroform for 4 h was found to give a maximum yield of plumbagin.

RESULTS AND DISCUSSION

Fig. 1 shows plots of the capacity factor and resolution *versus* percentage of *n*-hexane in the mobile phase. The effect of variation in *n*-hexane concentration on the recovery of plumbagin is shown in Fig. 2. Fig. 1 shows that the capacity factor difference between the two compounds increases with increasing *n*-hexane concentration. The resolution increases similarly. The recovery of both plumbagin and 2,2-dimethyl-5-hydroxy-6-acetylchromene is effected by the composition of the mobile phase. The solvents *n*-hexane–chloroform–2-propanol (75:25:2 to 35:65:2) are not efficient in eluting these compounds completely, and causes peak broadening, baseline shifts and smaller area counts, although a better resolution as is evident from Fig. 1. The mobile phases *n*-hexane–chloroform–isopropanol (10:90:2 to 25:75:2) provided a stable baseline, symmetrical peaks and reproducible

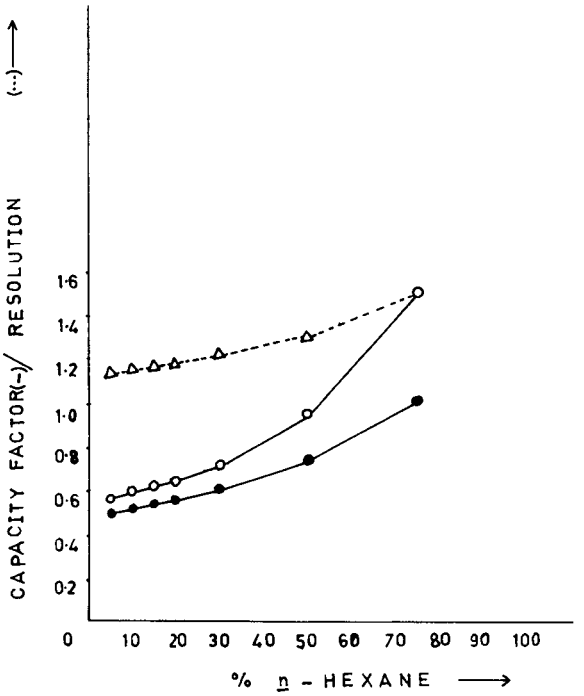

Fig. 1. Effect of *n*-hexane concentration in the mobile phase on the capacity factor (○ = plumbagin; ● = 2,2-dimethyl-5-hydroxy-6-acetylchromene) and the resolution (△).

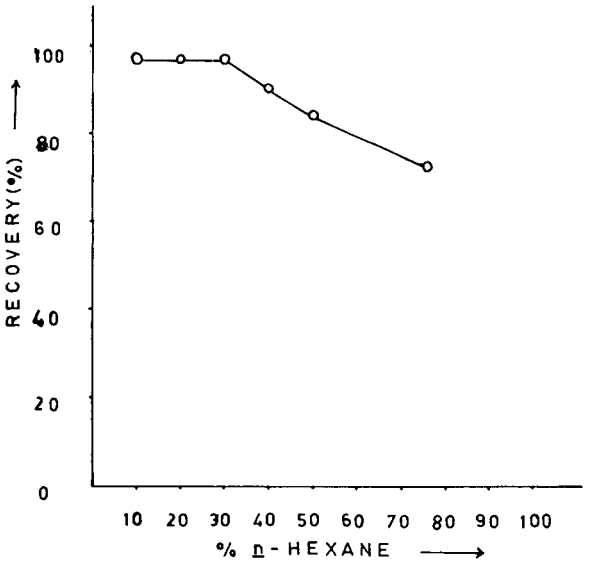

Fig. 2. Effect of *n*-hexane concentration in the mobile phase on the recovery of plumbagin.

area counts with lower resolution. Taking into consideration all these factors, the optimum conditions were fulfilled by using *n*-hexane–chloroform–2-propanol (30:70:2). The recovery of plumbagin was only 72% with *n*-hexane–chloroform–2-propanol (75:25:2), 84% with *n*-hexane–chloroform–2-propanol (50:50:2), 90% with *n*-hexane–chloroform–2-propanol (40:60:2) and the maximum of 97% with *n*-hexane–chloroform–2-propanol (30:70:2). All the recoveries were calculated by injecting a stock solution in each mobile phase.

Table I shows that the extraction of both plumbagin and 2,2-dimethyl-5-hydroxy-6-acetylchromene is not complete when extracted with *n*-hexane, as the amount is less than that extracted with chloroform for the same intervals. This further confirms that an increase in the *n*-hexane concentration in the mobile phase will decrease the recovery of the compounds.

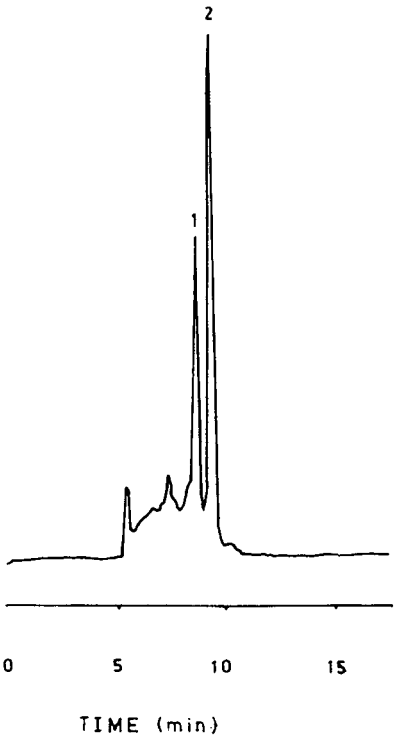

Fig. 3. HPLC separation of plumbagin and 2,2-dimethyl-5-hydroxy-6-acetylchromene from a plant extract on a μSpherogel column. UV detection at 267 nm. Mobile phase, *n*-hexane–chloroform–2-propanol (30:70:2); flow-rate, 1 ml/min. Peaks: 1 = 2,2-dimethyl-5-hydroxy-6-acetylchromene; 2 = plumbagin.

TABLE I

CONTENTS OF PLUMBAGIN AND 2,2-DIMETHYL-5-HYDROXY-6-ACETYLCHROMENE IN *PLUMBAGO ZEYLANICA* EXTRACTED FOR DIFFERENT TIME INTERVALS WITH *n*-HEXANE AND CHLOROFORM

Solvent	Plumbagin (%)				2,2-Dimethyl-5-hydroxy-6-acetylchromene (%)			
	1 h	2 h	4 h	6 h	1 h	2 h	4 h	6 h
n-Hexane	0.010	0.012	0.018	0.018	0.008	0.010	0.014	0.014
Chloroform	0.021	0.024	0.032	0.032	0.012	0.018	0.022	0.022

These observations led us to select the solvent system *n*-hexane–chloroform–2-propanol (30:70:2) for the optimum separation and determination of plumbagin. The separation of the two compounds from a plant extract is shown in Fig. 3. The numbers of theoretical plates for plumbagin and 2,2-dimethyl-5-hydroxy-6-acetylchromene were 3750 and 2240, respectively.

In conclusion, the HPLC method described is efficient and simple for the separation and determination of plumbagin and 2,2-dimethyl-5-hydroxy-6-acetylchromene in plant extracts.

ACKNOWLEDGEMENT

We are grateful to Dr. R.S. Thakur, Director, CIMAP, Lucknow, for his keen interest during the course of this work.

REFERENCES

1 G.V. Satyavati, A.K. Gupta and N. Tandon (Editors), *Medicinal Plants of India*, Vol. 2, Indian Council of Medical Research, New Delhi, 1987, p. 472.
2 P. Premakumari, K. Rathinam and G. Santhakumari, *Indian J. Med. Res.*, 65 (1977) 829.
3 M. Krishnaswamy and K.K. Purushothaman, *Indian J. Exp. Biol.*, 18 (1980) 876.
4 P. Premakumari and G. Santhakumari, *Indian J. Pharmacol.*, 7 (1975) 91.
5 G. Santhakumari, K. Rathinam and C. Seshadri, *Indian J. Exp. Biol.*, 16 (1978) 485.
6 N.G.K. Pillai, R.V. Menon, G.B. Pillai, S. Rajasekharan and C.P.R. Nair, *J. Res. Ayur. Siddha*, 2 (1981) 122.
7 A. Marston and K. Hostettmann, *J. Chromatogr.*, 295 (1984) 526.

Journal of Chromatography, 637 (1993) 213–218
Elsevier Science Publishers B.V., Amsterdam

CHROM. 24 995

Short Communication

Mass transfer in open-tubular supercritical fluid chromatography

Karel Janák*, Agneta Bemgård and Anders Colmsjö

Department of Analytical Chemistry, National Institute of Occupational Health, S-171 84 Solna (Sweden)

Ingela Hägglund and Lars G. Blomberg

Department of Analytical Chemistry, University of Stockholm, Arrhenius Laboratory, S-106 91 Stockholm (Sweden)

(First received October 28th, 1992; revised manuscript received February 8th, 1993)

ABSTRACT

Solute band broadening in 50 μm I.D. open tubular columns coated with PS-264 stationary phase has been evaluated in supercritical fluid chromatography. An improved method for on-column measurements of stationary phase swelling was used. For the conditions evaluated, a significant contribution to the total solute band broadening originating from stationary phase interactions was found. Possible sources of solute band broadening in the stationary phase are discussed.

INTRODUCTION

Recently, increasing attention has been paid to physicochemical interactions in a solute–supercritical fluid–stationary phase system. Different methods have been used to study the thermodynamics of phase-transfer processes, however the application of mass spectrometric tracer pulse chromatography seems to have been particularly fruitful [1–3]. Gibbs adsorption isotherms of carbon dioxide in a stationary phase as a function of pressure or density have thus been measured in different systems [3]. The swelling of the stationary phase as a result of the interaction with supercritical fluids is of particular interest in connection with the chromatographic process. Swelling was first studied in wide-bore columns by Springston *et al.* [4]. Shim and Johnston [5] correlated the swelling of a silicone rubber in supercritical carbon dioxide with the activity of carbon dioxide. It was thereby possible to predict the solute distribution between a polymer and a fluid phase. Further, these authors pointed out the influence of swelling on the accurate estimation of solute distribution coefficients by means of elution supercritical fluid chromatography (SFC) [6].

Unfortunately, understanding of the kinetics of these processes is less developed. The validity of the Golay equation [7] for evaluation of solute band broadening in open tubular columns under

* Corresponding author. On leave from Institute of Analytical Chemistry, Czech Academy of Sciences, 611 42 Brno, Czech Republic.

0021-9673/93/$06.00

SFC conditions is commonly accepted. However, the effects of supercritical fluid–stationary phase interactions ought to be considered as well. Possible effects of the swollen stationary phase on mass transfer were discussed but not evaluated in two papers in which a procedure for the measurement of swollen stationary phase film thickness was presented [4,8].

In this work solute band broadening in open tubular columns (OTCs) coated with PS-264 stationary phase has been evaluated in SFC. Using previously measured values for solute diffusion coefficients in supercritical carbon dioxide [9], solute band broadening originating from mobile phase diffusion has been directly estimated. Keeping extra-column effects at almost zero level by appropriate design of set-up [9], the remainder of the solute band broadening (contribution of mobile phase being subtracted) relates to the effects of mass transfer in the stationary phase. Corresponding effective diffusion coefficients of solutes were calculated. Possible contributions to solute band broadening in the stationary phase are discussed.

EXPERIMENTAL

Column preparation

A fused-silica capillary was silylated with methylhydro (3–4%) dimethyl (96–97%) polysiloxane, PS-124.5 (ABCR, Karlsruhe, Germany), using 1% solution in pentane. The dynamically coated capillary was heated at a rate of 5°C/min to 300°C and maintained at this temperature for 4 h. After rinsing with 0.5 ml of pentane and 0.5 ml of dichloromethane, the capillary was statically coated with PS-264 stationary phase (Fluka, Buchs, Switzerland) from a solution in pentane and dichloromethane (1:1) corresponding to film thickness (d_f) = 0.5 μm. Dicumylperoxide was added to the coating solution in the amount corresponding to 1% of stationary phase weight as a radical initiator of stationary phase cross-linking. Stationary phase immobilization was achieved by heating the column with sealed ends from 40 to 175°C at a rate of 5°C/min and keeping the temperature at 175°C for 20 min. The column was tested in GC by injection of a mixture of C_{12}–C_{17} *n*-alkanes and biphenyl and then washed with 1 ml of pentane and 1 ml of dichloromethane and retested in the same way. The decrease in k' values after rinsing corresponded to a reduction in d_f from 0.5 to 0.44 μm.

Instrumentation

Solute band broadening was measured on an apparatus slightly modified from that described for measurements of diffusion coefficients in supercritical carbon dioxide [9] (Fig. 1). A Suprex SFC/200A supercritical fluid chromatograph (Pittsburgh, PA, USA) was equipped with a pneumatically actuated Valco injection valve Model C14W (Valco Instruments, Houston, TX, USA) with a 0.06-μl internal loop. A fused-silica column, 6.67 m × 50 μm I.D., coated with methylpolysiloxane PS-264, d_f = 0.44 μm, was connected to the injection valve via a flow splitter, the other end being connected to a variable-flow restrictor 0.40 m × 9 μm (R_1) via a low-dead-volume butt connector, MVSU 004 (SGE, Austin, TX, USA). A back-pressure μLC-500 micropump (Isco, Lincoln, NE, USA) controlling mobile phase velocity by adjustment of the pressure drop over the variable-flow restrictor was connected to this restrictor and a restrictor, 0.35 m × 9 μm (R_2), ending in the jet of the flame ionization detector via a low-dead-volume ZT.5 Valco T-piece. As was proven in a previous paper [9], this apparatus exhibited no measurable extra-column effects. The chromatograph was connected to an ELDS 900 laboratory data

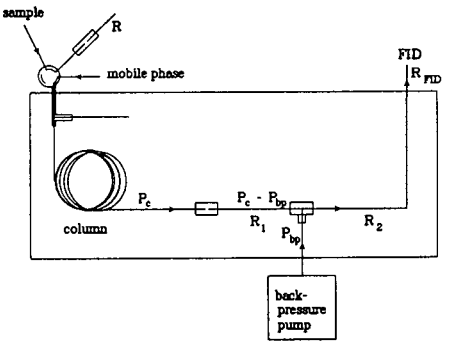

Fig. 1. Apparatus scheme for the band broadening measurement. R_1, R_2 and R_{FID} are restrictors; P_c and P_{bp} are column pressure and back-pressure, respectively; $P_c - P_{bp}$ is pressure drop over the variable flow restrictor R_1.

system (Chromatography Data System, Kungshög, Stenhamra, Sweden).

Measurement of the stationary phase swelling

The thickness of the swollen stationary film was measured by the on-column chromatographic method [4]. A modified procedure using the apparatus for measurement of diffusion coefficients in supercritical fluids [9] was used (Fig. 2). The column effluent (F_C) was split between an empty tube (F_T), 2.24 m × 50 μm, connected to a flame ionization detector via a variable-flow restrictor, R_1, and to the flame ionization detector (F_s) via a restrictor, 0.15 m × 5 μm (R_s). The flow-split ratio (C) was calculated from the corresponding areas of peaks of the same solute eluted from the column through the R_s restrictor (area A_C) and from the empty tube through the variable-flow restrictor R_1 (area A_T). Thus $C = (F_s/F_T) = (A_C/A_T)$. The column was prepared from the same batch of fused-silica capillary as the empty tube.

Measuring the hold-up time in the empty tube, t_m^T, and calculating dead time in the column, t_m^C, according to Guardino *et al.* [10] using C_6–C_{13} *n*-alkanes, the film thickness of the swollen stationary phase, d_f^*, was obtained from the formula:

$$d_f^* = r_T\left[1 - \sqrt{(1+C)\frac{L_T t_m^C}{L_C t_m^T}}\right] \quad (1)$$

where r_T is the radius of the empty tube and L_T and L_C are the lengths of the empty tube and the column, respectively.

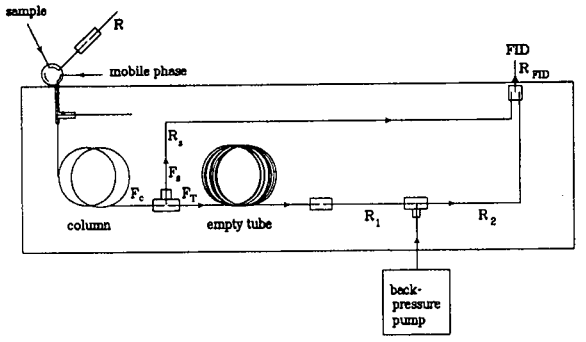

Fig. 2. Apparatus scheme for the measurement of the stationary phase swelling. R_s, R_1, R_2 and R_{FID} are restrictors and F_C, F_s and F_T are column flow, effluent split flow and empty tube flow, respectively.

Band-broadening measurements

Broadening of the solute zone in the column was estimated for C_8–C_{13}, C_{15} *n*-alkanes, dodecanone and biphenyl by injection of their solution in pentane, 10 mg/ml, on the column at 100 atm, 125°C, using 50–100 ms time split and a flow-split ratio of 1:4 to 1:10. Mobile phase velocity was adjusted to 28.8–41.2 mm/s by a back-pressure device [9] using supercritical carbon dioxide. The mixture was injected six or seven times at five different velocities.

Data handling

Chromatograms were registered at a speed of 4.55 Hz. An optimization programme was obtained by means of a least-squares fit of the measured values (H_i, u_i) to the Golay equation [7,11]. For capacity ratio the mean of all capacity ratios for each solute at all applied mobile phase velocities, and for column radius the difference $r_T - d_f^*$, were substituted into the Golay equation.

RESULTS AND DISCUSSION

Accurate estimation of the film thickness of swollen stationary phases is a prerequisite for evaluation of stationary phase contribution to total solute band broadening. The on-column chromatographic method is considered to be less precise than mass spectrometric tracer pulse chromatography [6]. However, it does not necessitate any special instrumentation, and precision can be increased by avoiding manipulation of the columns during measurements. Thus, an accurate ratio of volumetric flows can be measured, which is not the case if the columns are reconnected to the restrictor (possible flow change in the low-dead-volume connector). Unfortunately, none of these methods is able to distinguish between the adsorbed layer of carbon dioxide on the surface of the stationary phase and the swollen stationary phase film thickness itself. As one to three monolayers of carbon dioxide were proven to be sorbed on the surface of common adsorbents [12], a stagnant layer

should be supposed on the surface of a polymeric stationary phase film as well.

The film thickness of the swollen stationary phase at 100 atm, 125°C, was estimated to be 1.28 μm (S.D. = 0.09 μm, $n = 10$), which corresponds to a swelling factor of 1.9 (S.D. = 0.3). This is somewhat higher than that found by Springston *et al.* [4] for SE-30 at 89 atm, 40°C, which was 1.0 ± 0.6. The difference might originate from different degree of cross-linking. In this case, 88% immobilization degree has been obtained, which is sufficient to get stable stationary phase film and keep the column efficiency. Thus, possible changes in the stationary phase diffusivity due to excessive cross-linking were avoided.

In Table I, effective solute diffusion coefficients in the stationary phase measured in SFC [$D_s(\text{eff.})^{SF}$] are summarized together with corresponding solute diffusion coefficients in the supercritical fluid phase (D_m^{SF}). Variation in measurements of swollen film thickness (R.S.D. = 7%) gives a relative standard deviation for effective solute diffusion coefficients of 14%. The standard deviation of solute capacity ratios was less than 2.7%, which had almost no effect on the variation of solute effective diffusion coefficients, R.S.D. < 2.5%. Compared with the effective solute diffusion coefficients in the same stationary phase estimated from data measured by GC [$D_s(\text{eff.})^{G}$] [11] and the data obtained with similar polysiloxane phases [13], the values measured in SFC are at least one order of magnitude lower. Similarly, Horká *et al.* [14] showed that the diffusion in the stationary phase in OTLC is dependent on the type of mobile phase used. In theoretical calculations of the effect of stationary phase film thickness on efficiency in open tubular SFC [15,16] and LC [16], the stationary phase diffusion was assumed to be independent of the mobile phase. Such an assumption may produce misleading conclusions.

Evaluation of solute band broadening in the stationary phase under GC conditions revealed a significant contribution of mobile phase–stationary phase film interphase resistance to the total solute band broadening [11]. Including this effect, the extended Golay equation can be written:

$$H = B/u + C_m u + (C_s + C_i)u \quad (2)$$

where:

$$C_s = \frac{2k' d_f^{*2}}{3(1+k')^2 D_s} \quad (3)$$

$$C_i = \frac{2k' d_f^{*}}{(1+k')^2 k_d} \quad (4)$$

C_m, C_s and C_i are resistance to the mass transfer in the mobile phase, stationary phase and in the interphase between these phases, respectively. D_s is the solute diffusion coefficient in the swollen stationary phase and k_d is the desorption rate constant. In a previous paper [11], values of solute diffusion coefficients independent of film thickness were obtained (D_s^G) and desorption rate constants (k_d^G) were calculated for the same stationary phase as used here. Similarly, using GC values of solute diffusion coefficients independent of stationary phase film thickness,

TABLE I

SOLUTE DIFFUSION COEFFICIENTS IN STATIONARY PHASE PS-264 AT 125°C AND 100 atm (1 atm = 101 325 Pa)

Solute	D_m^{SF} $\times 10^3$ (mm^2/s)	$D_s(\text{eff.})^{SF}$ $\times 10^3$ (mm^2/s)	k_d^{SF} (mm/s)	$D_s(\text{eff.})^{G}$ $\times 10^3$ (mm^2/s)	D_s^G $\times 10^3$ (mm^2/s)	k_d^G (mm/s)
C_{11}	47	0.0474	0.115	0.54	1.35	2.90
C_{12}	45	0.0472	0.115	0.49	1.33	2.50
C_{13}	44	0.0488	0.119	0.51	1.33	2.67
C_{15}	41	0.0225	–	–	–	–
C_{12} on	43	0.0715	–	–	–	–
Biphenyl	50	0.0072	0.017	0.70	2.12	3.37

desorption rate constants for SFC conditions (k_d^{SF}) were calculated. Compared with GC conditions, k_d^{SF} is affected not only by solute interaction with stationary phase, but by solute solubility in the mobile phase as well. Lower solubility of biphenyl compared with the *n*-alkanes used in supercritical carbon dioxide corresponds to lower k_d^{SF} values. However, possible effects of a stagnant layer of supercritical carbon dioxide are included in these values.

As has been recently found in OTCs coated with Carbowax 20M, a stagnant layer of mobile phase has a significant influence on solute band broadening under LC conditions [14]. Accordingly, further extension of the Golay equation for evaluation of all contributions is necessary:

$$H = B/u + C_m u + (C_s + C_i + C_{SM})u \quad (5)$$

where C_{SM} is the contribution to mass transfer from the stagnant layer, which can be expressed according to ref. 17 as:

$$C_{SM} = \frac{2(1 - \Phi + k')^2 d_f^{*2}}{3(1 - \Phi)(1 + k')^2 D_{SM}} \quad (6)$$

where Φ is the part of the mobile phase in the swollen stationary phase film and D_{SM} is solute diffusion coefficient in the stagnant layer. Separate evaluation of C_i and C_{SM} terms is not possible from these experiments. The total contribution of the stationary phase to solute band broadening was estimated and the percentage contributions of resistance to solute mass transfer in mobile and in stationary phases at a velocity, 20 mm/s, commonly used in SFC were calculated from the measured data and are expressed in Table II. The contribution of the stationary phase to solute band broadening is commonly considered to be low under SFC conditions [15,16], but in the present work mass transfer in the stationary phase contributed about 50% to the total solute band broadening.

Further progress in the understanding of mass transfer effects in the stationary phase under SFC conditions can be achieved if a non-retained solute with good solubility in supercritical carbon dioxide is used for estimation of stagnant layer contributions. By subtracting this contribution to solute band broadening in columns differing in film thickness, contribution of interphase resistance can be obtained.

TABLE II

EFFECTS OF THE MASS TRANSFER TERMS ON HEIGHT EQUIVALENT TO A THEORETICAL PLATE (HETP) IN SFC AT 125°C, 100 atm, AND VELOCITY 2 cm/s CALCULATED ACCORDING TO EQN. 5

Column: 6.67 m × 50 μm; PS-264, $d_f^* = 1.28$ μm

Solute	HETP (mm)	k'	$C_m \times u$ (%)	$(C_s + C_i + C_{SM}) \times u$ (%)
C_{12}	0.17	1.94	38	59
C_{13}	0.17	2.76	46	52
C_{15}	0.23	5.62	44	54
C_{12} on	0.14	3.76	61	36

In summary, it was found that, for the conditions evaluated, effective diffusion in the stationary phase was one order of magnitude lower when applying SFC conditions than when GC conditions were applied. As a consequence, the contribution to band broadening from mass transfer in the stationary phase was higher than reported earlier. Thus, unacceptable band broadening would appear at lower film thicknesses than previously thought.

REFERENCES

1 M.I. Selim and J.R. Strubinger, *Fresenius' Z. Anal. Chem.*, 330 (1988) 246.
2 M. Roth, *J. Microcol. Sep.*, 3 (1991) 173.
3 C.R. Yonker and R.D. Smith, *J. Chromatogr.*, 550 (1991) 775.
4 S.R. Springston, P. David, J. Steger and M. Novotny, *Anal. Chem.*, 58 (1986) 997.
5 J.-J. Shim and K.P. Johnston, *AIChE J.*, 35 (1989) 1097.
6 J.-J. Shim and K.P. Johnston, *AIChE J.*, 37 (1991) 607.
7 M.J.E. Golay, in V.J. Coates, H.J. Noebels and I.S. Fagerson (Editors), *Gas Chromatography*, Academic Press, New York, 1958, p. 36.
8 M. Novotny and P. David, *J. High Resolut. Chromatogr. Chromatogr. Commun.*, 9 (1986) 647.
9 K. Janák, I. Hägglund, L.G. Blomberg, A.K. Bemgård and A.L. Colmsjö, *J. Chromatogr.*, 625 (1992) 311.
10 X. Guardino, J. Albaigés, G. Firpo, R. Rodriguez-Viñals and M. Gassiot, *J. Chromatogr.*, 118 (1976) 13.
11 A. Bemgård, L. Blomberg and A. Colmsjö, *Anal. Chem.*, 61 (1989) 2165.
12 J.F. Parcher and J.R. Strubinger, *J. Chromatogr.*, 479 (1989) 251.

13 J.M. Kong and S.J. Hawkes, *J. Chromatogr. Sci.*, 14 (1976) 279.
14 M. Horká, M. Krejcí and V. Kahle, *J. Microcol. Sep.*, 4 (1992) 305.
15 S.M. Fields, R.C. Kong, M.L. Lee and P.A. Peaden, *J. High Resolut. Chromatogr. Chromatogr. Commun.*, 7 (1984) 423.
16 P.J. Schoenmakers, *J. High Resolut. Chromatogr. Chromatogr. Commun.*, 11 (1988) 278.
17 S.J. Hawkes, *J. Chromatogr.*, 68 (1972) 1.

Journal of Chromatography, 637 (1993) 219–223
Elsevier Science Publishers B.V., Amsterdam

CHROM. 24 958

Short Communication

Determination of ephedrine and pseudoephedrine in Chinese herbal preparations by capillary electrophoresis

Ying-Mei Liu and Shuenn-Jyi Sheu*

Department of Chemistry, National Taiwan Normal University, 88, Sec. 5, Roosevelt Road, Taipei (Taiwan)

(First received November 24th, 1992; revised manuscript received February 5th, 1993)

ABSTRACT

A simple, rapid and accurate capillary electrophoresis method was developed for the assay of ephedrine and pseudoephedrine in Chinese herbal preparations. The buffer solution used was a 0.01 *M* valine solution with the pH adjusted to 10.0 with ammonia solution (7.2 *M*). The linear calibration range was 0.008–0.240 mg/ml ($r = 0.9996$) for both compounds and the recoveries were 98.0–102.3% for ephedrine and 99.0–101.5% for pseudoephedrine. The relative standard deviation was 0.86% for ephedrine and 0.87% for pseudoephedrine ($n = 6$) respectively. The contents of these two alkaloids in Ephedrae Herba-containing Chinese herbal preparations could easily be determined within 3 min.

INTRODUCTION

Ephedrae Herba (Ma-Huang) is a commonly used Chinese herbal drug intended for diaphoretic purposes, and is known to contain mainly (−)-ephedrine and (+)-pseudoephedrine [1]. It may combine with other herbs to form a sudorific, surface-internal acting, vitality-regulating or carminative formula [2]. At present, the best method to evaluate the quality of Ephedrae Herba-containing Chinese herbal preparations is to determine the contents of ephedrine and pseudoephedrine by HPLC [3,4]. However, owing to the complicated components in Chinese herbal formulations, the use of HPLC is restricted owing to the long time required (about 30 min), interference from alkaloidal peaks and contamination of the chromatographic column, which is difficult to clean. Capillary electrophoresis (CE) is a recently developed technique that offers short analysis times and easy thorough cleaning of the capillary, only small amounts of sample are required and autosampling is possible. It has given good results in the analysis of Chinese herbs [5–7]. In this study, CE was applied to various Ephedrae Herba-containing formulations with satisfactory results. Hence CE appears to be a suitable method for analyses of Chinese herbal preparations, especially for large numbers of samples and for quality control in pharmaceutical plants.

EXPERIMENTAL

Reagents and materials

Ephedrine hydrochloride and pseudoephedrine hydrochloride were purchased from Aldrich (Milwaukee, WI, USA) and valine from Merck (Darmstadt, Germany). Methyltriphenylphos-

* Corresponding author.

0021-9673/93/$06.00

phonium iodide, used as an internal standard, was prepared from triphenylphosphine and methyl iodide [8]. Deionized water from a Milli-Q system (Millipore, Bedford, MA, USA) was used to prepare all buffer and sample solutions. Methanol was of HPLC grade. Ammonia solution (7.2 *M*) was of extra-pure grade. Ephedrae Herba-containing Chinese herbal preparations were provided by Sun-Ten Pharmaceutical Manufactory.

Preparation of Chinese herbal preparation extracts

A 0.5-g sample of Chinese herbal preparation was extracted with 70% methanol (3 ml) by stirring at room temperature for 30 min, then centrifuged at 1500 *g* for 10 min. Extraction was repeated three times. The extracts were combined and filtered through a No. 1 filter-paper. After the addition of 1.0 ml of internal standard solution (0.6 mg of methyltriphenylphosphonium iodide in 1 ml of 70% methanol), the Chinese herbal preparation extract was diluted to 10 ml with 70% methanol. This solution was passed through a 0.45-μm filter and *ca.* 0.8 nl (5-s hydrostatic sampling) of the filtrate was injected directly into the capillary electrophoresis system.

Apparatus and conditions

All analyses were carried out on a Waters Quanta 4000 CE system equipped with a UV detector set at 185 nm and a 60 cm × 75 μm I.D. uncoated capillary (Millipore) with the detection window placed at 52.5 cm. The conditions were as follows: sampling time, 5 s, hydrostatic; run time, 3 min; applied voltage, 20 kV (constant voltage, positive to negative polarity); temperature, 26.5–27.0°C. The electrolyte was a buffer solution that contained 0.01 *M* valine and adjusted to pH 10.0 with ammonia solution. The electrolyte was filtered through a 0.45-μm filter before use.

Solution for linearity response

Eight concentrations of ephedrine and pseudoephedrine in the range 0.008–0.240 mg/ml were prepared. Each concentration was analysed three times.

Solution for recovery studies

Different amounts of ephedrine and pseudoephedrine standard were added to two samples of Chinese herbal preparations of known alkaloidal content and the mixtures were extracted and analysed using the proposed procedure.

RESULTS AND DISCUSSION

Analytical conditions

In the study of Ephedrae Herba crude drugs [5,9], we found that a buffer solution containing 0.005 *M* barium hydroxide and 0.02 *M* isoleucine and adjusted to pH 10.0 with ammonia solution could give a good resolution of the six ephedrine alkaloids (ephedrine, pseudoephedrine, norephedrine, norpseudoephedrine, methylephedrine and methylpseudoephedrine) and setting the detection wavelength at 185 nm could enhance the alkaloidal signals. However, surveys of a number of commercial Ephedrae Herba-containing Chinese herbal preparations showed that generally only ephedrine and pseudoephedrine were present in the test solutions. These two compounds are now used as marker substances on the evaluation of Chinese herbal preparations by HPLC [3]. Therefore, it would be desirable to have a far simpler method with a shorter analysis time that can be applied to various Ephedrae Herba-containing formulations, though it may only be able to separate ephedrine and pseudoephedrine well.

From the analysis of Ephedrae Herba [5], we knew that amino acids were good counter ions for ephedrine and pseudoephedrine and the use of ammonia solution for pH adjustment could shorten the analysis time and enhance the absorption signals. Hence we tried to prepare the buffer solutions with alanine, valine, isoleucine, leucine separately and adjusted their pH values with ammonia solution, and found that all these amino acids were suitable for this purpose. After a series of experiments, it was found that 0.01 *M* valine solution (pH 10.0, adjusted with ammonia solution) could resolve ephedrine and pseudoephedrine within 3 min. In comparison with buffer solutions of different concentrations, two concentrations (0.02 and 0.005 *M*) of valine solution were prepared. It was found that at the

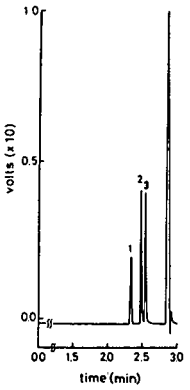

Fig. 1. Capillary electropherogram of a mixture of ephedrine and pseudoephedrine. Peaks: 1 = internal standard (methyltriphenylphosphonium iodide), 0.060 mg/ml; 2 = pseudoephedrine, 0.080 mg/ml; 3 = ephedrine, 0.080 mg/ml.

higher concentration of valine solution, the absorption signals of ephedrine and pseudoephedrine became very weak, whereas at the lower concentration, the peaks of ephedrine and pseudoephedrine were found to be partially overlapped. Comparison was also made with buffer solutions of different pH. Two buffer solutions of pH 10.5 and 9.5 were prepared. It was found that at high pH, the separation was good, but the absorption signals of ephedrine and pseudoephedrine were decreased and the analysis time was prolonged to 4 min, whereas at the lower pH, the separation was not good.

An electrolyte containing 0.01 *M* valine solution and adjusted to pH 10.0 with ammonia solution was found to produce the best resolu-

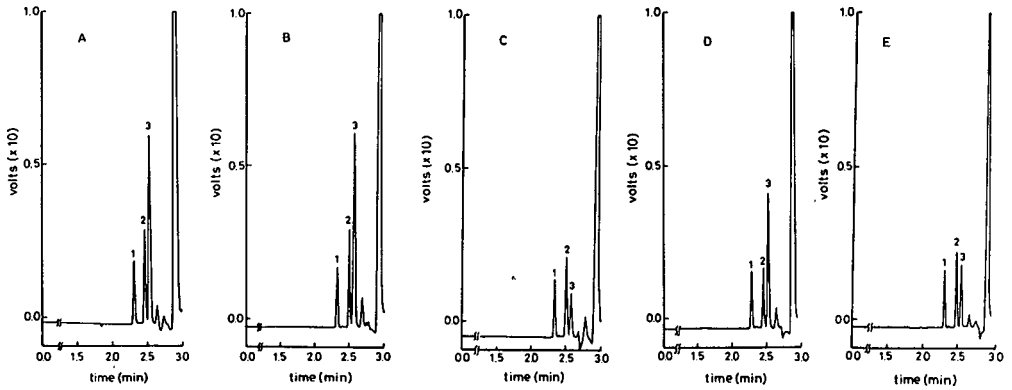

Fig. 2. Capillary electropherogram of Chinese herbal preparations: (A) Ma-huang-tang; (B) Ma-hsing-kan-shih-tang; (C) Ko-ken-tang; (D) Ta-ching-lung-tang; (E) Ma-hsing-i-kan-tang. Peaks as in Fig. 1.

TABLE I

RECOVERY OF EPHEDRINE AND PSEUDOEPHEDRINE FROM CHINESE HERBAL PREPARATIONS ($n = 3$)

Sample[a]	Alkaloid	Added (μg)	Found (μg)	Recovery (%)
Ma-huang-tang	Ephedrine	200	196	98.0
		400	395	98.8
	Pseudoephedrine	200	198	99.0
		400	396	99.0
Ma-hsing-kan-shih-tang	Ephedrine	200	204	102.0
		400	409	102.3
	Pseudoephedrine	200	202	101.0
		400	406	101.5

[a] See footnote to Table II.

TABLE II

CONTENTS OF EPHEDRINE AND PSEUDOEPHEDRINE IN CHINESE HERBAL PREPARATIONS ($n = 3$)

Sample[a]	Ephedrine (mg/g)	Pseudoephedrine (mg/g)	Total (mg/g)
1	0.49	0.43	0.92
2	0.59	0.21	0.80
3	0.23	1.57	1.80
4	1.31	0.44	1.75
5	0.45	0.36	0.81
6	1.77	0.87	2.64
7	0.81	0.36	1.17
8	0.89	1.68	2.57
9	3.45	0.62	4.07
10	0.86	1.04	1.90
11	2.92	1.29	4.21
12	4.30	1.71	6.01
13	2.85	1.30	4.15
14	4.54	1.66	6.20
15	0.49	0.67	1.16
16	2.14	0.89	3.03
17	1.27	0.60	1.87
18	0.98	0.45	1.43
19	1.03	0.48	1.51

[a] Names and compositions of the Ephedrae Herba-containing Chinese herbal formulations: **1** = *Ching-pi-tang:* Pueriae Radix, Cinnamomi Cortex, Zingiberis Rhizoma, Ligustici Rhizoma, Glycyrrhizae Radix, Platycodi Radix, Ephedrae Herba, Paeoniae Radix, Gypsum Fibrosum, Rhei Rhizoma, Coicis Semen, Magnoliae Flos, Zizyphi Fructus; **2** = *Fang-feng-tung-sheng-san:* Angelicae Radix, Paeoniae Radix, Gardeniae Fructus, Ligustici Rhizoma, Forsythiae Fructus, Schizonepetae Herba, Ledebouriellae Radix, Natrium Sulfuricum, Ephedrae Herba, Zingiberis Rhizoma, Rhei Rhizoma, Atractylodis Rhizoma, Menthae Herba, Platycodi Radix, Scutellariae Radix, Glycyrrhizae Radix, Talcum, Gypsum Fibrosum; **3** = *Hsiao-ching-lung-tang:* Ephedrae Herba, Cinnamomi Ramulus, Glycyrrhizae Radix, Paeoniae Radix, Zingiberis Siccatum Rhizoma, Asari Herba Cum Radice, Pinelliae Tuber, Schizandrae Fructus; **4** = *Hsiao-hsu-ming-tang:* Ledebouriellae Radix, Cinnamomi Ramulus, Ephedrae Herba, Armeniacae Semen, Ligustici Rhizoma, Paeoniae Radix, Ginseng Radix, Glycyrrhizae Radix, Scutellariae Radix, Aristolochiae Fangchi Radix, Aconiti Tuber, Zingiberis Rhizoma; **5** = *Hsu-ming-tang:* Ephedrae Herba, Cinnamomi Ramulus, Ginseng Radix, Angelicae Radix, Ligustici Rhizoma, Zingiberis Siccatum Rhizoma, Glycyrrhizae Radix, Armeniacae Semen, Gypsum Fibrosum; **6** = *Hua-kai-san:* Ephedrae Herba, Mori Cortex, Perillae Semen, Poria, Armeniacae Semen, Citri Leiocarpae Exocarpium, Glycyrrhizae Radix; **7** = *I-yi-jen-tang:* Ephedrae Herba, Cinnamomi Ramulus, Angelicae Radix, Paeoniae Radix, Atractylodix Rhizoma, Glycyrrhize Radix, Coicis Semen; **8** = *Ko-ken-tang:* Paeoniae Radix, Cinnamomi Ramulus, Zingiberis Rhizoma, Glycyrrhizae Radix, Zizyphi Fructus, Puerariae Radix, Ephedrae Herba; **9** = *Kuei-chih-shao-yao-chih-mu-tang:* Cinnamomi Ramulus, Paeoniae Radix, Glycyrrhize Radix, Ephedrae Herba, Zingiberis Rhizoma, Atractylodis Rhizoma, Anemarrhenae Rhizoma, Ledebouriellae Radix, Aconiti Tuber; **10** = *Ma-hsing-i-kan-tang:* Ephedrae Herba, Armeniacae Semen, Glycyrrhizae Radix, Coicis Semen; **11** = *Ma-hsing-kan-shih-tang:* Ephedrae Herba, Armeniacae Semen, Glycyrrhizae Radix, Gypsum Fibrosum; **12** = *Ma-huang-fu-tzu-hsi-hsin-tang:* Ephedrae Herba, Aconiti Tuber, Asari Herba Cum Radice; **13** = *Ma-huang-tang:* Ephedrae Herba, Cinnamomi Ramulus, Armeniacae Semen, Glycyrrhizae Radix; **14** = *Shen-mi-tang:* Ephedrae Herba, Glycyrrhizae Radix, Armeniacae Semen, Perillae Folium, Magnoliae Cortex, Bupleuri Radix, Citri Leiocarpae Exocarpium; **15** = *Shih-shen-tang:* Ephedrae Herba, Paeoniae Radix, Glycyrrhizae Radix, Puerariae Radix, Angelicae Dahuricae Radix, Cimicifugae Rhizoma, Ligustici Rhizoma, Perillae Folium, Citri Leiocarpae Exocarpium, Cyperi Rhizoma; **16** = *Ta-ching-lung-tang:* Ephedrae Herba, Armeniacae Semen, Cinnamomi Ramulus, Zingiberis Rhizoma, Zizyphi Fructus, Glycyrrhize Radix, Gypsum Fibrosum; **17** = *Ting-chuan-tang:* Pinelliae Tuber, Zingiberis Rhizoma, Ginkgo Semen, Ephedrae Herba, Glycyrrhizae Radix, Fararae Flos, Mori Cortex, Perillae Semen, Armeniacae Semen, Scutellariae Radix; **18** = *Wu-chi-san:* Glycyrrhizae Radix, Angelicae Dahuricae Radix, Ligustici Rhizoma, Atratylodis Lanceae Rhizoma, Aurantii Fructus, Platycodi Radix, Ephedrae Herba, Zingiberis Rhizoma, Pinelliae Tuber, Zingiberis Siccatum Rhizoma, Paeoniae Radix, Citri Leiocarpae Exocarpium, Magnoliae Cortex, Angelicae Radix, Cinnamomi Cortex, Poria, Allii Fistulosi Bulbus; **19** = *Wu-yao-shun-chi-san:* Ephedrae Herba, Glycyrrhizae Radix, Angelicae Dahuricae Radix, Ligustici Rhizoma, Linderae Radix, Citri Leiocarpae Exocarpium, Platycodi Radix, Aurantii Fructus, Bombyx Batryticatus, Zingiberis Siccatum Rhizoma.

tion. Fig. 1 is an electropherogram showing the separation of authentic ephedrine and pseudoephedrine with migration times of 2.3 min for the internal standard, 2.5 min for pseudoephedrine and 2.6 min for ephedrine. The separation of these two constituents can be completed within 3 min. As the methanol–water extracts of Chinese herbal preparations were injected directly, the results were as good as those obtained with pure chemical samples without interference with each peak and the analysis could also be completed within 3 min, as shown in Fig. 2.

Calibration graphs for ephedrine and pseudoephedrine

Calibration graphs (peak-area ratio, y, *vs.* concentration, x, mg/ml) were constructed in the range 0.008–0.240 mg/ml. The regression equations of these curves and their correlation coefficients were calculated as follows: pseudoephedrine, $y = 26.35x + 0.03$ ($r = 0.9996$); ephedrine, $y = 26.61x + 0.05$ ($r = 0.9996$).

System suitability test

The reproducibility (relative standard deviation) of the proposed method, on the basis of peak-area ratios for six replicate injections, was 0.86% (intra-day) and 2.1% (inter-day) for ephedrine and 0.87% (intra-day) and 1.7% (inter-day) for pseudoephedrine.

The results of standard addition recovery studies of ephedrine and pseudoephedrine from sample composites of Chinese herbal preparations are given in Table I. The recoveries were 98.0–102.3% for ephedrine and 99.0–101.5% for pseudoephedrine. All the tailing factors of the three peaks (internal standard, pseudoephedrine and ephedrine) are very close to unity.

Determination of ephedrine and pseudoephedrine in Chinese herbal preparations

When the test solutions of extracts of Chinese herbal preparations were analysed by CE under the selected conditions, the calculated contents of ephedrine and pseudoephedrine given in Table II were obtained. Each peak of the extracts in various Chinese herbal preparations showed no interference. These results indicate that the proposed CE method is suitable for the determination of ephedrine and pseudoephedrine in Chinese herbal preparations. Moreover, this method not only uses the methanol–water extract directly, but also offers autosampling. In addition to its rapid and accurate performance, consecutive injections can be made within 5 min with a thoroughly cleaned capillary. Therefore, it should be especially useful for large numbers of samples and for quality control in pharmaceutical plants.

ACKNOWLEDGEMENT

Financial support from the National Science Council, Republic of China, is gratefully acknowledged.

REFERENCES

1 H.Y. Hsu, Y.P. Chen, S.J. Sheu, C.H. Hsu, C.C. Chen and H.C. Chang, *Chinese Material Medica —A Concise Guide*, Modern Drug Press, Taipei, 1984, pp. 31–32.
2 S.Y. Huang, *A Collective Commentary to Herbal Formulas*, Ba-Teh Education and Culture Press, Taipei, 1987, pp. 1–10.
3 M. Harada, Y. Kano, A. Akahori, Y. Ichio, O. Miura and H. Suzuki, *Iyakuhin Kenkyu*, 19 (1988) 852.
4 M. Harada, Y. Ogihara, Y. Kano, A. Akahori, Y. Ichio, O. Miura, K. Yamamoto and H. Suzuki, *Iyakuhin Kenkyu*, 20 (1989) 1300.
5 Y.M. Liu and S.J. Sheu, *J. Chromatogr.*, 600 (1992) 370.
6 Y.M. Liu and S.J. Sheu, *J. Chromatogr.*, 623 (1992) 196.
7 Y.M. Liu and S.J. Sheu, *J. Chromatogr.*, 634 (1993) 329.
8 H.E. Baumgarten, *Org. Synth., Coll. Vol.*, 5 (1973) 751.
9 Y.M. Liu, S.J. Sheu, S.H. Chiou, H.C. Chang and Y.P. Chen, *Planta Med.*, in press.

Author Index

Atmospheric Oxidation and Antioxidants, Volume II

edited by **G. Scott**

Oxidation by molecular oxygen is one of the most practically important of all chemical processes. It is the basis of energy production in animals and, at the same time, a major cause of irreversible deterioration and ultimate death. Man uses oxygen positively in the production of energy by combustion, and many important industrial processes in the petrochemical industry are based on the controlled oxidation of hydrocarbons. At the same time, oxidation is the main cause of deterioration of foodstuffs and of many industrial polymers.

It is clearly of great practical importance that the mechanisms of oxidation and its prevention should be understood in order to utilise the reactions of oxygen more effectively but, equally important, to control the adverse effects of oxygen on man-made products and in biological systems. The three volumes of this work are directed towards these objectives. Although complementary to one another, the three volumes form a single whole and it is hoped that, by frequent cross-reference, the reader will be enabled to utilise ideas and experience from other disciplines to enlighten his own.

Volume II examines the oxidation chemistry of carbon-based materials in more detail with emphasis on the technological phenomena that result from the attack of oxygen and the practical procedures developed to prevent them.

Contents: 1. Lubricating Oil Oxidation and Stabilisation *(T. Colclough).* Introduction. Effect of Basestock Composition on Oxidation Stability. The Performance of Lubricants in Engines. Bench Oxidation Tests. Catalysis by Metals and Nitrogen Oxides. Actions and Interactions of Antioxidants.
2. Deterioration of Edible Oils and Foodstuffs *(S.P. Kochhar).* Introduction. Food Oils and Fats. Types of Lipid Deterioration. Antioxidants and Mechanisms of Their Action. Concluding Remarks.
3. Oxidation and Stabilisation of Polymers during Processing *(G. Scott).* The Significance of the Processing Operation. Mechanodegradation of Polymers. Chemical Plasticisation (Peptisation) of Rubbers. The Effect of Temperature during Mechanooxidation. Processing of Thermoplastic Polymers. Stabilisation of Polymers during Processing. Effect of Melt Stabilisers on Subsequent Environmental Ageing.
4. The Physical Chemistry of Polymer Oxidation and Stabilisation *(N.C. Billingham).* Introduction. Surface Heterogeneity of Polymer Oxidation. Macroscopic Heterogeneity of Oxidation. Molecular Heterogeneity of Oxidation. Solubility of Polymer Additives. Mobility of Polymer Additives. Loss of Additives from Polymers. Physical Effects in Accelerate Ageing. Conclusions.
5. Macromolecular and Polymer-Bound Antioxidants *(G. Scott).* Solubility, Diffusivity and Volatility of Antioxidants. Environmental Impact of Additives in Polymers. Effect of Processing on Antioxidant Effectiveness. Antioxidants Based on Large Molecules. Polymer-Bound Antioxidants.
6. Metal Catalysed Oxidation and its Inhibition *(Z. Osawa).* Introduction. General Features of the Role of Metallic Compounds. Examples of the Effects of Metallic Compounds on Degradation. Inhibition of Metal-Catalyzed Degradation. Conclusions.
7. Ozone Degradation and Antiozonants *(R.P. Lattimer, R.W. Layer, C.K. Rhee).* Introduction. Chemistry of Ozone Attack. Physical Aspects in Ozone Cracking. Desirable Properties of Antiozonants. Hydrocarbon Waxes. Chemical Antiozonants. Mechanism of Action of Chemical Antiozonants. Manufacture and Production. Alternatives to Antiozonants. Testing. Health and Safety Factors. Uses and Formulations.
8. Photodegradation and Photostabilisation *(G. Scott).* Weathering of Polymers. Photodegradation and Biodegradation. Photooxidation. Photolysis and Photooxidation. Stabilisation of Polymers Against the Effects of Light.
9. Synergism and Antagonism *(G. Scott).* Factors Affecting Antioxidant Performance. Synergistic Effects of Antioxidants and Stabilisers. Antagonism.
10. Fire Retardant Polymeric Materials *(C. Camino).* Introduction. Evaluation of Polymer Combustion. Fire Retardants. Inorganic Hydroxides. Halogen-Based Fire Retardants. Intumescent Systems. Conclusions.
11. Degradation and Stabilisation of Polymers Subjected to High Energy Radiation *(D.J. Carlsson).* Introduction. Primary Radiation Processes in Polymers. Secondary Reactions in Irradiated Polymers. Inhibition of Radiation Degradation Reactions. γ-Stabilisation and Radiolysis Reactions.
Subject Index.

© 1993 xiv + 542 pages
Price: US $ 254.25 / Dfl. 445.00
ISBN 0-444-89616-3

Volumes I, II, III
Set price: US $ 557.00 / Dfl. 975.00
Set ISBN 0-444-89618-X

ELSEVIER
SCIENCE PUBLISHERS

ORDER INFORMATION

For USA and Canada
ELSEVIER SCIENCE PUBLISHERS
Judy Weislogel, P.O. Box 945
Madison Square Station,
New York, NY 10160-0757
Tel: (212) 989 5800
Fax: (212) 633 3880

In all other countries
ELSEVIER SCIENCE PUBLISHERS
P.O. Box 211, 1000 AE Amsterdam
The Netherlands
Tel: (+31-20) 5803 753
Fax: (+31-20) 5803 705

US$ prices are valid only for the USA & Canada and are subject to exchange rate fluctuations; in all other countries the Dutch guilder price (Dfl.) is definitive. Customers in the European Community should add the appropriate VAT rate applicable in their country to the price(s). Books are sent postfree if prepaid.

PUBLICATION SCHEDULE FOR THE 1993 SUBSCRIPTION

Journal of Chromatography and *Journal of Chromatography, Biomedical Applications*

MONTH	1992	J	F	M	A	M	J	
Journal of Chromatography	623–627	628/1 628/2 629/1 629/2	630/1 + 2 631/1 + 2 632/1 + 2 633/1 + 2	634/1 634/2	635/1 635/2 636/1 636/2	637/1 637/2 638/1 638/2	639/1 639/2 640/1 + 2	The publication schedule for further issues will be published later.
Cumulative Indexes, Vols. 601–650								
Bibliography Section				649/1			649/2	
Biomedical Applications		612/1	612/2	613/1	613/2 614/1	614/2 615/1	615/2 616/1	

INFORMATION FOR AUTHORS

(Detailed *Instructions to Authors* were published in Vol. 609, pp. 437–443. A free reprint can be obtained by application to the publisher, Elsevier Science Publishers B.V., P.O. Box 330, 1000 AH Amsterdam, Netherlands.)

Types of Contributions. The following types of papers are published in the *Journal of Chromatography* and the section on *Biomedical Applications:* Regular research papers (Full-length papers), Review articles, Short Communications and Discussions. Short Communications are usually descriptions of short investigations, or they can report minor technical improvements of previously published procedures; they reflect the same quality of research as Full-length papers, but should preferably not exceed five printed pages. Discussions (one or two pages) should explain, amplify, correct or otherwise comment substantively upon an article recently published in the journal. For Review articles, see inside front cover under Submission of Papers.

Submission. Every paper must be accompanied by a letter from the senior author, stating that he/she is submitting the paper for publication in the *Journal of Chromatography.*

Manuscripts. Manuscripts should be typed in **double spacing** on consecutively numbered pages of uniform size. The manuscript should be preceded by a sheet of manuscript paper carrying the title of the paper and the name and full postal address of the person to whom the proofs are to be sent. As a rule, papers should be divided into sections, headed by a caption (*e.g.*, Abstract, Introduction, Experimental, Results, Discussion, etc.) All illustrations, photographs, tables, etc., should be on separate sheets.

Abstract. All articles should have an abstract of 50–100 words which clearly and briefly indicates what is new, different and significant. No references should be given.

Introduction. Every paper must have a concise introduction mentioning what has been done before on the topic described, and stating clearly what is new in the paper now submitted.

Illustrations. The figures should be submitted in a form suitable for reproduction, drawn in Indian ink on drawing or tracing paper. Each illustration should have a legend, all the *legends* being typed (with double spacing) together on a *separate sheet.* If structures are given in the text, the original drawings should be supplied. Coloured illustrations are reproduced at the author's expense, the cost being determined by the number of pages and by the number of colours needed. The written permission of the author and publisher must be obtained for the use of any figure already published. Its source must be indicated in the legend.

References. References should be numbered in the order in which they are cited in the text, and listed in numerical sequence on a separate sheet at the end of the article. Please check a recent issue for the layout of the reference list. Abbreviations for the titles of journals should follow the system used by *Chemical Abstracts.* Articles not yet published should be given as "in press" (journal should be specified), "submitted for publication" (journal should be specified), "in preparation" or "personal communication".

Dispatch. Before sending the manuscript to the Editor please check that the envelope contains four copies of the paper complete with references, legends and figures. One of the sets of figures must be the originals suitable for direct reproduction. Please also ensure that permission to publish has been obtained from your institute.

Proofs. One set of proofs will be sent to the author to be carefully checked for printer's errors. Corrections must be restricted to instances in which the proof is at variance with the manuscript. "Extra corrections" will be inserted at the author's expense.

Reprints. Fifty reprints will be supplied free of charge. Additional reprints can be ordered by the authors. An order form containing price quotations will be sent to the authors together with the proofs of their article.